Phase Diagrams and Thermodynamic Properties of the 70 Binary Alkali Halide Systems Having Common Ions

James Sangster[a] and Arthur D. Pelton

Centre de Recherche en Calcul Thermochimique Ecole Polytechnique, Campus de l'Université de Montréal, P.O. Box 6079, Station A, Montreal, Quebec, Canada H3C 3A7

Received October 25, 1985; revised manuscript received April 6, 1987

A very extensive literature survey of all available phase diagram and thermodynamic data has been carried out for all 40 possible common-anion binary systems (AX-BX) and all 30 possible common-cation binary systems (AX-AY) involving the alkali halides (A,B = Li, Na, K, Rb, Cs; X, Y = F, Cl, Br, I). A critical analysis and evaluation of these data have been performed with a view to obtaining a "best" evaluated phase diagram and a set of "best" evaluated thermodynamic parameters for each system. To this end, a computer-assisted coupled analysis of the phase diagram data and the thermodynamic data for each system has been employed. Mathematical expressions for the thermodynamic properties of all known phases have been obtained which are consistent with the measured thermodynamic properties and phase diagrams as well as with established thermodynamic principles and theories of solution behavior. The parameters of these expressions are reported here and have been used to generate the computer-calculated diagrams in the compilation.

Key words: alkali halides; molten salts; phase diagrams; thermodynamic properties.

Contents

[a] Permanent address: Sangster Research Laboratories, Suite M-3, 1270 Sherbrooke St. W., Montreal, Quebec, Canada H3G 1H7

List of Tables

List of Figures

1. Introduction

Molten salt phase diagrams are of central importance in metallurgy and materials science. They contribute to our knowledge of the behavior of materials in many applications and provide information relating to ionic interactions in solution.

There exists a wealth of data on phase diagrams of the alkali halides, particularly in compendia.[1-7] In these sources, as in the general literature, there is a relative lack of critical evaluation of these data. There have been some attempts at systematic evaluation,[2,4] but these have not exploited the contribution of a thermodynamic simultaneous analysis of the data.

For the common-ion binary alkali halide systems, there exists also a large amount of data on mixing and excess properties,[8] in both the liquid and solid states. The following section of the present report describes the computer-coupled thermodynamic/phase diagram analysis used in the critical evaluation of phase diagram data. This procedure enables the evaluator to test the thermodynamic consistency within and among all reported phase diagram and excess property measurements. This procedure, we believe, results in a much more rigorous and objective assessment of all data than has hitherto been possible. Furthermore, it enables a thermodynamically correct "smoothing" of the experimental data to be performed, and a "best" phase diagram to be calculated.

For each of the 70 systems, the details of the evaluation procedure and the phase diagram for that system are grouped together. Not all reported experimental points are shown on the phase diagram in each case. However, all references found for each system have been included and discussed. The evaluated "best" equations for the thermodynamic properties of all phases are given. The phase diagrams shown were calculated from these equations and are considered to be the "best" evaluated diagrams which can be deduced from the data currently available. The "probable maximum inaccuracy" of the evaluated phase diagram has been estimated for each system. Phase boundaries indicated by dashed lines are considered to be less accurately known.

Tabulated summaries of the thermodynamic properties of all phases represented in the evaluated phase diagrams, together with a topological classification of the diagrams, i.e., according to type (simple eutectic, etc.) are found in the Appendix. There is also a summary of the temperatures and Gibbs energies of fusion and transformation of the pure halides. While most of the pure component data were taken from a recent standard source,[9] a re-evaluation using more up-to-date data was found necessary in a few cases as indicated.

It should be noted that for all 70 binary systems reported here, one consistent set of melting points for the pure salts has been adopted. In many reported experimental binary phase diagrams, the melting points of the pure salts differ significantly from these values. Account was taken of this problem in the evaluations.

2. Computer-Coupled Thermodynamic/ Phase Diagram Analysis

2.1. Introduction

As well as providing a set of self-consistent thermodynamic equations which simultaneously reproduce the thermodynamic properties and the phase diagram of the system, the technique of coupled thermodynamic/phase diagram analysis yields a thermodynamically correct "smoothing" of the experimental data. Furthermore, discrepancies among various sets of data can often be resolved in this way, and error limits can more easily be assigned. Unknown or uncer-

tain phase boundaries can often be estimated with good precision and, conversely, some reported phase boundaries can be rejected as being inconsistent with the thermodynamic properties of the system. Finally, such a thermodynamic analysis is the first step in estimating ternary and higher order phase diagrams from binary data. A short bibliography on computer-coupled thermodynamic/phase diagram analysis and calculation[10–17] should suffice to orient the reader. The principles of simultaneous least-squares optimization of thermodynamic and phase diagram data are described in Ref. 10. The interactive computer programs which were used in the optimizations and phase diagram calculations are described in Ref. 11. (These programs are available "on-line" or on diskette, and further information may be obtained from the authors.)

2.2. Thermodynamic Relationships

For equilibrium between a solid and a liquid phase in a binary system with components A and B, we may write

$$RT \ln a_A^l - RT \ln a_A^s = -\Delta_{fus} G_A^\circ, \quad (1)$$

where a_A^l and a_A^s are the activities of A on the liquidus and solidus at temperature T. Here, $\Delta_{fus} G_A^\circ$ is the Gibbs energy of fusion of A at T and R is the gas constant. Setting the ideal activities equal to the mole fractions x^l and x^s we may write

$$RT \ln x_A^l / x_A^s + G_A^{E(l)} - G_A^{E(s)} = -\Delta_{fus} G_A^\circ, \quad (2)$$

where $G^{E(l)}$ and $G^{E(s)}$ are the partial excess Gibbs energies of A in the liquid and solid. These are zero in an ideal solution. Note that

$$G_A^{E(l)} = RT \ln \gamma_A^l, \quad (3)$$

$$G_A^{E(s)} = RT \ln \gamma_A^s, \quad (4)$$

where γ^l and γ^s are the activity coefficients in the liquid and solid.

An equation identical to Eq. (2) can be written for the other component, B. If the Gibbs energies of fusion are known, and if the excess Gibbs energies are also known as functions of temperature and composition, then these two equations can be solved simultaneously by numerical methods to calculate the liquidus and solidus lines. Conversely, if the liquidus and solidus are known along with the excess Gibbs energies for one phase, then the excess Gibbs energies for the other phase can be calculated.

The integral excess Gibbs energy G^E is related to the partial excess Gibbs energies by the following equation:

$$G^E = x_A G_A^E + x_B G_B^E. \quad (5)$$

Conversely, the partial properties can be obtained from the integral property from the following equation:

$$G_i^E = G^E + (1 - x_i) \frac{dG^E}{dx_i}, \quad (6)$$

where i = A or B.

The excess Gibbs energy can be written as

$$G^E = H^E - TS^E, \quad (7)$$

where H^E and S^E are the excess enthalpy and entropy, respectively. In most cases it can be assumed that H^E and S^E are independent of temperature. In only four of the 70 systems in the present compilaton were the data of sufficient precision and available over a wide enough temperature range to merit inclusion of a temperature-dependent term in the expressions for H^E and S^E. The details are discussed under the evaluations for these particular systems. For the remainder of the present section, it will be assumed that H^E and S^E are independent of temperature.

2.3. Polynomial Expressions of Excess Properties

For phases (solid and liquid) with extended ranges of solubility, H^E and S^E may be expanded as polynomials in the mole fractions as follows:

$$H^E = x_A x_B (h_0 + h_i x_B + h_2 x_B^2 + \cdots), \quad (8)$$

$$S^E = x_A x_B (s_0 + s_i x_B + s_2 x_B^2 + \cdots), \quad (9)$$

where the h_i and s_i are empirical coefficients. Corresponding expressions for the partial properties can be obtained by differentiating Eqs. (8) and (9) via Eq. (6) to give

$$H_A^E = \sum_{i=0} h_i (x_B - i x_A) x_B^{i+1}, \quad (10)$$

$$S_A^E = \sum_{i=0} s_i (x_B - i x_A) x_B^{i+1}, \quad (11)$$

$$H_B^E = x_A^2 \sum_{i=0} h_i (i+1) x_B^i, \quad (12)$$

$$S_B^E = x_A^2 \sum_{i=0} s_i (i+1) x_B^i, \quad (13)$$

whence:

$$G_A^E = RT \ln \gamma_A = H_A^E - TS_A^E, \quad (14)$$

$$G_B^E = RT \ln \gamma_B = H_B^E - TS_B^E. \quad (15)$$

The empirical coefficients h_i and s_i are found by the simultaneous optimization of the thermodynamic and phase diagram data. If only the first terms (h_0,s_0) in the empirical series Eqs. (8) and (9) are nonzero, then the solution is termed "regular." If two terms are required to fit the data then the system is called "subregular." Experience has shown that most alkali halide solutions approximate quite closely to regular or subregular behavior. No more than four terms were required in Eqs. (8) and (9) for any of the 70 systems, and usually one or two terms sufficed. If only limited experimental data are available, then the assumption of regular or subregular behavior will yield an acceptable approximation.

Experience with alkali halide solutions has also shown that the enthalpic term H^E in Eq. (7) is generally larger in magnitude than the entropic term TS^E. Hence, if available data are limited, it is a reasonable assumption to set $S^E = 0$ and to assume that G^E is temperature independent.

As a general rule, the larger the cations and/or anions and the smaller the difference between the radii of the two cations in a common-anion binary system (or between the two anions in a common-cation binary system), the more closely the above approximations (one- or two-term polynomial expansions; $S^E = 0$) are obeyed.

2.4. Solid Solutions with Limited Solubility: Henrian Behavior

In certain systems, limited solid solubility of only a few mole percent of one component in the other is observed. Such solid solutions may be considered to be Henrian solutions. That is, letting component A be the solvent, the activity of A is ideal (Raoultian):

$$a_A^s = x_A^s \text{ and } G_A^{E(s)} = 0. \quad (16)$$

For the solute, B, the activity coefficient $\gamma_B^s = a_B^s/x_B^s$ is independent of composition. Hence, $G_B^{E(s)} = RT \ln \gamma_B^s$ is also independent of composition, and can, to a reasonable approximation, be taken to be independent of temperature:

$$G_B^{E(s)} = RT \ln \gamma_B^s = \text{constant}. \quad (17)$$

In such cases of limited solid solubility of solute B in solvent A, we note that Eq. (2) alone is sufficient to permit $G_A^{E(l)}$ to be calculated along the liquidus, if the solidus and liquidus lines are known, since $G_A^{E(s)} = 0$.

2.5. Limiting Slopes of Liquidus Lines: Estimation of Solid Solubility

In some systems, the extent of solid solubility is not known. In such cases, the measured limiting slope of the liquidus line (dx^l/dT) at $x^l = 1$ (pure A) can permit the extent of solid solubility to be estimated. In the limit at $x_A = 1$, both the liquid and solid phases become Henrian such that $G^{E(s)}$ and $G^{E(l)}$ both approach zero. Similarly, for $x_A \approx 1$, the Gibbs energy of fusion of A is well approximated by the expression $\Delta_{fus}H^\circ_A(1 - T/T_{fus(A)})$, where $\Delta_{fus}H^\circ_A$ is the enthalpy of fusion of A at its melting point, $T_{fus(A)}$. Differentiation of Eq. (2) in the limit at $x_A = 1$ then gives

$$\frac{dx_A^l}{dT} - \frac{dx_A^s}{dT} = \frac{\Delta_{fus}H_A^\circ}{R(T_{fus(A)}^\circ)^2}, \quad \text{when } x_A = 1. \quad (18)$$

From the known enthalpy of fusion and the measured limiting liquidus slope, dx^l/dT, the limiting solidus slope dx^s/dT can be calculated. If this is close to zero, then the solid solubility is of limited extent.

2.6. Optimization Procedure

The actual steps followed in an optimization will vary from system to system. Details are given under the evaluation for each system. However, some general observations can be enunciated.

In 53 of the 70 systems, $H^{E(l)}$ in the liquid phase has been measured calorimetrically by Prof. O. Kleppa and coworkers. These data, which are very reliable, have been fitted to 1-, 2-, or 3-membered series as in Eq. (8).

In the cases of systems with limited solid solubility, Eq. (2) was then used under the assumption of Henrian solid behavior, to calculate excess Gibbs energies along the A- and B-liquidus lines. That is, $G_A^{E(s)}$ was set equal to zero for the solvent, according to Eq. (16). Combining these excess Gibbs energies with the already fitted calorimetric liquid enthalpies permitted the excess liquid entropy $S^{E(l)}$ to be calculated and then smoothed by representation as a 1- or 2-member (very exceptionally a 3 or 4 member) polynomial as in Eq. (9). The Henrian constant of Eq. (17) could then be calculated from the measured solubility limits for each of the two solid solutions. In those few systems for which calorimetric liquid enthalpies were not available, $S^{E(l)}$ was set equal to zero, and the values of $G^{E(l)} = H^{E(l)}$ obtained from the phase diagram were then smoothed by polynomial representation as in Eq. (8).

In the cases of systems with complete solid miscibility, $H^{E(s)}$ has been measured calorimetrically in only a few cases. In general, in these systems it must be assumed that $S^E = 0$ in either the liquid or solid phase or in both. If $G^{E(s)}$ for the completely miscible solid phase is positive, then there will be a zone of demixing (i.e., a miscibility gap) in the solid whose boundaries and consolute point can be calculated from the equation for $G^{E(s)}$. Conversely, if the miscibility gap has been measured experimentally, then these data can be used to help determine the coefficients in the expression for $G^{E(s)}$ (Ref. 10).

Some of the systems studied contain intermediate compounds. In no cases have the Gibbs energies of fusion of these compounds been measured. However, once $H^{E(l)}$ and $S^{E(l)}$ have been determined, the Gibbs energies of fusion of the compounds can be calculated from their measured liquidus lines via Eq. (2) if they are assumed to be stoichiometric compounds. Their Gibbs energies of formation from the pure component salts can then also be calculated.

In a few systems, activities of components have been measured by auxiliary methods. The number of such systems is small. The following is a summary showing the number of systems for which different data types were available.

Systems with phase diagram and/or thermodynamic data:	70
Systems with emf (electromotive force) data:	7
Systems with vapor pressure data:	2
Systems with mass spectrometric data:	2

For all those systems having auxiliary data, the pertinent sources are mentioned and discussed under the section for the appropriate system, and all references have been retained. These data could also be used in principle in the data optimization, but were in fact not used for this purpose. This is because these data, compared to available calorimetric or phase diagram data, were too sparse or inaccurate.

An example will illustrate this conclusion. The system KCl(A) + NaCl(B) has been widely studied; good phase diagram and thermodynamic data exist for both liquid and solid phases (26 references). From the phase diagram/thermodynamic property optimization for this system, as reported in this work, it was found that the quantities

$$H^E(l) = x_A x_B(-2050 - 272x_B) \text{ J mol}^{-1}, \quad (19)$$

$$S^E(l) = 0, \quad (20)$$

(assumed independent of temperature) were sufficient to describe the liquid phase. Equation (19) represents the excess enthalpy as determined calorimetrically by Kleppa.[18] Measurements of activities by other methods have also been reported. In Table 1, results for the excess chemical potential of NaCl in the liquid are shown, as found by three methods:

TABLE 1. System KCl(A) + NaCl(B). Excess chemical potential of NaCl, $\overline{G}_B^E$, in the liquid as determined by emf and phase diagram/thermodynamic analysis technique

	G_B^E, kJ mol^{-1}		
x_B	This work[a]	emf[b]	emf[c]
0.24	−1.26	···	3.63
0.29	−1.11	···	3.21
0.40	−0.82	···	1.45
0.43	−0.74	3.51	···
0.47	−0.65	2.34	···
0.51	−0.56	2.90	0.85
0.58	−0.54	2.43	···
0.63	−0.33	2.41	0.17
0.72	−0.19	1.59	···
0.75	−0.15	···	0.70
0.78	−0.12	1.15	···
0.82	−0.08	1.34	···
0.88	−0.04	···	0.28
0.91	−0.02	0.21	···
0.95	−0.01	···	0.13

[a] Quantity assumed to be independent of temperature.
[b] Reference 19, data at 880 °C.
[c] Reference 20, data at 885 °C.

(i) Eqs. (19) and (20), (ii) emf Ref. 19, and (iii) emf Ref. 20. Both emf studies report rather large positive deviations from ideality. If Eq. (19) is taken to represent the excess enthalpy, then the partial excess entropy of NaCl, as determined by emf, may be as large as -3 J mol^{-1} K^{-1} at the equimolar composition. As Forland and Thulin[20] point out, this is an improbably large deviation for this system, and instead they attribute the deviation to the presence of a liquid junction potential in the original emf measurements. That this is probably the case is supported also by independent NaCl activity measurements made by mass spectrometry[21] on the liquid. The results of these measurements, done in the interval 700–810 °C and extrapolated to 880 °C, indicate that $\overline{G}_B^E$ is slightly negative, and that the partial excess entropy $\overline{S}_B^E$ is very small ($\approx$0.4 J mol^{-1} K^{-1} at the equimolar composition).

In conclusion, we favored phase diagram and thermodynamic data in our optimization and excluded other types of data, because the latter were sparse and uncertain. Electromotive force measurements in systems containing alkali metals are particularly difficult, due to spurious effects. The interpretation of vapor pressure data is not entirely unambiguous and precise measurement is difficult. The mass spectrometric data may be accurate, depending upon the species whose ion currents are used to derive activities.

Only in the case where no phase diagram or thermodynamic data were at hand, but auxiliary data were available, would we consider the use of auxiliary data in the optimization. This was never the case among the 70 systems reported here. In such a hypothetical case, auxiliary data would be considered together with qualitative and quantitative estimates drawn from phase diagram and thermodynamic properties of analogous systems already studied.

3. The Evaluations

3.1. Common-Anion Systems

a. Fluorides

LiF(A)+NaF(B)

Earlier work on this system[22,23] with the visual-polythermal method indicated a eutectic at $x_B = 0.39$ at 652 °C. The most recent results,[24,25] obtained by thermal and differential thermal analysis, gives 649 °C and 0.39, with a limited solubility of LiF in NaF of about 8.5 mol% at the eutectic temperature. From this solubility, a Henrian activity coefficient of LiF in NaF, relative to the solid standard state at the eutectic temperature was calculated as

$$RT \ln \gamma_A = 18\,895 \text{ J mol}^{-1}, \quad (21)$$

which was assumed to be independent of temperature. The liquidus limiting slope at the LiF side does not suggest a solid solution; Holm[24] estimates less than 1% solubility of NaF in LiF.

The excess enthalpy of the liquid has been measured by two laboratories[26–28]; the more recent results of Kleppa[28] (measured at 1087 °C and assumed independent of T) have been used in the present calculation:

$$H^E(l) = x_A x_B(-7565 + 368x_B) \text{ J mol}^{-1}. \quad (22)$$

Small excess entropy terms were calculated

$$S^E(l) = x_A x_B(-1.607 - 1.124x_B) \text{ J mol}^{-1} \text{ K}^{-1}, \quad (23)$$

which enabled the liquidus to be reproduced within 5 °C of Holm's[24] results, as well as this author's eutectic temperature and composition.

Probable maximum inaccuracy in calculated diagram: (Fig. 1): ± 5 °C.

KF(A)+LiF(B)

Several investigations[2,29–34] report a eutectic in the range 487–493 °C at $x_B = 0.50$. The Russian investigators[22,29–32,34] used the visual-polythermal method, while Aukrust *et al.*[33] used thermal analysis and high-temperature filtration supplemented by visual observation in some cases. The limiting liquidus slopes of the phase diagram of the

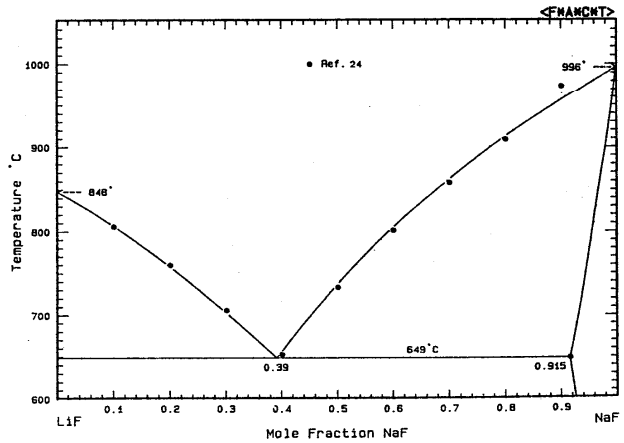

FIG. 1. The system LiF(A) + NaF(B).

American authors[33] suggest a solid solubility of no more than 2% at either end, and calculations were performed under the assumption of no solid solubility.

The excess enthalpy of this system has been reported by two laboratories[26,28,35] and the more recent and reliable data of Hong and Kleppa[28] were used in the present work:

$$H^{E}(1) = x_A x_B(-19\,251 - 1205x_A + 4732x_A^2)\ \text{J mol}^{-1}. \quad (24)$$

The use of small excess entropy terms

$$S^{E}(1) = x_A x_B(-1.375 - 3.146x_B)\ \text{J mol}^{-1}\ \text{K}^{-1}, \quad (25)$$

enabled a good fit (within 5 °C) to the liquidus of Aukrust *et al.*[33]

The calculated eutectic is at $x_B = 0.51$ at 492 °C.

Probable maximum inaccuracy in calculated diagram (Fig. 2): ⊥ 5 °C.

LiF(A)+RbF(B)

Two investigations of this system by Russian authors[36,37] report a eutectic at 448–450 °C and $x_B = 0.50$; the visual-polythermal method was used. Later American work[38,39] provided liquidus and solidus data points in the range $0.2 \leqslant x_B \leqslant 0.7$, obtained from cooling curve experiments. The American authors report a eutectic at 470 °C, $x_B = 0.56$ as well as the presence of an incongruently melting compound LiF·RbF (peritectic $x_B = 0.53$,457 °C). The crystal structure parameters of the intermediate compound were determined separately.[40] A recent report of a quaternary system limited by the LiF + RbF binary system[41] cites Thoma's[39] results, and there are apparently no more recent new data than these. Since the American work is more complete than the other, liquidus points were read off the published diagram[39] and were used for the present calculation, together with the reported invariant points.

The excess enthalpy has been measured by direct calorimetry at 898 °C by Holm and Kleppa,[26] whose results are used here:

$$H^{E}(1) = x_A x_B(-17\,155 - 6275x_A)\ \text{J mol}^{-1}. \quad (26)$$

None of the investigators reports or mentions solid solubility, although some solubility of LiF in RbF might be expected. None was assumed in the present work. With the assumption of $H^{E}(1)$ given by Eq. (26) three $S^{E}(1)$ coefficients were calculated:

$$S^{E}(1) = x_A x_B(-22.166 + 49.002x_B - 33.980x_B^2)\ \text{J mol}^{-1}\ \text{K}^{-1}. \quad (27)$$

The calculated phase diagram based on Eqs. (26) and (27) reproduced the experimental[39] liquidus curves within 10 °C, and the eutectic and peritectic points exactly. Although this is a good representation, its accuracy is possible only through the adoption of the very asymmetrical $S^{E}(1)$ expression, Eq. (27). If the diagram is calculated with $S^{E}(1) = 0$ and with Eq. (26) for $H^{E}(1)$, then the RbF liquidus is reproduced almost exactly (within 2 to 3 °C), but the LiF liquidus is up to 100 °C lower than the reported. These results suggest that the experimental diagram may be in error, probably on the LiF side.

The calculated Gibbs energy of fusion of the compound 0.5(LiF·RbF) is

$$\Delta_{fus}G^{\circ} = 13\,700 - 18\,316T\ \text{J/mol}. \quad (28)$$

Probable maximum inaccuracy in calculated diagram (Fig. 3): RbF liquidus, ± 20 °C; LiF liquidus, ± 40 °C.

CsF(A)+LiF(B)

Tabulated data for this system are not available from the literature, although phase diagrams have been published, based on the work of Russian[42,43] and American[39,44] investigators. Bukhalova and Sementsova[42] used a thermographic method, recording the differential heating and cooling curves. They report the compound LiF·CsF melting congruently at 494 °C, with eutectics at $x_B = 0.40$, 479 °C and $x_B = 0.525$, 490 °C. Later work by Russian authors[45–48] on ternary and higher systems limited by the LiF + CsF binary system confirm the presence of a congruently melting compound, and two eutectics (487–490 °C, 474–479 °C). In contrast, Barton *et al.*[44] from cooling curve and thermal gradient quenching experiments find an incongruently melting compound (peritectic at $x_B = 0.45$, 495 °C) and eutectic at

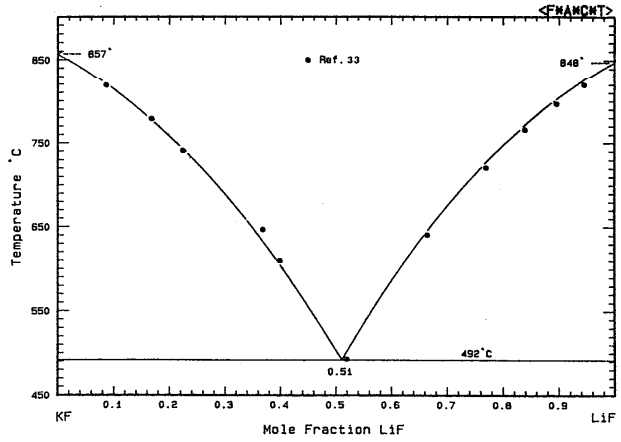

FIG. 2. The system KF(A) + LiF(B).

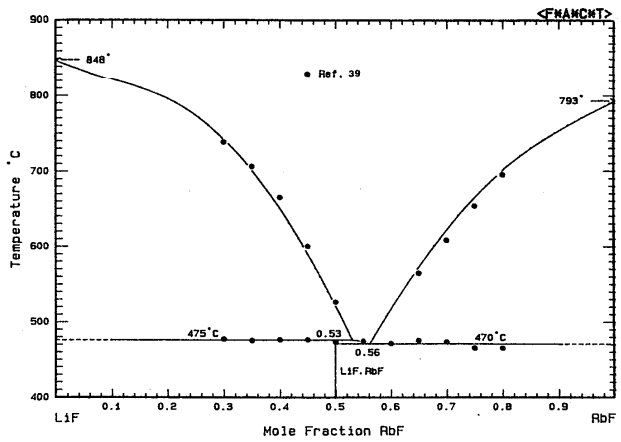

FIG. 3. The system LiF(A) + RbF(B).

$x_B = 0.37$, 475 °C. Deadmore and Machin,[49] also from cooling curve analysis, confirm the findings of Barton *et al.*, reporting only the peritectic ($x_B = 0.46$, 488 °C) and eutectic ($x_B = 0.36$, 470 °C). Calculations in the present work were performed separately on the Russian[42] and American[44] work; the data used included the invariant points reported in each case, and liquidus points at 0.1 mole fraction intervals read off published diagrams.[39,43]

None of the investigations[39,42–49] mentions solid solubility, although some solubility of LiF and CsF might be expected. Calculations were performed in the present work under the assumption of zero solid solubility. The excess enthalpy was measured at 751 °C in solid–liquid mixing experiments by Holm and Kleppa,[26] whose results are used here:

$$H^E(1) = x_A x_B (-11\,050 - 7450x_B - 5525x_A x_B)\ \text{J mol}^{-1}. \quad (29)$$

Under the assumption that $G^E(1)$ is given by Eq. (29), a phase diagram was calculated. At the eutectic temperatures of 479 and 490 °C reported in Ref. 42, the calculated liquidus compositions were $x_B = 0.39$ and $x_B = 0.535$, in very good agreement with the reported[42] eutectic compositions. In addition, the calculated CsF liquidus was everywhere within 5 °C of the Russian[42] results. However, the LiF liquidus was up to 40 °C below that reported in Ref. 42. The corresponding deviations from the American[44] results were larger. Hence, fitting either measured phase diagram would require a very asymmetrical and unusual $S^E(1)$. The fact that the CsF liquidus and both eutectic points were well fitted by the very simple assumption that $S^E(1) = 0$ suggests that this assumption may be valid and that the reported LiF liquidus curves may be in error. The calculated phase diagram shown here is based upon a $G^E(1)$ given by Eq. (29), and a congruently melting compound as indicated by Bukhalova and Sementsova.[42] The calculated Gibbs energy of fusion of the compound 0.5 (CsF·LiF) is

$$\Delta_{fus}G^\circ = 17\,950 - 23.400T\ \text{J/mol}. \quad (30)$$

The entropy of fusion is reasonable, thus giving further support to the calculated diagram.

In summary, however, these findings do not permit an unequivocal choice among the two reported diagrams[42,44] and the calculated diagram.

Probable maximum inaccuracy in calculated phase diagram (Fig. 4): CsF liquidus, ± 15 °C; LiF liquidus, ± 35 °C.

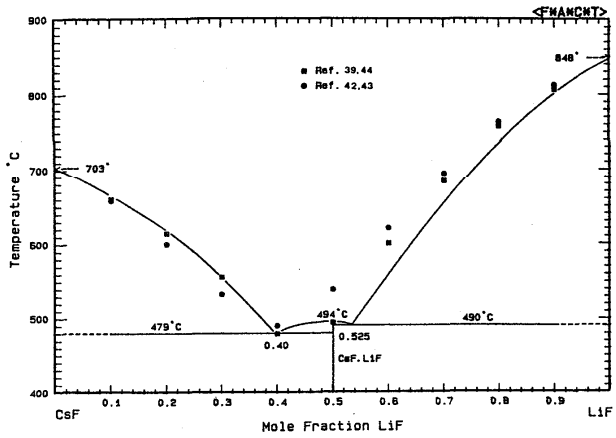

FIG. 4. The system CsF(A) + LiF(B).

KF(A)+NaF(B)

Data defining the liquidus in earlier investigations[50–54] are generally within 10 °C of the most recent work of Holm.[24] The Russian investigators used the visual-polythermal method[51–53] or a combination of visual-polythermal and cooling curve methods.[50,54] Holm[24] used thermal and differential thermal analysis. All agree on the eutectic composition, $x_B = 0.40$, but the reported eutectic temperature lies in the range 699[50] to 721 °C.[24] Holm's work appears to be the most carefully done, and hence was chosen for this study. He found negligible solid solubility at the NaF side of the diagram, but 5 mol % at the KF side, at the eutectic temperature. From this solubility, a Henrian activity coefficient of NaF in KF, relative to the solid standard state at the eutectic temperature was calculated as

$$RT \ln \gamma_B = 24\,770\ \text{J mol}^{-1}, \quad (31)$$

which was assumed to be independent of temperature.

The excess enthalpy of the liquid has been measured in two laboratories,[27,28] and the more recent and reliable data of Hong and Kleppa,[28] (measured at 1087 °C and assumed independent of T) have been used here:

$$H^E(1) = -355x_A x_B\ \text{J mol}^{-1}. \quad (32)$$

One excess entropy coefficient was calculated:

$$S^E(1) = -2.541x_A x_B\ \text{J mol}^{-1}\ \text{K}^{-1}. \quad (33)$$

This allowed the measured diagram[24] to be reproduced closely. The calculated eutectic is 719 °C at $x_B = 0.40$. The calculated NaF liquidus is within 2 °C of the measured,[24] while on the KF side it is 4 to 5 °C below the measured.[24] The earlier measurements[50–54] of this liquidus are also slightly below Holm's values, however, and hence agree closely with the calculated liquidus.

Probable maximum inaccuracy in calculated diagram (Fig. 5): ± 5 °C.

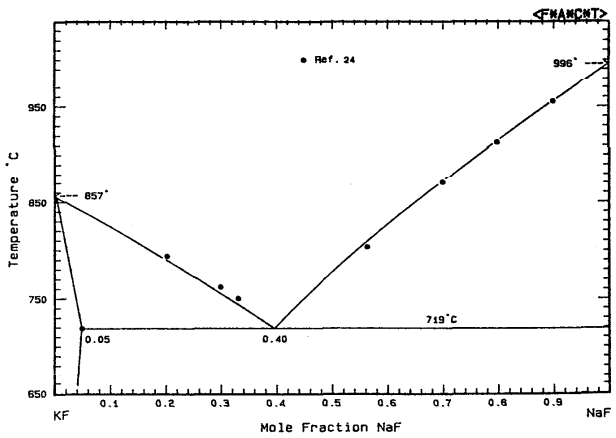

FIG. 5. The system KF(A) + NaF(B).

NaF(A)+RbF(B)

Data defining the liquidus have been reported in three independent investigations.[24,36,55] In the earlier work[36,55] the visual-polythermal method was used, and the reported eutectic was 644 or 675 °C, $x_B = 0.67$ or 0.73. In the most recent work by Holm,[24] determinations were made by thermal analysis, differential thermal analysis (DTA), and quenching; special care was taken with RbF, as it is very hygroscopic. The possibility of solid solution was examined closely, and it was concluded that solid solution in both components was less than 1%. The earlier work cites no solid solution, and this is consistent with the limiting slopes of the reported[24] liquidus. Holm's work appears to be the most carefully done, and his data were used for the present calculations (eutectic 667 °C, $x_B = 0.672$).

The excess enthalpy of this system has been measured in two laboratories.[26,27] The results of Holm and Kleppa[26] at 1008 °C were used in the present work, as they were obtained by direct calorimetry rather than by drop calorimetry.[27] The excess enthalpy is small and can be represented by the following equation[26]:

$$H^E(1) = 375 x_A x_B \text{ J mol}^{-1}. \quad (34)$$

With the use of this excess enthalpy (assumed independent of T) and the experimental phase diagram points,[24] three excess entropy coefficients were calculated:

$$S^E(1) = x_A x_B (-2.658 + 4.140 x_B - 4.702 x_B^2) \text{ J mol}^{-1} \text{ K}^{-1}, \quad (35)$$

which enable the reported liquidus[24] to be reproduced within 3 °C, except for two points (within 10 °C) which appear distinctly higher than the calculated curve. Holm's eutectic is reproduced exactly.

Probable maximum inaccuracy in calculated diagram (Fig. 6): ± 5 °C.

CsF(A)+NaF(B)

Liquidus data are available in two studies[49,56] both by thermal analysis (cooling curves). In the Russian report,[49] the liquidus shown an unlikely inflection near pure NaF, which is absent in the other work. The phase diagram of Deadmore and Machin[56] therefore was used as the basis of the present calculations. In these reports and others,[42,57] the eutectic falls in the range 610–618 °C, $x_B = 0.20$–0.24. No solid solubility was observed by Samuseva and Plyushchev[56] in the range 1–98 mol % NaF. This was confirmed by x-ray analysis of quenched samples at $x_B = 0.25$, 0.5, and 0.75,[49] and corroborated by limiting liquidus slopes of the chosen[49] phase diagram.

The excess enthalpy of this system has been measured at several temperatures between 820 and 1100 °C[27] by drop calorimetry. In a preliminary calculation, the excess enthalpy at 820 °C was used with the chosen eutectic point (610 °C, $x_B = 0.238$). This calculation indicated that the excess Gibbs energy of the system at the eutectic is small [$G^E(1) \approx 300$ J mol^{-1}] with a very negative excess entropy [$S^E(1) \approx -5$ J mol^{-1} K^{-1}]. The latter finding is improbable in reality, in comparison with other similar systems. The calculated phase diagram showed deviations from the measured[49] of up to 50 °C. For these reasons, and considering the fact that $H^E(1)$ was measured by an indirect technique, it was deemed better to derive thermodynamic quantities from the phase diagram. Thus in a second calculation it was assumed that $G^E(1) = H^E(1)$, independent of temperature, and the following result was obtained:

$$H^E(1) = x_A x_B (955 + 2718 x_B) \text{ J mol}^{-1}. \quad (36)$$

With the use of this excess enthalpy, the eutectic[49] was reproduced exactly, and liquidus points on the NaF side reproduced within 5 °C (within 15 °C for two scattered points). The calculated CsF liquidus followed the measured one, at a displacement corresponding to the uncertainty in the melting point of CsF (that is, the melting point of CsF reported in Ref. 49 is 23 °C lower than the chosen value in Table A1).

Probable maximum inaccuracy in calculated diagram (Fig. 7): ± 10 °C.

KF(A)+RbF(B)

Data defining the liquidus, obtained by the visual-polythermal method, have been reported in tabular form,[38] and as a smooth curve in a phase diagram[39,59] obtained from analysis of cooling curves. Both studies report continuous

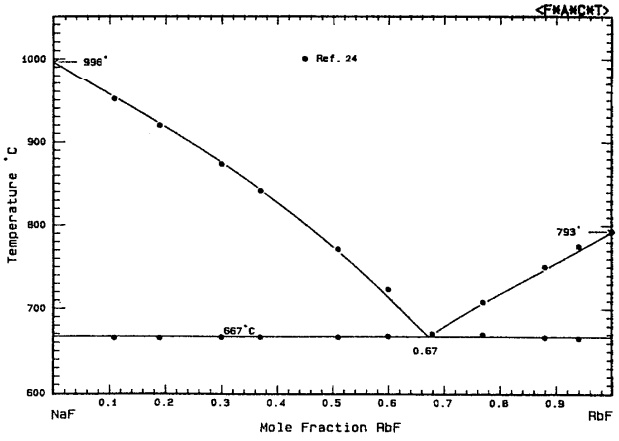

FIG. 6. The system NaF(A) + RbF(B).

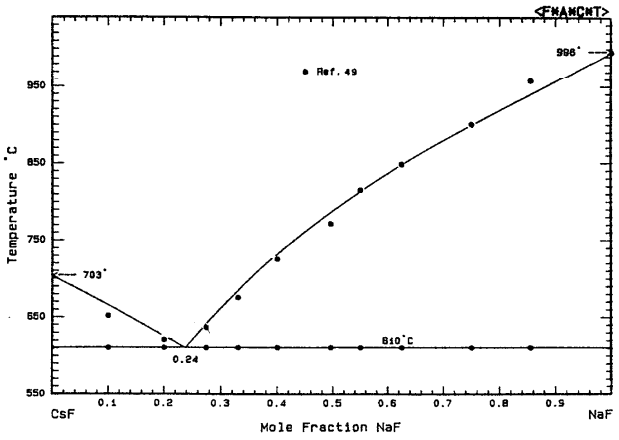

FIG. 7. The system CsF(A) + NaF(B).

solid solution. A temperature minimum at 770 °C, $x_B = 0.72$ is indicated by the American authors,[59] but none by the Russian authors.[58] Although the melting point of RbF reported in the Russian work[58] is 13 °C below the chosen value in Table A1, this work was taken as a guide to the general shape of the liquidus. There are no data defining the solidus.

The excess enthalpy has been measured at 898 °C by direct calorimetry by Holm and Kleppa,[26] whose result is used here:

$$H^E(l) = 360 x_A x_B \text{ J mol}^{-1}. \quad (37)$$

This was taken as the excess free energy of the liquid, independent of temperature for the present calculations. The phase diagram was calculated with this assumption, and with the assumption that the solid exhibits regular solution behavior. The phase diagram based upon the value

$$G^E(s) = 2500 x_A x_B \text{ J mol}^{-1}, \quad (38)$$

is shown, and is proposed as the most reasonable reconstruction for the system. The calculated liquidus closely approximates the experimental,[58] when allowance is made for the difference in reported melting point of RbF. There is a very shallow temperature minimum at $x_B \approx 0.84$. The calculated consolute temperature for solid demixing is − 125 °C.

Probable maximum inaccuracy in calculated diagram (Fig. 8): ± 15 °C.

CsF(A)+KF(B)

Data for the liquidus are to be found in one study,[60] which reports the eutectic at 625 °C and $x_B = 0.43$. Another report confirms these values,[61] while a third[62] gives the eutectic temperature as 627 °C. All determinations were performed by thermal analysis. Samuseva and Plyushchev[60] report "up to" 15 mol % solid solubility of KF in CsF and none detectable (< 3%) on the KF side. The latter finding is corroborated by the limiting liquidus slope at the KF side. The authors, however, show the solidus curve at the CsF side to be convex toward this axis. The difference between the limiting liquidus and solidus slopes at the CsF side indicates that this is not correct.

There is a large uncertainty in the observed melting point of CsF. Therefore, a thermodynamic optimization was performed with liquidus data for compositions between the eutectic and pure KF only. From these data a single excess enthalpy coefficient was calculated:

$$H^E(l) = 2028 x_A x_B \text{ J mol}^{-1}, \quad (39)$$

based on the assumption that $G^E(l) = H^E(l)$ and that $H^E(l)$ is independent of temperature. From the calculated activities of KF and CsF in the liquid at the eutectic, a solid solubility of KF in CsF of 25 mol % was deduced, although this value must, of course, be taken as only very approximate. Furthermore, a Henrian activity coefficient for KF in solid solution at the eutectic temperature, given by

$$RT \ln \gamma_B = 10\,448 \text{ J mol}^{-1}, \quad (40)$$

was calculated which is here assumed to be independent of temperature.

With the use of these values for $H^E(l)$ and $RT \ln \gamma_B$, a phase diagram was calculated, which reproduced the observed[60] eutectic point exactly. The KF liquidus was reproduced to within 10 °C, except for one point near pure KF, which may be accounted for by the discrepancy in the melting point of KF. The CsF-side liquidus differs significantly from the measured.[60] It is to be noted, however, that both the calculated solubility of KF in CsF (25%) at the eutectic temperature and the curvature of the solid solubility curve are thermodynamically consistent with the observed[60] KF side of the diagram. In this respect the calculated diagram is more probably correct than the experimental in this region.

Probable maximum inaccuracy of calculated liquidus (Fig. 9): ± 10 °C.

CsF(A)+RbF(B)

There is apparently only one report of the measured phase diagram of this system.[60] The reported diagram however shows a temperature minimum in the solidus without a corresponding minimum for the liquidus; it thus violates the phase rule. The data were obtained by thermal analysis, and so the reported liquidus is probably more accurate than the solidus. The shape of the liquidus was, therefore, taken as a guide for the present calculations, in which it was assumed that $G^E(l) = 0$, as a reasonable approximation. The solid phase was assumed to be a regular solution. The calculated liquidus, based on an excess Gibbs energy of solid solution of

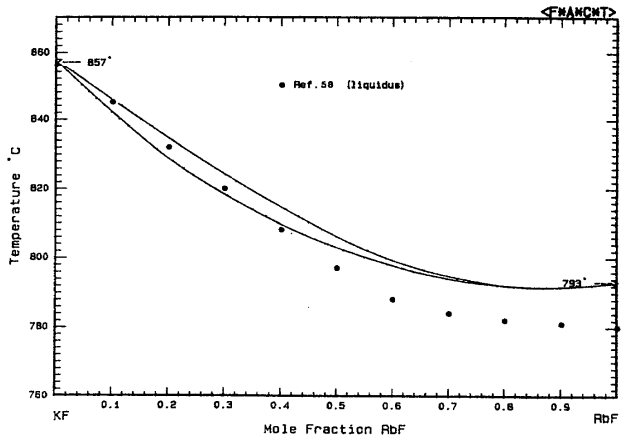

FIG. 8. The system KF(A) + RbF(B).

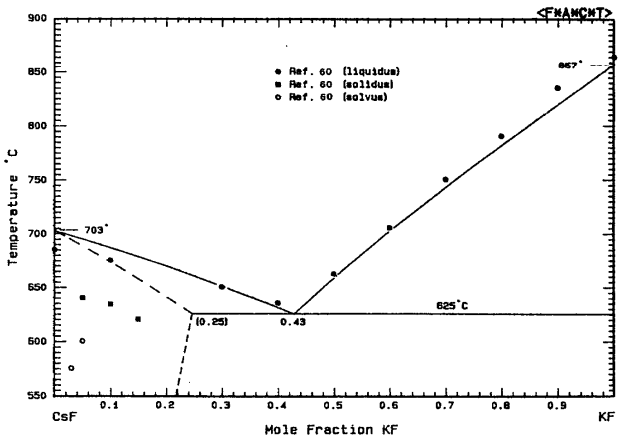

FIG. 9. The system CsF(A) + KF(B).

$$G^E(s) = 2000 x_A x_B \text{ J mol}^{-1}, \quad (41)$$

corresponded closely to the observed,[60] with due allowance for differences between the melting points of the pure substances as reported by[60] and as listed in Table A1. The two-phase region, as calculated, is much narrower than the reported, and there is no temperature minimum. The calculated phase diagram, moreover, is thermodynamically consistent, and probably corresponds more faithfully to true behavior than the published one. The calculated consolute temperature for solid demixing is − 155 °C.

Probable maximum inaccuracy of calculated diagram (Fig. 10): ± 15 °C.

b. Chlorides

LiCl(A)+NaCl(B)

Data defining the liquidus have been tabulated in several studies,[63–71] determined by thermal analysis[63–65,70,71] and visual-polythermal methods.[66,69] Lamplough[65] examined only dilute solutions of LiCl in NaCl. Some authors report a minimum and complete solid miscibility at the liquidus temperature, while others report a eutectic and intermediate compounds. Table 2 summarizes the reported minima and invariant points.

In addition, a few authors[71–74] report, on the basis of small breaks in the liquidus curve, a LiCl homomorphic transition at 565 °C, $x_B = 0.185$. There are no confirmatory reports by x-ray or other methods, and the existence of such a transformation has been doubted.[1] This transformation is shown on the phase diagram in a authoritative compilation,[80] although no phase transformation of LiCl is known.[81]

Evidence for the existence of intermediate compounds is based on breaks in the liquidus curves in binary and ternary systems. Other methods were also used.[67,72,77,78,82] X-ray analysis of cooled solid samples[67,77,82] failed to detect compounds. Chesnokov *et al.*[78] used DTA, x-ray, and crystallo-optical analyses, but reported only the 575 °C peritectic from thermal analysis. Smits *et al.*[83] examined the NaCl + 2LiCl composition by x ray and found no compounds. Akopov and Bergman,[72] in addition to cooling curves, also performed heating experiments at selected compositions, and report breaks at 575 and 610 °C, corresponding to two compounds. Thus, although the existence of compounds has been claimed to be established[68,69,72] there is a lack of independent confirming evidence. Finally, all reported liquidi at their lowest temperatures are flat (i.e., zero slope) rather than sharp (finite slope), indicating that the system has a minimum and not a eutectic. This is true even of those authors[68,69] who claim a eutectic rather than a minimum.

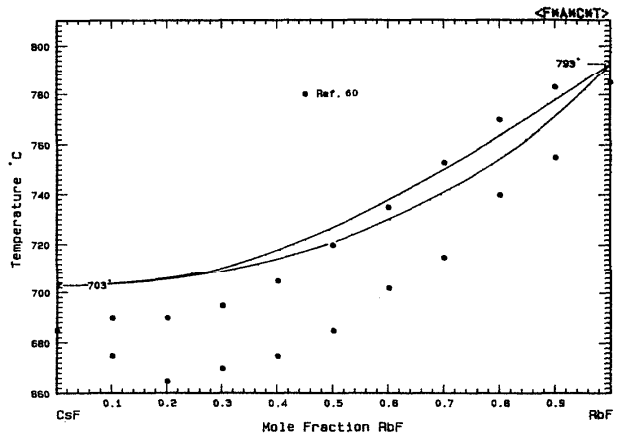

FIG. 10. The system CsF(A) + RbF(B).

TABLE 2. Reported minima and invariant points of the system LiCl(A) + NaCl(B)

	T/°C	x_B	Ref.
Minimum	552	0.27	63
	553	0.28	64
	528	0.29	66
	555	0.25	77
Eutectic	553	0.215	67
	553	0.27	71
	551	0.245	68,69
	558	0.21	72
	546	0.3	73
	553	0.285	74
	548	0.27	75
	554	0.26	76
Peritectic	575	0.33	67
near 575 °C	572	0.36	68,69
	575	0.33	71
	576	0.4	73
	575	0.39	78
	575	0.37	77
	575	0.37	74
	570	0.36	79
	570	0.375	75
	575	0.37	72
Peritectic	622	0.5	68,69
near 620 °C	610	0.53	72
	618	0.5	75
	618	0.5	79
	610	0.47	74
	620	0.5	73

Data defining the solidus were obtained by thermal analysis only[63,66,70] and indicate continuous solid solution. The presence (but not the extent) of solid solution was confirmed by x-ray diffraction.[77,78] The presence of appreciable solid solution is denied by some,[68,69,72] but this statement[68] does not take into account any more recent disconfirming evidence. Moreover, the limiting slopes of the liquidus[67,68] indicate extensive solid solubility.

The consolute point for solid–solid miscibility has been reported as 314 °C, $x_B = 0.35$ from cooling curves,[63] 271 °C and $x_B = 0.42$ from optical investigation of thin sections,[64] ≈400 °C from heating curves[66] and > 500 °C from thermographic analysis.[77]

The excess enthalpy of the liquid was obtained by Hersh and Kleppa[84] by calorimetric solid–liquid mixing experiments at 740 °C. Their results are used here:

$$H^E(l) = -4686 x_A x_B \text{ J mol}^{-1}. \quad (42)$$

In a preliminary calculation, Eq. (42) was used and the system was treated as having a eutectic and no solid solubility. The observed liquidus[68] could not be satisfactorily reproduced. Subsequently, the system was treated as one with continuous solid solution at the liquidus temperature. A phase diagram was calculated with $G^E(l)$ assumed to be given by Eq. (42), and $G^E(s)$ given by Eq. (43):

$$G^{E}(s) = x_B x_A (9800 - 5200x_B) \text{ J mol}^{-1} \quad (43)$$

both independent of temperature. The calculated liquidus is within 6 °C of the experimental,[64,67,68] except at $T > 670$ °C, where the experimental liquidi themselves[63,64,66–68] diverge to some extent. In summary, the thermodynamic analysis indicated that the assumption of eutectic and intermediate compounds is inconsistent with the flatness of the liquidus at its lowest temperature, and supports the existence of a minimum.

The calculated minimum is 554 °C, $x_B = 0.28$. The calculated consolute temperature for solid–solid demixing is 241 °C at $x_B \approx 0.33$. Since there is significant residual uncertainty concerning the existence of compounds, and the extent of solid solubility, the solidus and solid miscibility gap, as calculated, are less accurate than the calculated liquidus.

Probable maximum inaccuracy in calculated liquidus (Fig. 11): ± 10 °C.

Probable maximum inaccuracy in calculated solidus (Fig. 11): ± 25 °C.

KCl(A)+LiCl(B)

Data defining the liquidus obtained from thermal analysis in several investigations[33,63,64,70,85 88] are in good agreement. The spread in the measured liquidus temperatures is essentially the same as the spread in the melting points of the pure components as reported by the different investigators (KCl, ± 13 °C, LiCl, ± 6 °C).The eutectic as reported, lies in the range 348 to 361 °C at $x_B = 0.58$ to 0.595. Investigation of the limit of solid solubility by thermal analysis in the earlier work[63] indicated less than 5 mol % at either end; the limiting liquidus slopes confirm this finding.The most recent tabulated liquidus points are those of Murgulescu and Sternberg[88]; these agree well (within 10 °C) with points read off the phase diagram of Aukrust *et al.*[33]

The activity of LiCl has been deduced from emf measurements on the liquid at 640[89] and 722 °C.[90]

The excess enthalpy of the liquid has been reported by two groups.[84,91] Hersh and Kleppa[84] performed solid–liquid mixing experiments at 740 °C, and since their work is more detailed and covers a wider concentration range than that of Markov *et al.*,[91] their results are used here:

$$H^{E}(l) = x_A x_B (-17\,570 - 377x_B) \text{ J mol}^{-1}. \quad (44)$$

Thermodynamic analysis using this excess enthalpy indicated that a eutectic temperature of 355 °C is most consistent with a simple entropy function, and hence is to be preferred over the low and high extremes reported. Two excess entropy terms were calculated:

$$S^{E}(l) = x_A x_B (-7.627 + 4.958x_B) \text{ J mol}^{-1} \text{ K}^{-1}, \quad (45)$$

to give a calculated eutectic composition of $x_B = 0.595$. The calculated liquidus is everywhere within 10 °C of those of the most recent investigations.[33,88]

Probable maximum inaccuracy of calculated diagram (Fig. 12): ± 10 °C.

LiCl(A)+RbCl(B)

Data defining the liquidus have been tabulated in five independent investigations.[63,85,86,88,92] The methods used were cooling curves,[63,85,88] heating curves,[86] and visual-polythermal.[92] A summary of reported eutectics and peritectics is given as follows:

	T/°C	x_B	Ref.
Eutectic	312	0.4475	63
	318	0.417	85
	316	0.4225	86
	312	0.445	37
	312	0.43	94
	297	0.405	92
	305	0.45	88
Peritectic	323	0.462	85
	321	0.46	86
	328	0.45	92

The presence of a peritectic is indicated by a pronounced discontinuity in the liquidus curve of three studies.[85,86,92] In the other studies, the liquidus data points were not numerous enough in the region $0.4 < x_B < 0.5$ to show this. Richards and Meldrum[85] assign the composition LiCl·RbCl to the intermediate compound on the basis of analogy with similar systems, but did no solid phase analysis. Keitel[86] studied thin solid sections optically, and deduced 1:1 stoichiometry. Il'yasov *et al.*[92] give no basis for this composition. Only very recently[93] has this 1:1 compound been isolated and characterized by x-ray measurements.

Zhemchuzhnyi and Rambach[63] observed a "eutectic"

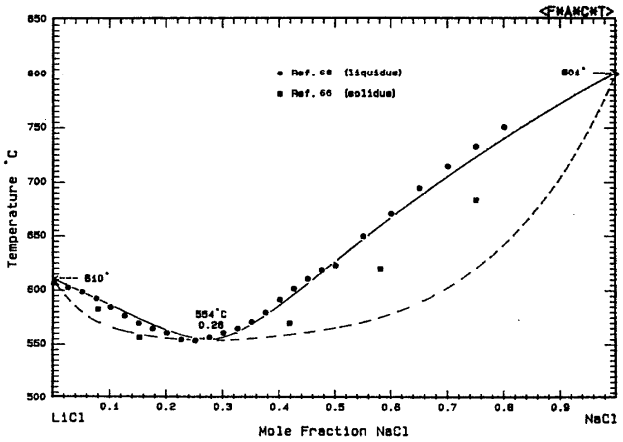

FIG. 11. The system LiCl(A) + NaCl(B).

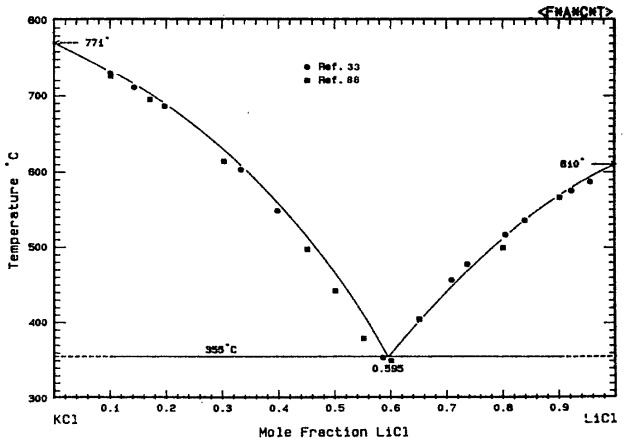

FIG. 12. The system KCl(A) + LiCl(B).

arrest over the range $0.22 \leqslant x_B \leqslant 0.96$. The limiting liquidus slopes of four liquidi[63,86,88,92] all indicate that the solid solubility at either end is probably smaller than these figures indicate, and so zero solid solubility was assumed in the present calculations.

The activity of LiCl in the liquid has been deduced from emf measurements at 652 °C.[90]

The excess enthalpy of the liquid has been measured by Hersh and Kleppa[84] at 740 °C by direct calorimetry; their result is used here:

$$H^E(l) = x_A x_B(-17\,866 - 4812x_A - 3975x_A x_B)\ \text{J mol}^{-1}. \quad (46)$$

With the use of this excess enthalpy and the liquidus points of three studies,[85,86,88] two excess entropy coefficients were calculated:

$$S^E(l) = x_A x_B(-7.352 - 6.725x_B)\ \text{J mol}^{-1}\ \text{K}^{-1}. \quad (47)$$

The liquidus calculated with Eqs. (46) and (47) reproduced the experimental liquidus points[85,86,88] within 8 °C with few exceptions. The calculated eutectic is 313 °C, $x_B = 0.422$. The peritectic is similarly calculated to be 324 °C, $x_B = 0.471$, and the Gibbs energy of fusion of the compound 0.5(LiCl·RbCl) is

$$\Delta_{fus} G^\circ = 8128.9 - 13.575T\ \text{J/mol}. \quad (48)$$

Probable maximum error in calculated liquidus (Fig. 13): ± 10 °C.

CsCl(A)+LiCl(B)

Data defining the liquidus have been tabulated in three studies.[85,95,96] The methods used were cooling curves with[85] and without[95] visual observation, and visual-polythermal.[96] All three liquidi are reasonably concordant (within 10 °C) except in the range $0.25 < x_B < 0.5$. In the most recent work[96] the liquidus is better defined over the entire composition range, and so Dergunov's[96] results were taken as reference for the present calculations. Apart from these three detailed reports of the liquidus, there have been a large number of later re-examinations of this system as a limiting edge of ternary phase diagrams. The reported invariant points are summarized in Table 3.

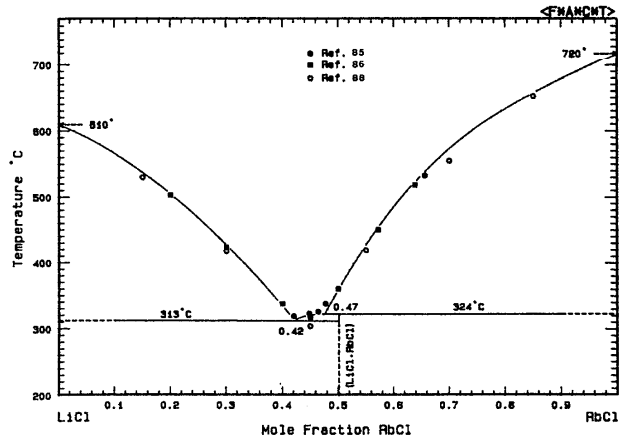

FIG. 13. The system LiCl(A) + RbCl(B).

TABLE. 3. Reported invariant points of the system CsCl(A) + LiCl(B)

	T/°C	x_B	Ref.
Eutectic	332	0.58	95
	323	0.593	85
	332	0.585	96
	315	0.61	97
	306	0.595	98
	314	0.575	99
	328	0.605	94
	307	0.62	100
	332	0.585	101
CsCl polymorphic transition	475	0.3	95
	390(?)	0.425(?)	96
	472	0.3	94
	472	0.3	101
	440(?)	0.375(?)	102
Peritectic near 380 °C	380	0.41	95
	381	0.43	102
	382	0.43	94
	382	0.425	101
	372	0.41	100
Peritectic(s) below 380 °C	351	0.5	95
	360	0.47	95
	357	0.465	85
	352	0.515	94
	352	0.5	101
	323(?)	0.515(?)	102

In addition, a LiCl homomorphic transition at 565 °C, $x_B = 0.875$ has been claimed,[94,101] based on small breaks in the liquidus curve. The existence of this transition has been doubted,[1] and there is no confirming evidence.[81]

The composition of the intermediate compounds has been determined by Korreng,[95] from heating curves, microscopic study of solidified melts, and observed temperature arrests during cooling. The peritectic near 380 °C he identified as involving LiCl·2CsCl. Between 380 °C and the eutectic temperature he postulates two peritectics representing another crystalline form of LiCl·2CsCl and CsCl·LiCl. That there is at least one peritectic in this region is corroborated by the unmistakable liquidus discontinuity of Richards and Meldrum,[85] checked by repeated determinations with specially purified CsCl (mp 645 °C). In the present work, the eutectic, CsCl transformation and LiCl·2CsCl peritectic were included as well-established invariant points. Another peritectic for CsCl·LiCl was provisionally included, representing one of other possible invariants of this system. This peritectic is not part of the calculated diagram. It was assigned a temperature of 354 °C which is an average of the reported peritectic temperatures below 380 °C. The compound LiCl·CsCl has been isolated and characterized by x-ray diffraction.[103] Its melting point is not known accurately, and its Gibbs energy of fusion cannot be calculated with sufficient precision from the phase diagram. For these reasons, this compound is not part of the calculated phase diagram; its stoichiometry is indicated in Fig. 14, and a peritectic temperature of 354 °C, an average of the reported temperatures below 380 °C, has been assigned to it.

Korreng[95] observed eutectic and peritectic arrests in the range $0.1 \leqslant x_B \leqslant 0.8$ and found no indication of solid solubility. The limiting slopes of the liquidus curves at either

end[95,96] suggest negligible solid solubility. None was assumed in the present calculations, although there has been no more recent study.

The activity of LiCl in the liquid has been deduced from emf measurements on the liquid[90] at 622 °C. Burylev[104,105] has performed vapor pressure measurements on the melt in the range 929–1148 °C.

The excess enthalpy of the liquid has been measured at 670 °C by Hersh and Kleppa[84] by direct calorimetry. Their result is used here:

$$H^E(l) = x_A x_B(-19\,456 - 7448x_B - 9080x_A x_B)\ \text{J mol}^{-1}. \quad (49)$$

On the basis of this excess enthalpy and the liquidus points of Dergunov,[96] two excess entropy coefficients were calculated:

$$S^E(l) = x_A x_B(-20.541 + 3.285x_B)\ \text{J mol}^{-1}\ \text{K}^{-1}. \quad (50)$$

A phase diagram was calculated with the use of the thermodynamic quantities of Eqs. (49) and (50). The calculated liquidus was everywhere within 10 °C of the experimental.[96] The calculated invariant points are as follows:

	°C	x_B
Eutectic	327	0.584
CsCl transformation	470	0.346
LiCl·2CsCl peritectic	382	0.440
(CsCl·LiCl peritectic)	(354)	(0.535)

The Gibbs energy of fusion of the 2:1 intermediate compound 0.67 (CsCl) 0.33 (LiCl) was calculated to be

$$\Delta_{fus}G^\circ = 16\,340 - 24.519T\ \text{J mol}^{-1}. \quad (51)$$

Probable maximum error in calculated diagram (Fig. 14): ± 10 °C.

KCl(A)+NaCl(B)

The liquidus curve has been investigated many times by methods of cooling curves[50,64,107–110,112,113,118] and temperature of first appearance of crystals.[106,111,114–117] The reported minimum varies between 640 and 670 °C. Most of the values lie near the most recently reported value[118] of 658 °C, at $x_B \approx 0.50$. An exception is the work of Coleman and Lacy,[117]

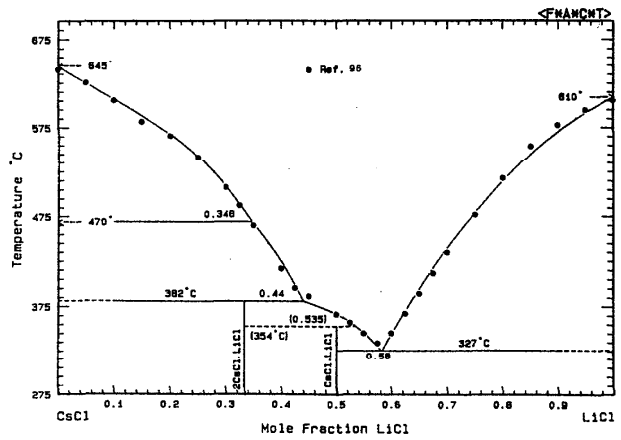

FIG. 14. The system CsCl(A) + LiCl(B).

indicating 645 °C. However this work, performed with a hot-stage microscope, is based on a technique which may be inherently less accurate than thermal analysis.

Points on the solidus curve have been measured by means of thermal analysis,[110,119] optical methods,[113,117] crystal growth analysis,[127] and conductivity.[128] The solidus curves reported by these authors are in poor agreement.

The excess enthalpy of the liquid has been measured at 810 °C by direct calorimetry by Hersh and Kleppa,[84] whose result is used here:

$$H^E(l) = x_A x_B(-2050 - 272x_B)\ \text{J mol}^{-1}. \quad (52)$$

The limits of solid miscibility have been investigated in numerous studies. Most of the earlier work (before 1950) was done by thermal or optical analysis, and the results were not concordant. They indicated a consolute point near 400 °C. An exception is Nacken,[120] who measured refractive indices of solidified melts, and who obtained 495 °C, $x_B = 0.65$. Later investigators[121–124] used x-ray diffraction at room or higher temperatures. Their results are generally concordant within 25 °C over the entire concentration range. The consolute point lies in the range 490 to 502 °C, $x_B = 0.5$ to 0.7. Studies of the kinetics of decomposition of the mixed crystals[125] showed that the approach to equilibrium is slow and may occur in several steps; thus the earlier work may have been in error because measurements were not taken at equilibrium.

The activity of NaCl in the liquid has been deduced from emf measurements by a number of authors[19,20,129–131] covering a temperature range from the liquidus minimum to 885 °C. Activities have also been obtained by mass spectrometry[21] from the liquidus minimum to 810 °C. The vapor pressure of the melt has been measured.[132–135]

The enthalpy of formation of metastable solid solutions, annealed at high temperature and quenched to room temperature, has been measured calorimetrically.[122,126] The results of these two studies agree within 200 J mol^{-1}.

A phase diagram was calculated, based upon Eq. (52) with $S^E(l) = 0$ for the liquid, and Eq. (53) for the solid phase:

$$G^E(s) = x_A x_B(14\,333 + 3278x_B + 32.796T - 5.593T\ln T)\ \text{J mol}^{-1}. \quad (53)$$

From Eq. (53) may be deduced other thermodynamic quantities for the solid state:

$$H^E(s) = x_A x_B(14\,333 + 3278x_B + 5.593T)\ \text{J mol}^{-1}, \quad (54)$$

$$S^E = x_A x_B(-27.203 + 5.593\ln T)\ \text{J K}^{-1}\ \text{mol}^{-1}, \quad (55)$$

$$C_p^E(s) = 5.593x_A x_B\ \text{J K}^{-1}\ \text{mol}^{-1}. \quad (56)$$

Equation (53) was derived from the liquidus points of Pelton *et al.*,[118] the most recent miscibility gap data,[124] and the enthalpy of formation of mixed crystals at room temperature.[122] The calculated liquidus is everywhere with 5 °C of the experimental.[118] The calculated solidus follows closely, but not exactly, the most recent experimental solidus.[117] The calculated minimum is 657 °C, $x_B = 0.506$. The calculated

consolute point is 500 °C, $x_B \approx 0.58$, and the envelope is within 30 °C of the experimental.[124] Equation (54) reproduces the experimental heats of formation at 25 °C[122] within 235 J mol^{-1}.

Probable maximum inaccuracy in calculated liquidus [Fig. 15(a)]: ± 5 °C.

Probable maximum inaccuracy in calculated solidus [Fig. 15(a)]: ± 15 °C.

Probable maximum inaccuracy in calculated consolute temperature (Fig. 15b): ± 20 °C.

NaCl(A)+RbCl(B)

Data defining liquidus and solidus have been tabulated in four studies,[63,88,136,137] obtained from cooling curves[63,88,136] supplemented by visual observation in two[63,88] and from DTA.[137] The reported eutectic data may be summarized as follows:

T/°C	x_B	Ref.
541	0.55	63
550	···	88
550	0.56	136
560	0.55	137
540	0.55	139

The plotted liquidus points of Murgulescu and Sternberg[88] do not allow an unambiguous extrapolated eutectic composition. The later studies[88,136,137] show good agreement in reported melting points of the pure salts (within 2 °C), but Zhemchuzhnui and Rambach[63] report a NaCl melting point 20 °C higher than the other authors. All but one of the liquidus points of Murgulescu and Sternberg[88] fall on or near the curve reported by Pelton and Flengas.[136] The phase diagram of the latest study[136] was therefore chosen as the most accurate to data.

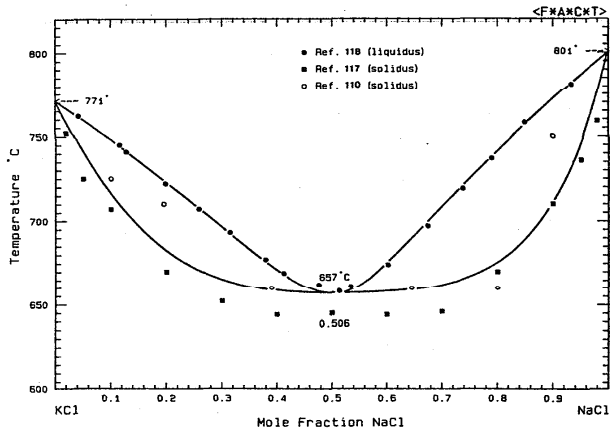

FIG. 15a. The system KCl(A) + NaCl(B), high temperature.

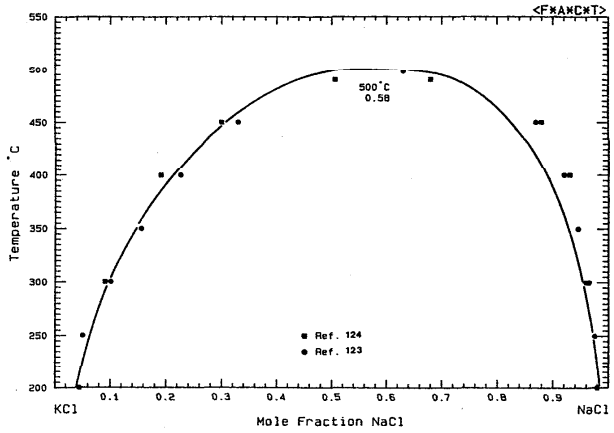

FIG. 15b. The system KCl(A) + NaCl(B), low temperature.

The limits of solid solubility, from temperature arrests, were reported by Zhemchuzhnui and Rambach[63] as $x_B = 0.02$ and 0.95 at the eutectic temperature. These limits were also determined by the method of interdiffusion by Short and Roy,[138] who found $x_B = 0.008$ and 0.94 at 515 °C. Tsubuki *et al.*[139] used x-ray diffraction and say only that there is "negligible" solid solubility. The results from interdiffusion,[138] were taken as a guide for the present calculations.

The activity of NaCl in the liquid has been deduced from emf measurements[19] at 865 °C.

The excess enthalpy of the liquid has been measured by direct calorimetry at 810 °C by Hersh and Kleppa,[84] whose result is used here:

$$H^E(l) = x_A x_B(-3222 - 335x_A)\ \text{J mol}^{-1}. \quad (57)$$

Two solid solution Henrian activity coefficients, relative to the solid standard state, were calculated to reproduce the experimental solubilities[138] at 515 °C. For RbCl in NaCl, this was

$$RT \ln \gamma_B = 31\,027\ \text{J mol}^{-1}, \quad (58)$$

and for NaCl in RbCl

$$RT \ln \gamma_A = 18\,325\ \text{J mol}^{-1}. \quad (59)$$

The values of $RT \ln \gamma$ were assumed to be independent of temperature.

The calculated liquidus, based on the excess enthalpy of Eq. (57) and an excess entropy given by

$$S^E(l) = x_A x_B(-0.677 - 5.245x_B)\ \text{J mol}^{-1}\ \text{K}^{-1}, \quad (60)$$

reproduced the experimental[136] eutectic exactly, and was everywhere within 2 °C of the reported[136] liquidus points. The calculated limits of solid solubility are $x_B = 0.01$ and 0.93 at the eutectic temperature (550 °C), while the values at 515 °C reproduce the experimental ones.[138]

Probable maximum inaccuracy in calculated diagram (Fig. 16): ± 5 °C.

CsCl(A)+NaCl(B)

Data defining the liquidus have been tabulated in three studies,[56,63,88] all of which used the cooling curve method. The system was also examined briefly as a limiting edge of ternary and quaternary systems.[140–142] The reported eutectic data are summarized as follows:

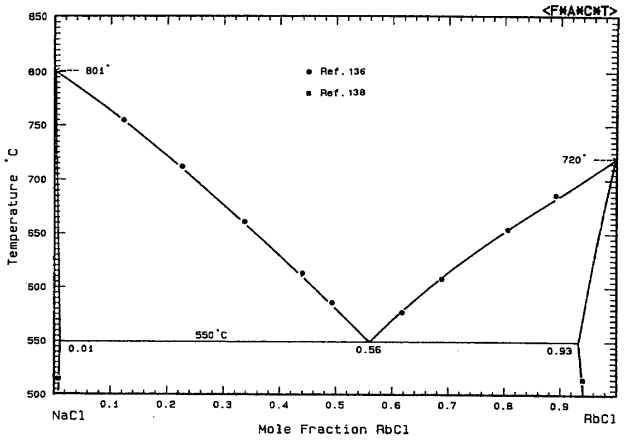

FIG. 16. The system NaCl(A) + RbCl(B).

T/°C	x_B	Ref.
493	0.34	63
490	0.345	56
486	0.35	88
493	0.34	140
494	0.36	141
495	0.34	142
493	0.346	144

In the earliest work,[63] the reported melting point of NaCl is 19 °C higher than the accepted value; also, Samuseva and Plyushchev[56] show a NaCl liquidus with a point of inflection, which is absent in the other reports. For these reasons, the data of the more recent work[88] were adopted for calculation purposes. Activities of NaCl in the liquid were deduced from emf measurements[19] at 880 °C. A eutectic halt was observed[56] in the range $x_B = 0.01$ to 0.99. This result, very low solid solubility, was confirmed by the limiting liquidus slopes of the phase diagram.[88] By an indirect method, Fullam[144] estimated that the solubility of NaCl in CsCl is less than 1 mol %.

The excess enthalpy of the liquid has been measured by Hersh and Kleppa[84] at 810 °C by direct calorimetry, and their results are used here:

$$H^E(l) = x_A x_B(-4310 + 418x_B)\ \text{J mol}^{-1}. \quad (61)$$

With this excess enthalpy, and the chosen phase diagram data,[88] two excess entropy coefficients were calculated:

$$S^E(l) = x_A x_B(-5.764 + 5.901x_B)\ \text{J mol}^{-1}\ \text{K}^{-1}. \quad (62)$$

A phase diagram, calculated with the liquid thermodynamic properties of Eqs. (61) and (62), reproduced all liquidus points[88] within 6 °C, and the eutectic[88] was reproduced exactly.

The cesium chloride solid-state transformation temperature was observed[56,63] from 100% CsCl to 1% CsCl without significant change, although the experimental[56,63] transformation temperature of the pure salt (455 °C) is much lower than the accepted value (470 °C). Weyand[143] has found that equilibrium thermal hysteresis occurs over a 20 to 50 °C range in pure CsCl, an effect which was not noted in earlier work.[56,63] Fullam[144] measured the transformation temperature in the interval $0 \leqslant x_B \leqslant 0.96$ by two independent techniques (DTA and thermal expansion). The transformation temperature is 466 ± 2 °C in the interval $0.01 \leqslant x_B \leqslant 0.96$. In the interval between 0% and 1% NaCl, the temperature is depressed from 474 °C (Fullam's value for pure CsCl) to 466 °C.

Probable maximum inaccuracy in calculated diagram (Fig. 17): $\pm$ 10 °C.

KCl(A)+RbCl(B)

For this system there exist tabulated data for the liquidus and solidus[63] and for the liquidus only.[86] Both studies used the method of cooling curves for the liquidus and solidus. Phase diagrams have been given for both phase boundaries[145] and for the liquidus only.[146,147] All investigations report a continuous solid solution at the liquidus temperature. Of the four reported liquidi, that of Zhemchuzhnyi and Rambach[63] lies highest (wtih a high KCl melting point of 790 °C) and that of Keitel[86] lies lowest (with a liquidus minimum of 715 °C). The others fall between these two. In those cases where both liquidus and solidus are reported,[63,145] the phase boundaries are particularly far apart (up to 15 °C). This behavior is improbable and may be in error. For these reasons, the liquidus reported by Dombrovskaya,[146] read off the published diagram,[147] was used as a guide to the present calculations. X-ray diffraction measurements on the melt cooled to room temperature[148–150] all indicate a single phase.

The excess enthalpy of the liquid has been measured by Hersh and Kleppa[84] at 810 °C by direct calorimetry, and their results are used here:

$$H^E(l) = 84x_A x_B\ \text{J mol}^{-1}. \quad (63)$$

On the assumption that $G^E(l)$ is given by Eq. (63), independent of temperature, and that the solid solution follows regular solution behavior, a phase diagram was calculated using a $G^E(s)$ given by

$$G^E(s) = 1500x_A x_B\ \text{J mol}^{-1}. \quad (64)$$

The calculated liquidus shows the same shape as the adopted reference liquidus,[146] with allowance for the difference in melting point of RbCl. The solidus is everywhere within 5 °C of the liquidus, and there is no minimum. In agreement with experiment, the calculated consolute point for solid–solid separation is below room temperature($-$ 184 °C).

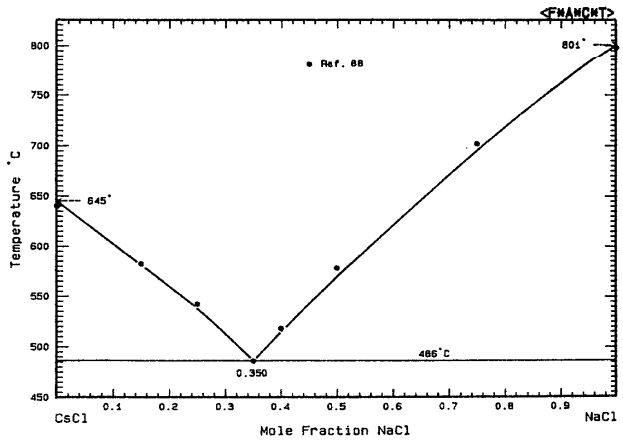

FIG. 17. The system CsCl(A) + NaCl(B).

Probable maximum inaccuracy in calculated diagram (Fig. 18): ± 10 °C.

CsCl(A)+KCl(B)

Data defining the liquidus have been tabulated in five studies,[63,86,151–153] in all of which thermal analysis was used. All report complete solid solubility at the liquidus temperature. Data for the minimum may be summarized as follows:

T/°C	x_B	Ref.
616	0.34	63
610	0.30	86
616	0.30	151
600	0.34	152
606	0.36	153
610	0.30	154
605	0.349	144

The most extensive study is the oldest,[63] but the reported KCl melting point is 20 °C higher than the accepted value. Keitel's[86] melting point of CsCl is 15 °C below the accepted value. The reported liquidus curves[63,86,151–153] differ by as much as 20 °C from each other. For these reasons, and also since the later work[152,153] includes only sparse data points, Dombrovskaya's[151] liquidus was chosen as a guide for present calculations. The melting points of the pure components in the chosen work[151] agreed well with the accepted values. Points at 0.1-mole fraction intervals were read off the smooth curve of the published phase diagram.[155]

Data for the solidus have been observed from the temperature of completed crystallization.[63,86] The data of the two studies agreed within 15 °C. The data of Ref. 63 are shown on the diagram because they are more numerous, and because they are probably more accurate in the region of the minimum.

The excess enthalpy of the liquid has been measured by direct calorimetry at 810 °C by Hersh and Kleppa,[84] and their results are used here:

$$H^E(l) = 795 x_A x_B \text{ J mol}^{-1}. \quad (65)$$

A phase diagram was calculated, based upon a $G^E(l)$ given by Eq. (65), independent of temperature, and a $G^E(s)$ given by Eq. (66):

$$G^E(s) = x_A x_B (5957 + 6044 x_B) \text{ J mol}^{-1}, \quad (66)$$

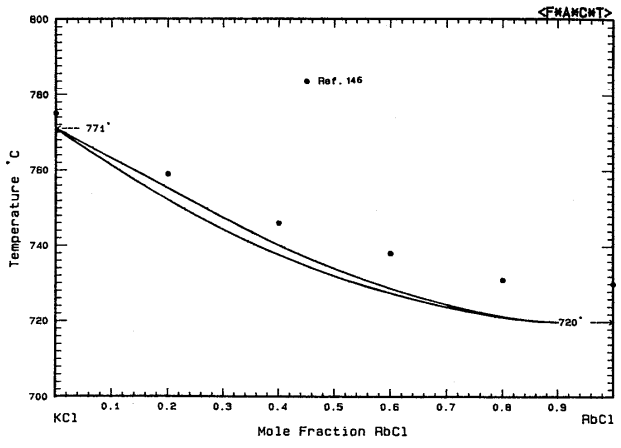

FIG. 18. The system KCl(A) + RbCl(B).

also assumed temperature independent. The calculated liquidus was everywhere within 7 °C of the experimental,[151] and the calculated minimum is 615 °C, $x_B = 0.36$. The two-phase region on the KCl side of the calculated phase diagram is considerably wider than the experimental.[63,86] Although both experimental solidi are closer to each other than to the calculated curve, the experimental method used—cooling curves—is not the best suited for solidus determination.

The earlier work[63,86] obtained a few points for the (α-β) CsCl phase transformation temperature in the range $0 \leqslant x_B \leqslant 0.15$. These were obtained from cooling curves[63] or by heating curves and crystallographic study of thin sections.[86] Later measurements used high-temperature x-ray diffractometry,[143,158,318] DTA and heating and quenching techniques,[144,156,318] thermal expansion,[144] and ionic conductivity.[159,161] All reports indicate that KCl depresses the CsCl transition temperature, but the extent of lowering varies considerably. At 2% KCl, the earlier work indicated a temperature between 440 and 450 °C[63,86]; in the later, 315 °C.[143] This great difference may be partly accounted for by the 20–30°C difference between the observed transition temperatures of pure CsCl[63,86,144,156,159,161,318] and partly by the fact that there is a 20–50 °C hysteresis effect in pure CsCl, which is increased by addition of KCl. The calculated CsCl transformation curve was based on the assumption of zero solubility of KCl in α-CsCl. This assumption may not be valid, as Tsubuki *et al.*[157] present a complete solid–solid phase diagram (in sketch form only) showing appreciable KCl solubility, and a miscibility gap in the β-CsCl + KCl region. The presence of a miscibility gap was confirmed by Weyand,[143] who reported a consolute temperature of 470 °C. If the α-CsCl phase is suppressed in the calculated diagram, the consolute temperature for β-CsCl + KCl solid is 360 °C. Shukla *et al.*[160] have measured the heat of formation of solid solutions at 25 °C calorimetrically.

Probable maximum inaccuracy in calculated liquidus (Fig. 19): ± 15 °C.

Probable maximum inaccuracy in calculated solidus (Fig. 19): ± 20 °C.

CsCl(A)+RbCl(B)

Data for the liquidus and solidus of this system have been tabulated in three studies,[63,86,162] obtained from cooling curves in all cases. All three report an unbroken series of solid solutions. The melting point of RbCl as reported by[63] is 6 °C higher than the accepted value, while that reported by Ref. 162 is 6 °C lower. For both liquidus and solidus, the data points of the three studies differ by as much as 10 °C. A temperature minimum is indicated (on the CsCl side) in two reports[63,162] but none in the third.[86] The existence of a minimum is problematical, since Keitel[86] reports a CsCl melting point 13 °C below the other investigators, and Wood *et al.*[162] show a minimum for which liquidus and solidus are separated by 9 °C, which is an impossible construction. All three reports show a liquidus–solidus separation of up to 10 °C, which in comparison with other systems of this type, is improbable. In view of these uncertainties, it was decided to take the liquidus of Wood *et al.*[162] as a guide for present calculations.

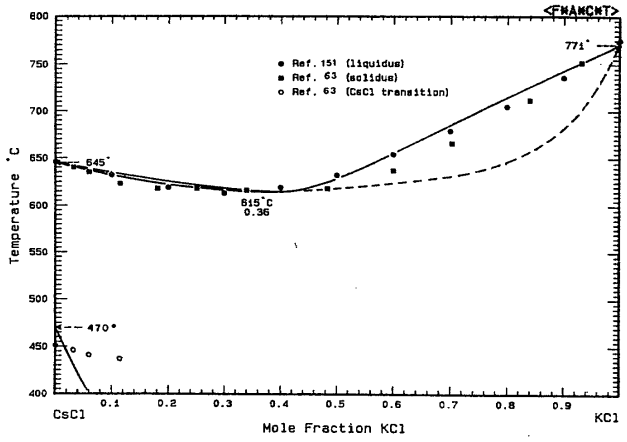

FIG. 19. The system CsCl(A) + KCl(B).

The excess enthalpy of the liquid has been measured at 810 °C by direct calorimetry by Hersh and Kleppa,[84] whose result is used here:

$$H^{E}(l) = 335 x_A x_B \text{ J mol}^{-1}. \quad (67)$$

On the assumption that both liquid and solid solutions are regular, and that the excess Gibbs energy of both phases is independent of temperature, a phase diagram was calculated in which $G^{E}(l)$ is given by Eq. (67) and $G^{E}(s)$ by Eq. (68):

$$G^{E}(s) = 2500 x_A x_B \text{ J mol}^{-1}. \quad (68)$$

The calculated phase diagram, as shown in Fig. 20, has a shallow minimum, but the existence of this minimum cannot be taken as established. It is sensitive to the solid solution thermodynamic parameter in Eq. (68), and as mentioned earlier, the experimental diagrams[63,86,162] are ambiguous in this respect.

The cesium chloride transition temperature in this system has been studied by thermal analysis[63,86,143,156] and by x-ray diffraction above room temperature.[143,162,163] Arends *et al.*[159,161] used ionic conductivity. All investigators indicate that the transformation temperature is depressed by RbCl but the extent of lowering differs in these studies. At $x_B = 0.14$, the reported temperatures are 425, 375, 310, and 260 °C.[63,143,162,163] Part of this difference may be due to the presence of a large thermal hysteresis effect of 20 to 50 °C, which is increased by the addition of RbCl. The enthalpy of formation of solid solution at room temperature has been measured calorimetrically.[160,165,166] The solid state at room temperature has also been examined by x-ray diffraction,[167,169] and the two-phase miscibility limits have been determined from the aqueous solubility isotherm and radioactive tracer analysis.[168,169] Makarov and Vlasov[168] estimated the excess Gibbs energy in the miscible regions of solid solution at room temperature from the activity coefficients of the salts in saturated and unsaturated aqueous solutions, with the use of the McKay–Perring method.[229]

The CsCl transformation temperature curve was calculated on the basis of a $G^{E}(s)$ given by Eq. (68) for the β-CsCl + RbCl region, and zero solid solubility of RbCl in α-CsCl. The curve shown in the figure, is suggestive only. Its slope depends on the factors already mentioned, and also on the assumed enthalpy of transition, here taken as 3766 J mol^{-1}; the experimental values lie however in the range 2.4 to 7.5 kJ mol^{-1}.[164] In any case, Weyand[143] reports appreciable solubility of RbCl in α-CsCl, as well as a solid–solid miscibility gap in the β-phase with a consolute temperature of about 470 °C. The consolute temperature for the β-phase calculated from Eq. (68) is − 123 °C. The result of Weyand is thus very doubtful.

Probable maximum inaccuracy in calculated liquidus (Fig. 20): ± 10 °C.

Probable maximum inaccuracy in calculated solidus (Fig. 20): ± 15 °C.

c. Bromides

LiBr(A)+NaBr(B)

Data defining the liquidus have been tabulated in two studies,[68,170] the first by cooling curves and the second by the visual-polythermal method. There is confusion in accounts of this system, as to whether it is one with continuous solid solutions, or whether it is one of the eutectic type with intermediate compounds. The limiting slopes of the experimental liquidi[68,170] indicate extensive solid solubility at both extremes. The reported minimum and invariant points are summarized in Table 4.

Data defining the solidus have been tabulated in the oldest study,[170] found from the temperature of complete crystallization. The same method was used in a later study (Ref. 173, data not tabulated). Kellner[170] used microscopic examination of thin sections, and Bugaenko *et al.*[173] used x-ray diffraction on cooled solid samples. Both groups concluded that there was continuous solid solution at high temperature. Kellner[170] reported the solid solutions to be stable down to room temperature, but suggested this was due to supercooling. Bugaenko *et al.*[173] found that the solid solutions had demixed at room temperature. Confirmatory x-ray evidence for continuous solid solutions was presented in a later report.[174] Tamman and Ruppelt[175] observed turbidity and translucence of solidified melts during slow cooling and heating. The change in optical properties took place over a considerable temperature range at a given composition, but approximate co-ordinates of the consolute point may be deduced from their data: $x_B = 0.4$, 155 to 265 °C. The bound-

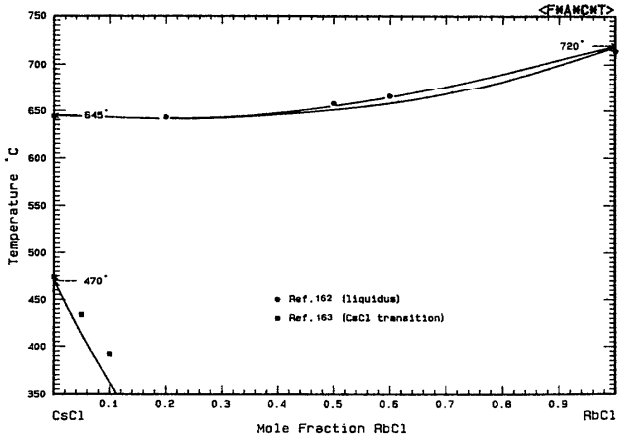

FIG. 20. The system CsCl(A) + RbCl(B).

TABLE 4. Reported minima and invariant points of the system LiBr(A) + NaBr(B)

	T/°C	x_B	Ref.
Minimum	524	0.2	170
	514	0.21	171
	510	···	172
Eutectic	510	0.2	173
Peritectics	512	0.29	68
	516	0.28	173
	537	0.405	68
	543	0.37	173

ary of the demixing region has been better defined by the x-ray diffraction measurements of Oonk *et al.*[176] Their measurements cover the temperature range 80–229 °C; they quote a consolute temperature of 240 °C.

In summary, those investigators who attempted to determine the solidus[170,173] found complete solid solubility. Some who determined the liquidus found breaks which suggested peritectics,[68,171–173] but there is no other confirmatory evidence to date for intermediate compounds. The phase diagram presented in the latest work[173] shows a liquidus with sharp minimum and two breaks, but coupled to a smooth solidus representing continuous solid solution. This is an impossible construction. It was decided, for the present study, that it would be reasonable to treat the system as one of continuous solid solution at high temperature.

The excess enthalpy of the liquid has been measured at 690 °C in solid–liquid calorimetric mixing experiments by Hersh and Kleppa,[84] and their result is used here:

$$H^E(l) = x_A x_B(-2971 - 586x_A)\ \text{J mol}^{-1}. \quad (69)$$

A phase diagram was calculated, based on an excess Gibbs energy of the liquid given by Eq. (69), and of the solid by Eq. (70):

$$G^E(s) = x_A x_B[9617 - 1.374T + x_B(2150 - 4.662T)]\ \text{J mol}^{-1}. \quad (70)$$

$H^E(l)$ was assumed to be independent of temperature. The calculated liquidus closely follows the experimental liquidus points of Ref. (68) on the NaBr side of the minimum and lies between the values of Ref. 68 and Ref. 170 on the LiBr side. The calculated minimum is 510 °C, $x_B = 0.26$. The calculated solidus–liquidus separation is greater than that shown in experiment[170,173] and cannot be taken as veridical. The calculated consolute point for solid demixing is 246 °C; both this datum and the calculated solid–solid phase boundary agree well with experiment.[176]

Probable maximum inaccuracy in calculated liquidus [Fig. 21(a)]: ± 15 °C.

Probable maximum inaccuracy in calculated solidus [Fig. 21(a)]: ± 40 °C.

Probable maximum inaccuracy in calculated consolute temperature (Fig. 21b): ± 20 °C.

KBr(A)+LiBr(B)

Data defining the liquidus have been reported in four independent studies.[33,170,177,178] Only in the oldest work[170] are there tabulated data. The investigation of Aukrust *et al.*[33] appears to be the most carefully done; data points, read off their published diagram were used in the present calculations. Kellner[170] obtained heating and cooling curves, and Aukrust *et al.*[33] performed cooling curve experiments. The following is a summary of the reported eutectic data:

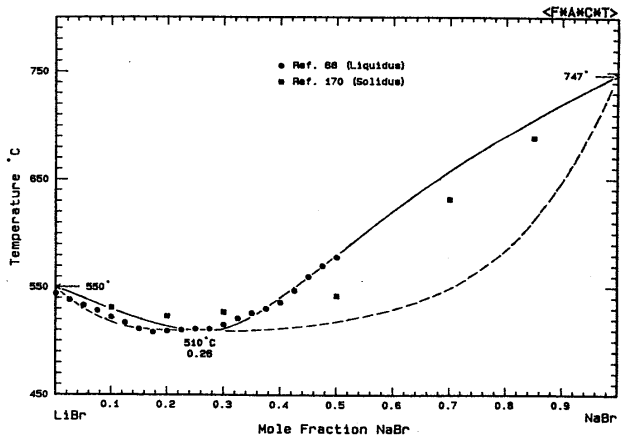

FIG. 21a. The system LiBr(A) + NaBr(B), high temperature.

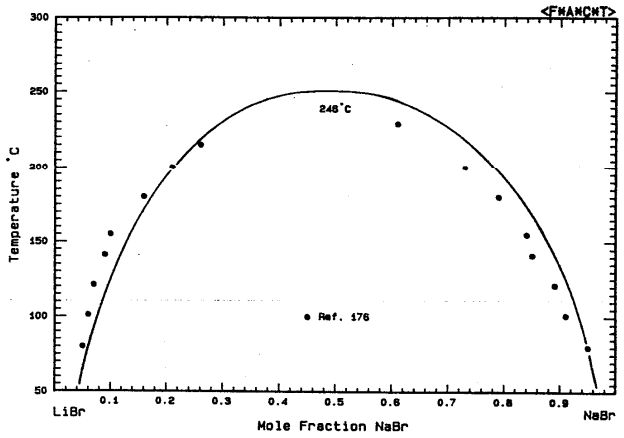

FIG. 21b. The system LiBr(A) + NaBr(B), low temperature.

T/°C	x_B	Ref.
348	0.60	170
320	0.68	177
328	0.60	33
330	0.60	178
318	0.60	179
318	0.605	180
318	0.60	181
325	0.615	171
334	0.62	182
334	0.61	183

Kellner[170] observed a eutectic arrest in the range $0.05 \leqslant x_B \leqslant 0.95$, and Aukrust *et al.*[33] used a radioactive tracer technique for detecting solid solubility. The later work[33] revealed no solid solubility, within experimental error. The limiting slopes of the experimental liquidus[33] confirm this finding.

The excess enthalpy of the liquid has been measured by direct calorimetry at 745 °C by Hersh and Kleppa,[84] whose result is used here:

$$H^E(1) = x_A x_B(-13\,222 - 1757x_B - 1967x_A x_B)\ \text{J mol}^{-1}. \quad (71)$$

With the use of this excess enthalpy, two excess entropy coefficients were calculated:

$$S^E(1) = x_A x_B(0.378 - 3.638x_B)\ \text{J mol}^{-1}\,\text{K}^{-1}, \quad (72)$$

which enabled the experimental diagram[33] to be reproduced within 5° over the entire composition range. The eutectic, 328 °C and $x_B = 0.60$ is reproduced exactly.

Probable maximum inaccuracy in calculated diagram (Fig. 22): ± 5 °C.

LiBr(A)+RbBr(B)

Data defining the liquidus have been reported in two studies,[70,184] both obtained by thermal analysis. The earlier data[70] were tabulated but the later were not, so they were read off the published diagram.[184] The melting points of the pure components as reported in the earlier work[70] are both much lower than accepted values (LiBr, by 23 °C; RbBr, by 14 °C). The two reported liquidus curves differ by as much as 48 °C, although the invariant points reported in these two studies are in good agreement. Other determinations[185,186] of the invariant points are not in good agreement with respect to temperature, as seen in Table 5.

In neither work[70,184] were second temperature arrests recorded outside the range $0.2 \leqslant x_B \leqslant 0.7$, so that solid solubility limits are experimentally undefined. On the LiBr side, the limiting liquidus slopes of both studies suggest no or very little solid solubility, and none was assumed in the present calculations. On the RbBr side, the liquidus points of Flor *et al.*[184] are all consistently above those of Gromakov and Gromakova.[70] The pronounced curvature of the liquidus of Ref. 184 suggests the presence of solid solubility. Since, however, the reported invariant points of the two studies are in remarkably good agreement, the assumption of significant solid solubility cannot be justified on these considerations alone. Consequently, zero solid solubility was assumed at the RbBr side also.

There are no independent determinations of the stoichiometry of the compound, which is assumed in the literature[70,184–186] to be 1:1. This stoichiometry was nominally assumed in the present calculations.

TABLE 5. Reported invariant points of the system LiBr(A) + RbBr(B)

	T/°C	x_B	Ref.
Eutectic	259	0.41	70
	258	0.40	184
	280	0.42	185
	287	0.405	186
Peritectic	271	0.45	70
	273	0.45	184
	290	0.47	185
	300	0.46	186

The excess enthalpy of the liquid has been measured by direct calorimetry at 700 °C by Hersh and Kleppa,[84] whose result is used here:

$$H^E(1) = x_A x_B(-16\,067 - 4018x_A - 4686x_A x_B)\ \text{J mol}^{-1}. \quad (73)$$

A phase diagram was calculated, based on the $H^E(1)$ of Eq. (73), assumed independent of temperature. The calculated invariant points are the following: eutectic, 260 °C, $x_B = 0.411$; peritectic, 272 °C, $x_B = 0.453$. The calculated liquidus follows the experimental points[70,184] closely on the LiBr side. On the RbBr side the calculated liquidus is closer to the points of Ref. 70, suggesting that on this side of the diagram, the results of Flor *et al.* may be in error.

The calculated Gibbs energy of fusion of the compound, of nominal 1:1 stoichiometry 0.5(LiBr·RbBr), is

$$\Delta_{fus}G^\circ = 10\,176 - 18.550T\ \text{J/mol}. \quad (74)$$

Probable maximum inaccuracy in calculated diagram (Fig. 23): ± 30 °C.

CsBr(A)+LiBr(B)

Data defining the liquidus have been tabulated in two studies[97,187] by thermal analysis and visual-polythermal methods, respectively. In both investigations there is a definite break in the liquidus indicating a peritectic, ascribed to the 1:1 compound, although there is no independent confirmation of this stoichiometry. A summary of the reported invariant points is as follows:

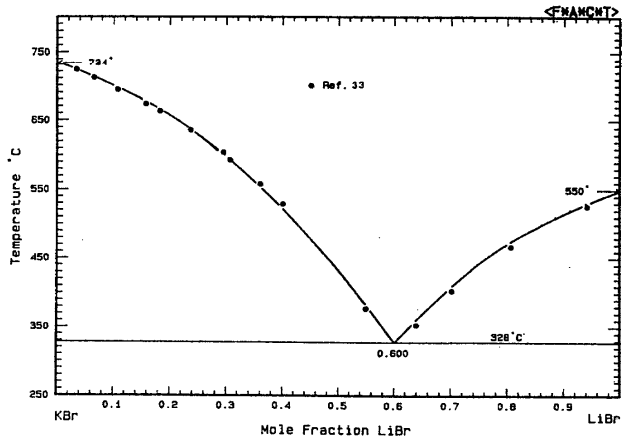

FIG. 22. The system KBr(A) + LiBr(B).

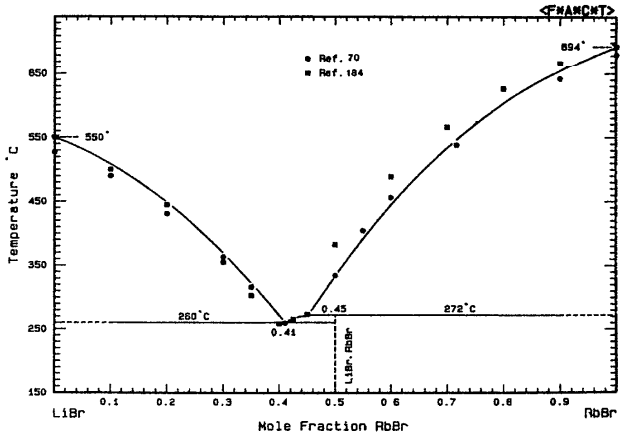

FIG. 23. The system LiBr(A) + RbBr(B).

	T/°C	x_B	Ref.
Eutectic	262	0.625	187
	276	0.635	97
	230	0.485	188
Peritectic	300	0.55	187
	313	0.5	97

Eutectic and peritectic halts were observed in the earlier work[187] in the range $0.05 \leqslant x_B \leqslant 0.95$, indicating little, if any solid solubility. The limiting slopes of the liquidus[97,187] at either end suggest no solid solubility, and hence none was assumed in the present calculations.

The excess enthalpy of the liquid has been measured by direct calorimetry at 700 °C by Hersh and Kleppa,[84] whose result is used here:

$$H^E(l) = x_A x_B(-18\,661 - 6485x_A - 3891x_A x_B)\ \text{J mol}^{-1}. \quad (75)$$

Three excess entropy coefficients were calculated, based on all the liquidus points of Il'yasov *et al.*, on those of Plyushchev and Samuseva[187] in the range $0 < x_B \leqslant 0.3$ and Eq. (75):

$$S^E(l) = x_A x_B(-15.171 + 7.010x_B + 15.051x_B^2)\ \text{J mol}^{-1}\,\text{K}^{-1}. \quad (76)$$

A phase diagram was calculated, based on Eqs. (75) and (76). The calculated liquidus lies within 8 °C of the experimental,[97] except near the LiBr extreme, where the difference between the reported data points of Refs. 97 and 187 diverge somewhat. The calculated invariant points are the following: eutectic 274 °C, $x_B = 0.613$; peritectic 311 °C, $x_B = 0.510$. The calculated Gibbs energy of fusion of the intermediate compound, of nominal 1:1 stoichiometry 0.5(LiBr·CsBr), is

$$\Delta_{fus}G^\circ = 11\,559 - 19.802T\ \text{J/mol}. \quad (77)$$

Probable maximum inaccuracy in calculated diagram (Fig. 24): ± 15 °C.

KBr(A)+NaBr(B)

Data defining the liquidus have been tabulated in three studies,[50,51,189] obtained from cooling curves[50,189] and the visual-polythermal method.[51] The reported melting points of pure components in the earliest work[50] are much higher (KBr, 23 °C; NaBr, 21 °C) than accepted values; those in the later work[51,189] are closer to the accepted. The liquidus of Ref. 51 lies consistently lower than those of Refs. 50 and 189. A summary of the reported values for the minimum is as follows:

T/°C	x_B	Ref.
643	0.54	50
626	0.50	51
644	0.46	189
630	···	190
638	0.5	191,192

Points defining the solidus were obtained in one study only[189] from cooling curves. All three investigations[50,51,189] indicated continuous solid solutions at the liquidus temperature.

The excess enthalpy of the liquid has been measured by direct calorimetry in two laboratories[193,84] at 860 and 770 °C, respectively. The results agree within 65 J mol^{-1}, but since the data of Hersh and Kleppa are both more numerous and cover a wider composition range, they are used here:

$$H^E(l) = x_A x_B(-2134 - 251x_B)\ \text{J mol}^{-1}. \quad (78)$$

The activity of NaBr in the liquid at 800 °C has been deduced from emf measurements.[195] The solid–solid miscibility gap has been investigated in two studies.[175,194] In the earlier work[175] the optical transmission was followed during heating and cooling; the other used x-ray diffraction. In the optical experiments, changes in transmission occurred over a wide temperature range (150–200 °C) at a given composition, and so the curve cannot be located precisely from these data. It is significant, however, that the highest temperature reported in this work was 395 °C at $x_B \sim 0.5$. The x-ray method[194] yielded a consolute point of 395 °C, $x_B = 0.65$.

The heat of formation of solid solutions, formed at high temperature and quenched to 25 °C, has been measured calorimetrically.[126] A phase diagram was calculated, based on the excess enthalpy of the liquid (assumed independent of temperature) given by Eq. (78), the liquidus of Bellanca,[189] the heats of formation of solid solution at 25 °C [126] and the assumption that the solid solution is regular over the experimental temperature range. The expression for the excess Gibbs energy of the solid is

$$G^E(s) = x_A x_B(11\,004 + 78.782T - 12.088T\ln T)\ \text{J mol}^{-1}. \quad (79)$$

Other thermodynamic properties may be deduced from Eq. (79):

$$H^E(s) = x_A x_B(11\,004 + 12.088T)\ \text{J mol}^{-1}, \quad (80)$$

$$S^E(s) = x_A x_B(-66.694 + 12.088\ln T)\ \text{J mol}^{-1}\,\text{K}^{-1}, \quad (81)$$

$$C_p^E(s) = 12.088x_A x_B\ \text{J mol}^{-1}\,\text{K}^{-1}. \quad (82)$$

The calculated minimum is 644 °C, $x_B = 0.49$, and Bellanca's liquidus is reproduced within 5° (one point is anomalous). The calculated consolute point for solid miscibility is 394 °C, $x_B = 0.48$. The experimental[126] heats of formation of solid solution at 25° are reproduced within an rms deviation

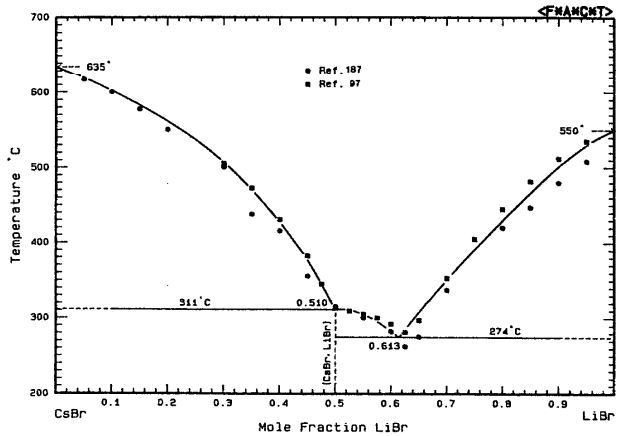

FIG. 24. The system CsBr(A) + LiBr(B).

of 175 J mol^{-1}. The miscibility gap envelope, as calculated, is symmetrical rather than skewed, as reported in one study.[194] Thermodynamic analysis revealed that the solid solution is regular both at the liquidus temperature and at 25 °C; it was assumed, as a reasonable approximation, that it is also regular at intermediate temperatures, e.g., in the region of the consolute point. The earlier determination of the envelope,[175] though apparently less precise, suggests that the envelope is more symmetrical than skewed.

Probable maximum inaccuracy of calculated liquidus (Fig. 25): ± 10 °C.

Probable maximum inaccuracy of calculated solidus (Fig. 25): ± 20 °C.

Probable maximum inaccuracy of calculated consolute temperature (Fig. 25): ± 30 °C.

NaBr(A)+RbBr(B)

Data defining the liquidus have been tabulated in two reports,[70,196] both obtained from thermal analysis. The liquidi of these two studies agree within 10 °C. The reported pure component melting points in both studies differ from accepted values (NaBr, 7 °C high; RbBr, 14 °C low). A summary of reported eutectic coordinates is as follows:

T/°C	x_B	Ref.
495	0.535	70
495	0.55	196
494	0.5	197
507	0.5	198

Samuseva and Plyushchev[196] observed the eutectic temperature arrest in the interval $0.05 \leqslant x_B \leqslant 0.95$. The limiting slopes of the experimental liquidi[70,196] do not indicate appreciable solid solubility, and none was assumed in the present calculations.

The excess enthalpy of the liquid has been determined by direct calorimetry at 770 °C by Hersh and Kleppa,[84] and their result is used here:

$$H^E(l) = x_A x_B(-3452 - 460x_A) \text{ J mol}^{-1}. \quad (83)$$

A phase diagram was calculated, based on the excess enthalpy of Eq. (83), assumed independent of temperature. The calculated liquidus agrees with experiment,[70,196] with due allowance for differences in pure component melting points and some experimental scatter on the NaBr side.

Probable maximum inaccuracy in calculated diagram (Fig. 26): ± 10 °C.

CsBr(A)+NaBr(B)

Data defining the liquidus have been tabulated in one study[199] obtained from thermal analysis (heating and cooling curves). The data points, though numerous, are rather scattered. The authors report this system as a simple eutectic (460 °C, $x_B = 0.375$). A later determination of the eutectic[200,201] yielded a somewhat different result (482 °C, $x_B = 0.43$). Samuseva and Plyushchev[199] observed eutectic halts in the range $0.02 \leqslant x_B \leqslant 0.99$, indicating essentially zero solid solubility. This result is supported by the results of zone melting experiments.[202] Because of scatter in the data, the limiting slopes of the experimental liquidus[199] are consistent with, but do not confirm, zero solid solubility. None was assumed in the present calculations.

Bokarev and Parshukov[203] carried out an x-ray diffraction and DTA examination of a 1:1 mixture of the components. They deduced the presence of a new crystalline phase above 450 °C; However, their DTA traces are consistent with a simple eutectic system and their results are not detailed enough to warrant consideration of a new phase.

The excess enthalpy of the liquid has been measured by direct calorimetry at 770 °C by Hersh and Kleppa,[84] whose result is used here:

$$H^E(l) = x_A x_B(-4728 - 209x_B) \text{ J mol}^{-1}. \quad (84)$$

A phase diagram was calculated, based on Eq. (84) representing the excess Gibbs energy of the liquid, independent of temperature. The calculated eutectic is 466 °C, $x_B = 0.413$, which is intermediate between the two experimental results.[199,201]

Probable maximum inaccuracy in calculated diagram (Fig. 27): ± 20 °C.

KBr(A)+RbBr(B)

Data defining the liquidus have been tabulated in two studies,[70,204] by thermal analysis[70] and the visual-polythermal method.[204] A shallow minimum near the RbBr extreme was found in both cases. The following is a summary of the

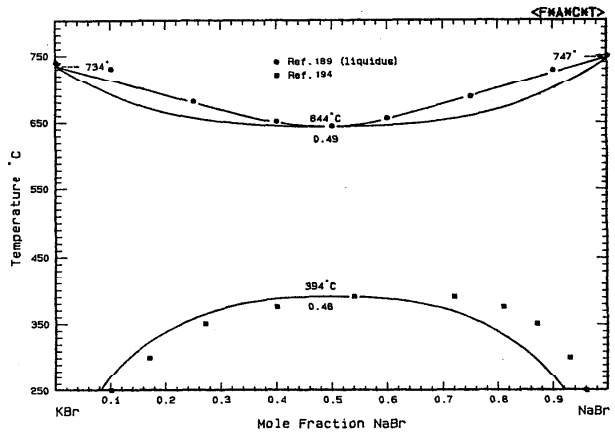

FIG. 25. The system KBr(A) + NaBr(B).

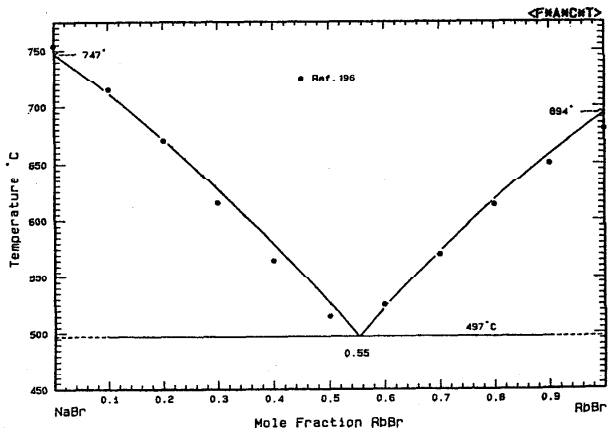

FIG. 26. The system NaBr(A) + RbBr(B).

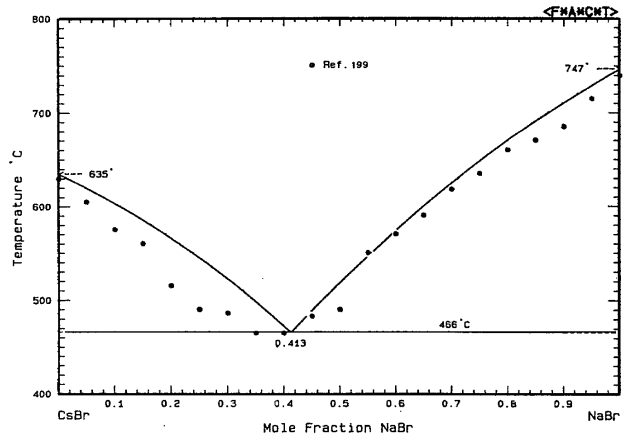

FIG. 27. The system CsBr(A) + NaBr(B).

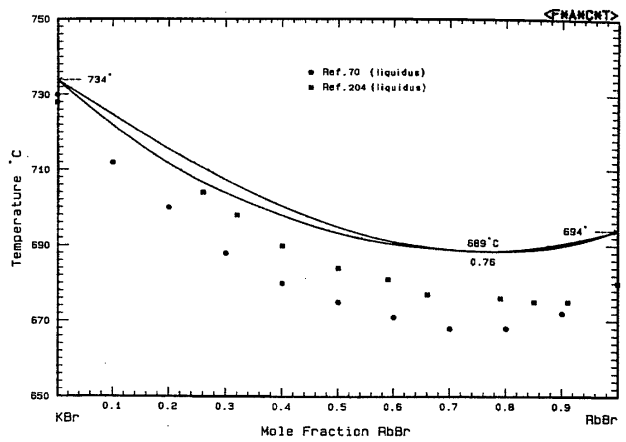

FIG. 28. The system KBr(A) + RbBr(B).

reported data for the minimum and authors' melting points for RbBr.

T/°C	x_B	Ref.	mp RbBr °C
668	0.8	70	680
675	0.85	204	680
673	0.91	205	682
686	0.6–0.95	198	690

There are no reported determinations of the solidus.

The excess enthalpy of the liquid has been measured by direct calorimetry at 770 °C by Hersh and Kleppa,[84] whose result is used here:

$$H^E(1) = 0. \quad (85)$$

Solid solutions have been examined at 25 °C by x-ray diffraction at the 1:1 composition[149] and over the entire composition range,[206] and both studies indicate complete solid solubility at this temperature.

A phase diagram was calculated, based on Eq. (85) and the assumption that the solid is regular. The calculated diagram shown in the figure was derived with the use of Eq. (86) in order to reproduce the shape of the reported[204] liquidus:

$$G^E(s) = 2000 x_A x_B \text{ J mol}^{-1}. \quad (86)$$

The calculated minimum is 689 °C, $x_B = 0.76$. The minimum is very shallow and close to the RbBr extreme, for whose melting point reported values differ significantly. For this reason the depth and position of the minimum cannot be determined with more precision than the discrepancy in the RbBr melting point. The calculated consolute temperature for solid demixing is − 153 °C, which is consistent with experiment.[149,206]

Probable maximum inaccuracy in calculated diagram (Fig. 28): ± 15 °C.

CsBr(A)+KBr(B)

Data defining the liquids have been tabulated in two studies[187,207] from thermal analysis and visual-polythermal methods, respectively. Points on the solidus also were determined by Plyushchev and Samuseva[187] by thermal analysis. All investigators describe this system as one with a minimum liquidus temperature and continuous solid solution. Data for the minimum liquidus temperature are summarized.

T/°C	x_B	Ref.
575	~0.4	187
586	0.35	207
570	0.35	185

In Ref. 187 the liquidus and solidus are reported to be 11 °C apart at the minimum, which is an impossible construction. The liquidus data of Ref. 207 are less scattered than those of Ref. 187 at the minimum, but the corresponding minimum temperatures are 11 °C apart.

A third temperature arrest was observed[187] at 356 ± 6 °C over the composition range $0.05 \leqslant x_B \leqslant 0.97$. This temperature arrest is ascribed[187] to demixing of solid solutions. This ascription is unlikely to be correct, since the phase envelope is essentially isothermal over most of the composition range. These authors[187] also examined solid solutions at room temperature by x-ray diffraction, and observed only pure components. Bokarev and Parshkov[203] performed DTA and x-ray studies on the solid at the 1:1 composition. They conclude that solid solutions based on CsBr undergo a phase transformation similar to CsCl. There is, however, no evidence for a phase transition of CsBr itself.[81] The solid state of this system has thus not been well characterized from experiment.

It has been pointed out only very recently[203] that solid CsBr and KBr have different crystal structures in the temperature range of the phase diagram (KBr, Fm3m and CsBr, Pm3m). This implies that there should be a region of solid–solid immiscibility, since the transition temperature at 1 atm of KBr has not been observed,[81] and that of CsBr is estimated to be above the melting point.[81,161] For calculating the phase diagram therefore, it was decided to treat the system as one having a eutectic and two solid phases. The CsBr-based (α) solid phase is treated as a Henrian solution. The KBr-based (β) solid phase is treated as a regular solution, with the use of the following expression for the Gibbs energy of the hypothetical Pm3m → Fm3m transition of CsBr:

$$\Delta G_{tr} = 4483 - 3.89T \text{ J mol}^{-1}. \quad (87)$$

This expression incorporates the extrapolated transforma-

tion temperature of 880 °C.[161] The enthalpy of transition, 4483 J mol^{-1}, was obtained by the present authors in the evaluation of the CsCl–CsBr system (see section on this system).

The excess enthalpy of the liquid has been measured at 770 °C by direct calorimetry by Hersh and Kleppa,[84] whose result is used here:

$$H^{E}(l) = 377 x_A x_B \text{ J mol}^{-1}. \quad (88)$$

For the α-solid phase, a Henrian activity coefficient for KBr in CsBr at the eutectic temperature given by

$$RT \ln \gamma_B = 8000 \text{ J mol}^{-1}, \quad (89)$$

was used. For the β-phase, the expression:

$$G^{E}(s,\beta) = 9000 x_A x_B \text{ J mol}^{-1}, \quad (90)$$

was used. Both quantities were assumed independent of temperature. The phase diagram, calculated with Eqs. (87)–(90), shows a calculated eutectic at 571 °C, $x_B = 0.400$. The calculated limits of solid solubility at the eutectic temperature are $x_B = 0.228$ and 0.591. The calculated eutectic temperature is closer to the low minimum observed temperature[185,187] rather than the high.[207] The calculated limits of solid solubility are suggestive only, and were chosen to approximate the observed solidus points[187] in the range $0.2 \leqslant x_B \leqslant 0.6$. The calculated solidus and solid–solid phase boundary are to be regarded as tentative only, since the question of the location of the solid miscibility gap and the existence of two solid phases has not been resolved.

Probable maximum inaccuracy in calculated liquidus (Fig. 29): ± 10 °C.

CsBr(A)+RbBr(B)

Data defining the liquidus have been tabulated in two studies[187,208] with the use of thermal analysis and visual-polythermal methods, respectively. Thermal analysis (heating curves) was also used[187] to obtain data for the solidus. The system is described by all investigators[187,202,208–211] as one with a minimum liquidus temperature and continuous solid solution. Data for the minimum are summarized as follows:

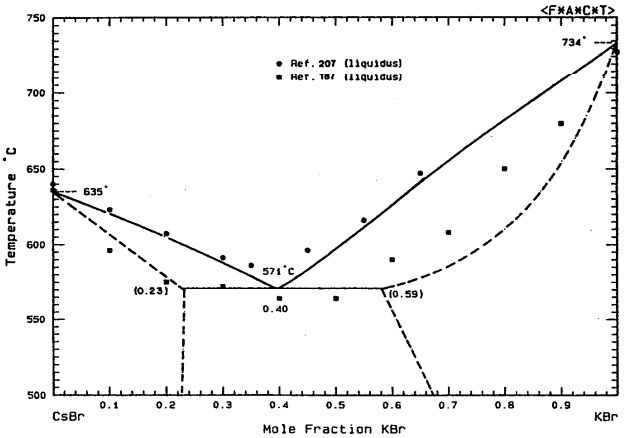

FIG. 29. The system CsBr(A) + KBr(B).

T/°C	x_B	Ref.
594	0.15	187
627	···	208
···	0.45	202
593	0.25	209
594	0.15	210
600	0.2	211

The liquidus data points of Ref. 187 show appreciable scatter, particularly near the minimum, where the curve is shown to be cuspate; this fact is inconsistent with the presence of a minimum, where the slope of the liquidus is zero. The solidus and liquidus in Ref. 187 are separated, on the RbBr side, by as much as 48 °C. This is unlikely in systems of this type. The liquidus of Ref. 208 is flat in the composition range $0 \leqslant x_B \leqslant 0.5$, perhaps due to the fact that the reported melting point of CsBr is 8 °C lower than the accepted value. This liquidus,[208] as reported, thus does not show a minimum.

The enthalpy of formation of solid solutions at 25 °C was measured calorimetrically,[165] and activity coefficients in solid solution were estimated from the aqueous solubility isotherm and activity coefficients in aqueous solution.[212,229] Solid solutions at the 1:1 composition were examined[203] at 25 °C by x-ray diffraction and by DTA from 100 °C to the solidus temperature. These authors claim the existence of a phase transformation in the range 190–220 °C with two solid solutions of different crystal structure. Neither CsBr nor RbBr, however, undergoes structural transformation at these temperatures.[81] It has been pointed out[203] that solid CsBr and RbBr have different crystal structures (RbBr, Fm3m and CsBr, Pm3m). This implies that there should be a region of solid–solid immiscibility, since the transition temperature of RbBr has not been observed,[81] and that of CsBr is estimated to be above the melting point.[81,161] For the present calculations, therefore, it was decided to treat the system as one having a eutectic and two solid phases. The CsBr-based (α) phase is treated as a Henrian solution. The RbBr-based (β) phase is treated as a regular solution, with the use of the following expression for the Gibbs energy of the hypothetical Pm3m → Fm3m transition of CsBr:

$$\Delta_{trs} G = 4483 - 3.89T \text{ J mol}^{-1}. \quad (91)$$

This expression incorporates the extrapolated transformation temperature of 880 °C.[161] The enthalpy of transition, 4483 J mol^{-1}, was obtained by the present authors in the analysis of the CsCl–CsBr system (see section on this system).

The excess enthalpy of the liquid has been measured by direct calorimetry at 710 °C by Hersh and Kleppa,[84] whose result is used here:

$$H^{E}(l) = 230 x_A x_B \text{ J mol}^{-1}. \quad (92)$$

For the calculation of the phase diagram, the Henrian activity coefficient of RbBr in CsBr (α-phase) at the eutectic temperature, relative to the solid standard state, is

$$RT \ln \gamma_B = 3000 \text{ J mol}^{-1}, \quad (93)$$

here assumed to be temperature independent. For the β-phase, the expression

$$G^{E}(s,\beta) = x_A x_B (1000 + 2000x_A) \text{ J mol}^{-1} \quad (94)$$

was used, also assumed to be temperature independent. A phase diagram was calculated with the use of Eqs. (91)–(94). The calculated eutectic is 615 °C, $x_B = 0.37$, and the calculated limits of solid solubility at this temperature are $x_B = 0.32$ and 0.46. The calculated eutectic temperature is nearer the high observed "minimum" temperature[208,211] rather than the low.[187,209,210] The calculated liquidus however, is close to the observed[187,208] in the RbBr-rich region, where both studies[187,208] are in better agreement with each other. Since the uncertainty in the nature of the solid state of this system is unresolved at present, the solid phase boundaries are suggestive only.

Probable maximum inaccuracy in calculated liquidus (Fig. 30): ± 20 °C.

d. Iodides

LiI(A)+NaI(B)

There is one report of this system,[213] in which liquidus points were determined from thermal analysis. The system is stated[213] to be one with continuous solid solution at liquidus temperature, with a minimum at 430 °C, $x_B = 0.1$. The reported experimental melting points of LiI and NaI are 23 and 18 °C, respectively, lower than accepted values, and the authors give no details of the purity of the iodides or of the ambient atmosphere of the melt during the experiments. The liquidus points, read off the published phase diagram, were used only as a guide for the present calculations. There are no reported measurements of the solidus.

The excess enthalpy of the liquid has been measured by Melnichak and Kleppa[214] at 740 °C by direct calorimetry, and their result is used here:

$$H^{E}(l) = x_A x_B (-3895 - 540x_A) \text{ J mol}^{-1}. \quad (95)$$

A phase diagram was calculated, based on Eqs. (95) and (96)

$$G^{E}(s) = 4000x_A x_B \text{ J mol}^{-1}, \quad (96)$$

both quantities assumed to be independent of temperature. The calculated minimum is 450 °C, $x_B = 0.207$. The calculated liquidus follows but is not coincident with the experimental.[213] Because the reported pure component melting points are significantly lower than accepted values, there is a corresponding irreducible uncertainty in the liquidus. The calculated solidus is suggestive only. From Eq. (96) it may be calculated that equilibrium solid–solid demixing occurs only below room temperature.

Probable maximum inaccuracy in calculated liquidus (Fig. 31): ± 15 °C.

KI(A)+LiI(B)

Liquidus points of this system have been reported,[215–217] obtained from cooling curves[215,217] and the visual-polythermal method.[216] Only in Refs. 216 and 217 are the data tabulated. A summary of the results is as follows:

	T/°C	x_B	Ref.
Eutectic	260	0.631	215
	286	0.632	216
	285	0.635	217

There is a discrepancy of 25 °C in the eutectic temperature. The reported KI melting point of Ref. 216 is 20 °C higher than the accepted value; the reported LiI melting points[215,216] are, respectively, 17 and 24 °C lower. All three groups[215–217] attest to the difficulty of preparing sufficiently pure anhydrous LiI from the trihydrate. The most careful preparation was done by Sridhar *et al.*[217] by dehydration *in vacuo* in stages of increasing temperature over a two week period. The salt was tested for dryness by addition of molten lithium; no gas evolution was observed. The salt itself was dissolved in water, the *p*H of which did not change, indicating the absence of Li_2O or LiOH. The cooling curve experiments were performed in a helium atmosphere. In view of the precautions taken in this work,[217] these results, although confined to the composition interval $0.575 \leqslant x_B \leqslant 0.7$, were chosen as the basis of the present calculations.

Eutectic arrests were observed in two studies,[215,217] the first covering a wider composition range $0.078 \leqslant x_B \leqslant 0.9$. The limiting liquidus slopes at both extremes suggest that there is negligible solid solubility, and none was assumed here.

The excess enthalpy of the liquid has been measured by direct calorimetry at 740 °C by Melnichak and Kleppa,[214] whose result is used here:

$$H^{E}(l) = x_A x_B (-11\,393 - 2824x_B) \text{ J mol}^{-1}. \quad (97)$$

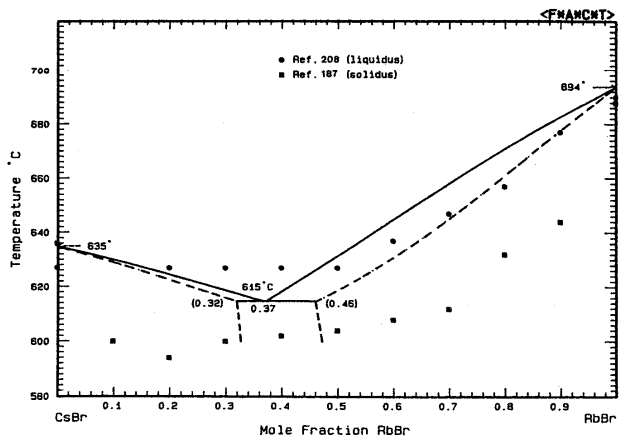

FIG. 30. The system CsBr(A) + RbBr(B).

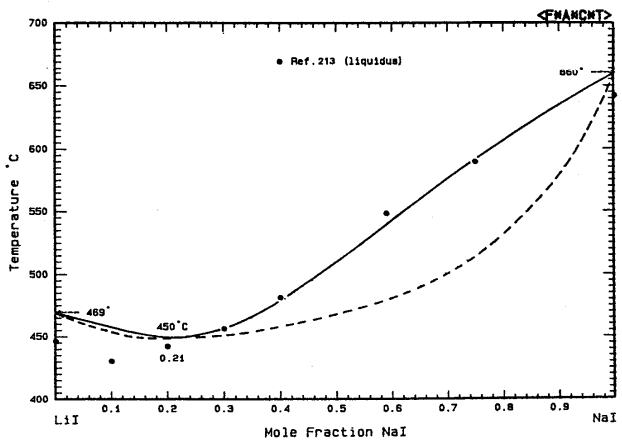

FIG. 31. The system LiI(A) + NaI(B).

A phase diagram was calculated, based on Eq. (97) together with a small entropy term:

$$S^E(1) = x_A x_B(-0.548 - 5.459x_B) \text{ J mol}^{-1}\text{ K}^{-1}. \quad (98)$$

The calculated eutectic is 285 °C, $x_B = 0.633$. This reproduces the chosen values[217] and the calculated liquidus falls within 5 °C of the experimental.[217]

Probable maximum inaccuracy in calculated diagram (Fig. 32): ± 25 °C.

LiI(A)+RbI(B)

Data defining the liquidus have been reported in one study,[217] from cooling curves. The data cover only a restricted range of compositions ($0.28 \leqslant x_B \leqslant 0.47$). The authors report a eutectic at 252 °C, $x_B \leqslant 0.38$ and a peritectic at 260 °C, $x_B = 0.4385$. A 1:1 stoichiometry for the compound is assumed[217] but is not verified; there are no other determinations.

The extent of solid solubility in this system, if any, if unknown. Structurally, this system resembles the other analogous halide systems LiF–RbF, LiCl–RbCl, and LiBr–RbBr. In none of these three cases are there experimental data defining solid solubility, although the limiting liquidus slopes in these systems do not indicate extensive solubility. In the present case there are not sufficient liquidus data for a comparison of limiting slopes. In common with the thermodynamic treatment of the fluoride, chloride, and bromide systems, no solid solubility is assumed in the present calculations.

The excess enthalpy of the liquid has been measured by direct calorimetry at 740 °C by Melnichak and Kleppa,[214] whose result is used here:

$$H^E(1) = x_A x_B(-15\,385 - 4351x_A) \text{ J mol}^{-1}. \quad (99)$$

With the use of Eq. (99), two excess entropy coefficients were calculated:

$$S^E(1) = x_A x_B(-7.188 + 12.507x_B) \text{ J mol}^{-1}\text{ K}^{-1}. \quad (100)$$

The calculated eutectic is 251 °C, $x_B = 0.375$ and peritectic 259 °C, $x_B = 0.430$. The calculated liquidus is within 10 °C of the experimental points.[217] The calculated Gibbs energy of fusion of the compound, of nominal 1:1 stoichiometry 0.5(LiI·RbI), is

$$\Delta_{fus}G^\circ = 20\,168 - 37.643T \text{ J/mol}. \quad (101)$$

Probable maximum inaccuracy in calculated diagram (Fig. 33): ± 30 °C.

CsI(A)+LiI(B)

There are no reports on the phase diagram of this system. The excess enthalpy of the liquid has, however, been measured at 740 °C by direct calorimetry[214] and the result

$$H^E(1) = x_A x_B(-17\,364 - 7623x_B) \text{ J mol}^{-1} \quad (102)$$

is used here to construct a tentative phase diagram.

It is useful for this purpose to compare this system with other related phase diagrams in the same series. One such series is CsF–LiF, CsCl–LiCl, CsBr–LiBr, and CsI–LiI. Another is CsI–LiI, RbI–LiI, and CsI–NaI. Apart from the present system, all have been critically evaluated from experimental data. All are eutectic systems, with or without a peritectic. Although the limits of solid solubility have not been determined experimentally, in all cases the limiting liquidus slopes do not indicate significant solubility. Thus for the present system, as a first approximation, it is reasonable to use Eq. (102) together with the assumption of zero solid solubility and the presence of a eutectic. From the thermodynamic analysis of the series of systems, it is probable that the excess entropy of the liquid in this system, while nonzero, is small and negative. In the absence of experimental phase diagram data, a numerical assignment cannot be made and a reasonable assumption is

$$S^E(1) = 0. \quad (103)$$

The compound 2CsI·3LiI has been isolated and its crystal structure determined by x-ray diffraction measurements.[218]

A phase diagram, calculated with the aid of Eqs. (102) and (103) and the assumptions indicated above, is shown in the figure. The calculated eutectic is 217 °C, $x_B = 0.66$. This eutectic temperature is consistent with those in the related systems:

Probable maximum inaccuracy in calculated diagram (Fig. 34): + 50 °C.

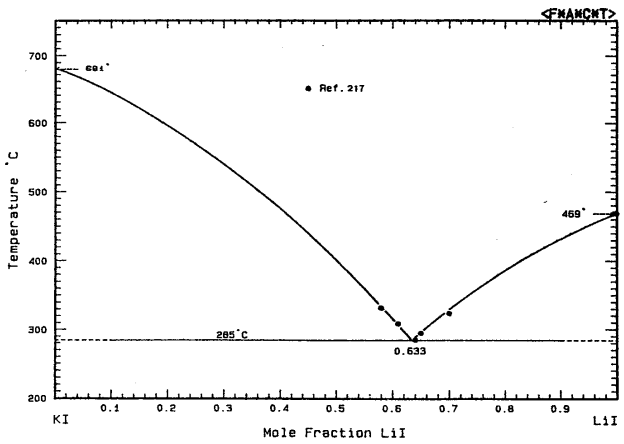

FIG. 32. The system KI(A) + LiI(B).

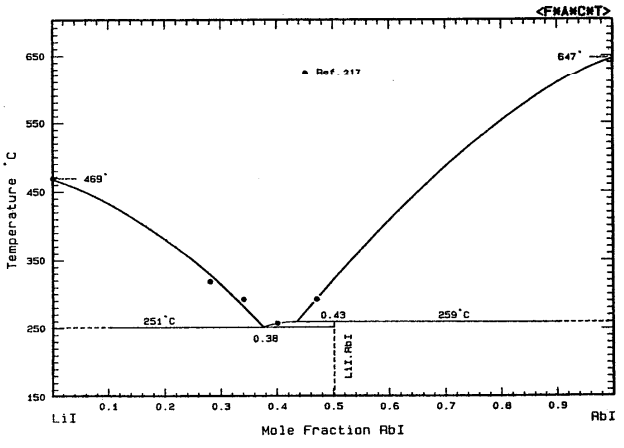

FIG. 33. The system LiI(A) + RbI(B).

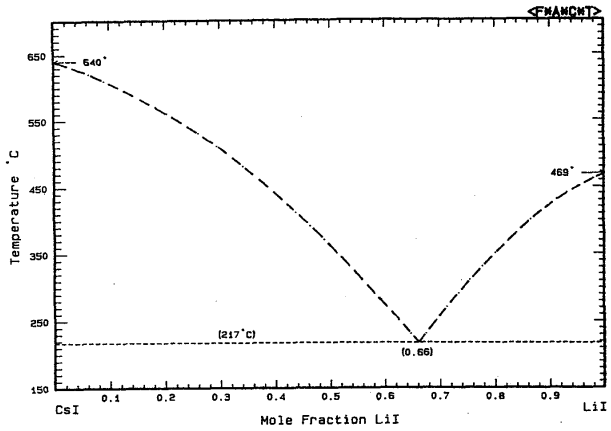

FIG. 34. The system CsI(A) + LiI(B).

KI(A)+NaI(B)

Data defining the liquidus have been tabulated in two independent studies, Ref. 50 and Refs. 219 and 220, from cooling curves and visual-polythermal methods, respectively. The system is one with continuous solid solutions at the liquidus temperature, and data for the minimum liquidus temperature are summarized.

T/°C	x_B	Ref.
583	0.62	50
584	0.58	219,220
580	0.6	221
~585	0.58	222

There are no measurements of the solidus.

The reported melting point of KI in Ref. 50 is 12 °C higher than the accepted value, while that of NaI in Refs. 219 and 220 is 7 °C lower. The later work[219,220] was chosen as a guide for the present calculations.

Data defining the solid miscibility gap are found in two reports,[123,175] obtained by optical transmission and x-ray diffraction methods, respectively. The later study[123] reports the consolute point as 240 °C, $x_B = 0.62$. The results of the earlier study[175] are not precise enough to locate this point, although the data suggest a temperature between 180 and 420 °C at $x_B \sim 0.67$.

The heat of formation of metastable solid solutions has been measured calorimetrically at 25 °C.[126] These results were used in the present calculations, as indicated below.

The excess enthalpy of the liquid has been measured by direct calorimetry by Kleppa and co-workers.[84,214,223] The latest measurements[214] were performed only near $x_B = 0.5$, while the earlier[84,223] were done over the whole composition range. At $x_B = 0.5$, the results of the three reports agree within 60 J. The parameters at 700 °C (Ref. 84) are used here:

$$H^E(l) = x_A x_B(-2113 - 209x_B) \text{ J mol}^{-1}. \quad (104)$$

A phase diagram was calculated, based on Eq. (104) for the liquid, and Eq. (105) for the solid:

$$G^E(s) = x_A x_B(10\,014 + 3073x_B - 18.203T + 1.831T \ln T) \text{ J mol}^{-1}. \quad (105)$$

Equation (105) was based on the liquidus points of Refs. 219 and 220, the solid miscibilty gap data of Ref. 123 and the heats of formation of solid solutions at 25 °C, Ref. 126. Other properties of the solid may be deduced from Eq. (105):

$$H^E(s) = x_A x_B(10\,014 + 3073x_B - 1.831T) \text{ J mol}^{-1}, \quad (106)$$

$$S^E(s) = x_A x_B(16.372 - 1.831 \ln T) \text{ J mol}^{-1}\text{ K}^{-1}, \quad (107)$$

$$C_p^E(s) = -1.831 x_A x_B \text{ J mol}^{-1}\text{ K}^{-1}. \quad (108)$$

The calculated liquidus minimum temperature is 580 °C at $x_B = 0.585$, and the calculated liquidus lies within 5 °C of the experimental.[219,220] The calculated consolute point for solid demixing is 240 °C, $x_B = 0.60$. The calculated envelope follows the experimental curve within 10 °C on the NaI side, but less closely on the KI side. Equation (106) reproduces the experimental enthalpy of formation at 25 °C, Ref. 126, within 300 J mol^{-1}.

Probable maximum inaccuracy in calculated liquidus (Fig. 35): ± 10 °C.

Probable maximum inaccuracy in calculated consolute temperature (Fig. 35): ± 25 °C.

NaI(A)+RbI(B)

Liquidus, solidus, and solvus points for this system were obtained[196] by thermal analysis, while data for liquidus only were found by the visual-polythermal method.[224] Il'yasov[224] states that the system is one with a minimum liquidus temperature and continuous solid solution, without giving any information concerning the solidus or the consolute temperature for solid demixing. He does not acknowledge the earlier work,[196] in which the system is described as eutectic, with appreciable solid solubility at both extremes. The following are the reported data for minimum and eutectic.

	T/°C	x_B	Ref.
Eutectic	475	0.50	196
Minimum	512	0.525	224

The liquidus points of Samuseva and Plyushchev[196] all fall below the theoretical limiting slopes for zero solid solubility at both NaI and RbI extremes; this suggests that this

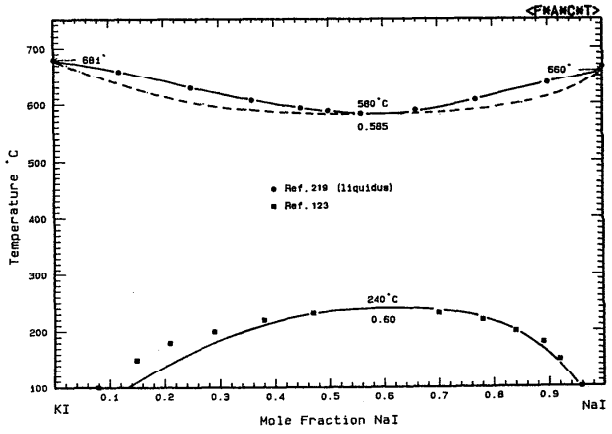

FIG. 35. The system KI(A) + NaI(B).

liquidus[196] is in error. The liquidus of Il'yasov,[224] however, is consistent with solid solubility at both ends; this liquidus[224] was therefore chosen as being closer to true behavior.

The limits of solid solubility at the eutectic temperature are stated[196] as $x_B = 0.15$ and 0.80. These were deduced from the results of thermal analysis only, and there are no confirmatory measurements by other methods.

The excess enthalpy of the liquid has been measured by direct calorimetry by Kleppa and co-workers[84,214] at 700 and 740 °C, respectively. In the later work[214] care was taken to exclude oxygen from the molten salts, and data were obtained over the complete concentration range, rather than near the 50–50 composition only. The later results[214] are used here:

$$H^E(l) = x_A x_B(-3569 - 397x_A) \text{ J mol}^{-1}. \quad (109)$$

The calculated phase diagram shown in the figure is based on Eq. (109), together with an excess entropy of the liquid given by

$$S^E(l) = -4.386 x_A x_B \text{ J mol}^{-1} \text{ K}^{-1} \quad (110)$$

and excess Gibbs energy of the solid given by

$$G^E(s) = 15\,190 x_A x_B \text{ J mol}^{-1}. \quad (111)$$

The calculated eutectic is 505 °C, $x_B = 0.50$ and the calculated limits of solid solubility at the eutectic temperature are $x_B = 0.18$ and 0.82. The extent of solid solubility in this system has not been established unambiguously, and so this part of the diagram is suggestive only.

Probable maximum inaccuracy in calculated liquidus (Fig. 36): ± 10 °C.

CsI(A)+NaI(B)

Data defining the liquidus have been tabulated in two studies,[56,207] from thermal analysis and visual-polythermal methods, respectively. Eutectic data are summarized as follows:

T/°C	x_B	Ref.
435	0.45	56
428	0.485	207
428	0.515	225

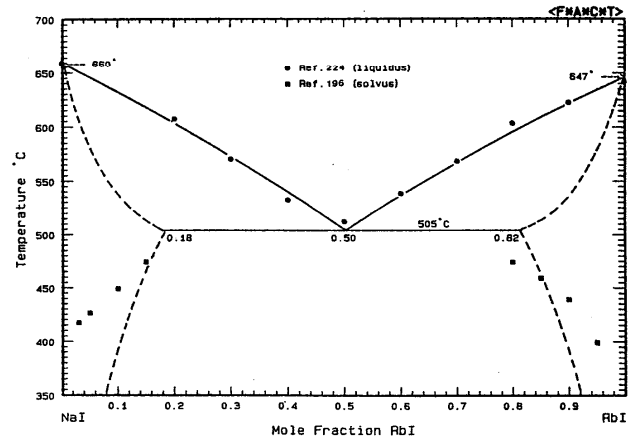

FIG. 36. The system NaI(A) + RbI(B).

The reported CsI melting point in Ref. 56 is 15 °C lower than the accepted value, and the liquidus points in this work show severe scatter near the eutectic. The agreement between the two liquidi[56,207] is poor in some parts of the diagram (80 °C) but good in others (1 °C). The liquidus of Ref. 207 was therefore taken as a guide for the present calculations.

Samuseva and Plyushchev[56] observed eutectic arrests in the composition interval $0.025 \leqslant x_B \leqslant 0.975$. The limiting slopes of the experimental liquidus Ref. 207 suggest negligible solid solubility at the CsI extreme. At the NaI side, the limiting slope indicates that solid solubility could be significantly greater than the 2.5% maximum suggested in Ref. 56. However, in view of the imprecision in the experimental points and in the absence of conclusive evidence of solid solubility here, it is reasonable to assume no solubility for the purpose of calculating the phase diagram.

The excess Gibbs energy of the liquid over the temperature interval 657–777 °C has been determined by mass spectrometric measurements of the vapor.[331] The $G^E(l)$ thus deduced may be represented by the expression $3374 x_A x_B$ J mol^{-1}, to within a rms deviation of 92 J mol^{-1}. This result—a positive excess Gibbs energy—is quite at variance with the negative calorimetric excess enthalpy discussed in the next paragraph.

The excess enthalpy of the liquid has been measured by Kleppa and co-workers[84,214] by direct calorimetry at 700 and 740 °C, respectively. In the earlier work[84] measurements were done near the 50–50 composition only, while in the later,[214] the whole composition range was covered. The later result is used here:

$$H^E(l) = x_A x_B(-5439 - 556x_B) \text{ J mol}^{-1}. \quad (112)$$

A phase diagram was calculated, based on Eq. (112) and a small excess entropy:

$$S^E(l) = x_A x_B(4.368 - 5.134x_B) \text{ J mol}^{-1} \text{ K}^{-1}. \quad (113)$$

The calculated eutectic is 428 °C, $x_B = 0.485$, identical to the experimental.[207] The calculated liquidus follows the shape of, but does not coincide with, the experimental.[207]

Probable maximum inaccuracy in calculated diagram (Fig. 37): ± 20 °C.

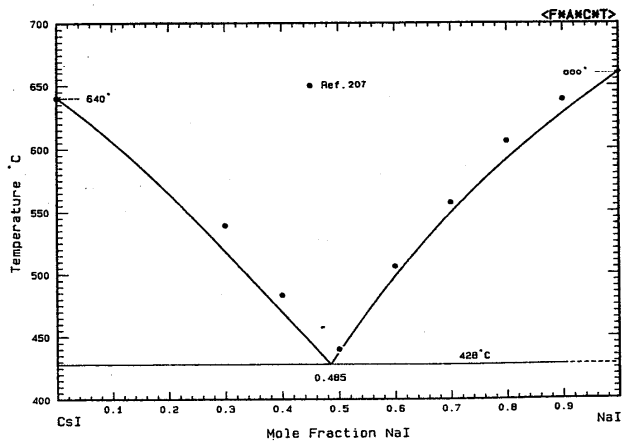

FIG. 37. The system CsI(A) + NaI(B).

KI(A)+RbI(B)

Data defining the liquidus have been tabulated in two studies,[226,224] obtained from thermal analysis and visual-polythermal methods, respectively. The system is one with continuous solid solution at the liquidus temperature. The earlier work[226] reports a minimum temperature for the solidus without a minimum in the liquidus, and the two curves are separated by as much as 55 °C. This construction violates the phase rule. Data for the minimum are summarized in the table:

T/°C	x_B	Ref.
...	...	226
514	0.63	224
626	0.7	227

The melting points of the pure salts, as reported in Ref. 226 are both higher than accepted values (KI, by 13 °C; RbI, by 9 °C). The very great discrepancy between Il'yasov's two reported minima[224,227] is not commented upon by him; neither does he mention the early work.[226] A rational choice for the position of the liquidus cannot be made from these reports alone.

The excess Gibbs energy of solid solutions at 25 °C has been determined from isopiestic data of mixed saturated KI–RbI aqueous solutions.[228] The data were treated according to the McKay–Perring method.[229] The results of this calculation may be represented by the following equation:

$$G^E(s) = 1700x_A x_B \text{ J mol}^{-1}, \quad (114)$$

which reproduces the observed values[228] within 60 J mol^{-1}.

The excess enthalpy of the liquid has been measured, at the 50–50 composition only, by direct calorimetry by Kleppa and co-workers.[84,214] In later work, at 740 °C, special care was taken to prevent oxidation of the iodides in the calorimeter. These results are used here and may be represented by

$$H^E(l) = -80x_A x_B \text{ J mol}^{-1}. \quad (115)$$

In order to calculate a phase diagram for this system, an estimate of the excess Gibbs energy of solid solutions at the liquidus temperature is needed. The published phase diagram data[224,226,227] do not allow an unambiguous estimate to be made. A comparison may be made, however, of the thermodynamic properties of the present system with other K–Rb halide binary systems:

	$H^E(l)/x_A x_B$ J mol^{-1}	$G^E(s)/x_A x_B$
KF + RbF	360	2500
KCl + RbCl	84	1500
KBr + RbBr	0	2000
KI + RbI	80	

The unknown $G^E(s)$ most probably lies between zero and $4000x_A x_B$ J mol^{-1}; a convenient estimate for calculation purposes is Eq. (114).

A phase diagram was calculated, based on Eqs. (114) and (115). It has a shallow minimum at 643 °C, $x_B = 0.74$. The calculated liquidus–solidus separation is everywhere less than 5 °C. The existence of a minimum is not unequivocably indicated, since the thermodynamic properties of the solid cannot be more precisely specified (the experimental data themselves are inconclusive). If there is a minimum, it probably does not lie lower than 623 °C [result for $G^E(s) = 4000x_A x_B$ J mol^{-1}]. In any case, Il'yasov's very low reported[227] minimum of 514 °C is not reasonable, since this would thermodynamically entail solid–solid separation at a temperature higher than 514 °C. The calculated consolute temperature for solid demixing is − 172 °C.

Probable maximum inaccuracy in calculated diagram (Fig. 38): ± 20 °C.

CsI(A)+KI(B)

Data defining the liquidus and solidus of this system are tabulated in one report,[226] determined by thermal analysis. All investigators[226,230,231] describe this system as one having a minimum liquidus temperature and continuous solid solutions, but the experimental liquidus[226] is cusp-shaped at the minimum, which is not thermodynamically consistent. Available data for the minimum are summarized as follows:

T/°C	x_B	Ref.
516	0.45	226
494	0.21	230
559	0.3	231

The large discrepancy in minimum temperature between Il'yasov's later work[231] and earlier reports[226,230] is neither acknowledged nor discussed by him. It is not possible, from these data, to define the liquidus minimum temperature more precisely than this.

The excess enthalpy of the liquid has been measured at 700 [84] and 740 °C [214] by Kleppa and co-workers by direct calorimetry. Both determinations were performed near the 50–50 composition only. In the later work, precautions were taken to exclude oxygen from the molten salts in the calorimeter; the results[214] are used here in the form

$$H^E(l) = -59x_A x_B \text{ J mol}^{-1}. \quad (116)$$

This excess enthalpy was assumed to be independent of temperature.

It has not hitherto been pointed out in this context,[226,230,231] that solid CsI and KI have different crystal structures (KI, Fm3m and CsI, Pm3m). This implies that there should be a region of solid–solid immiscibility, since the transition temperatures of either CsI or KI have not been

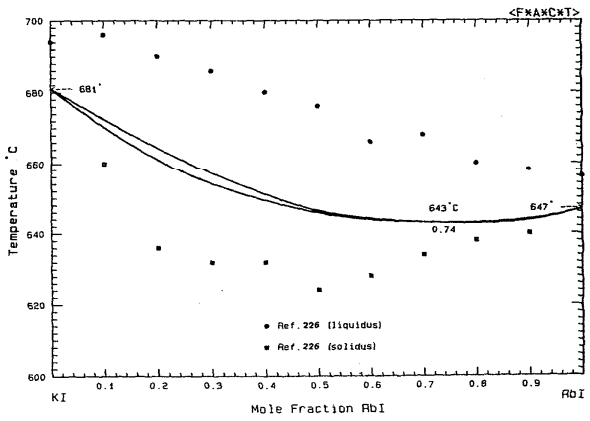

FIG. 38. The system KI(A) + RbI(B).

observed.[81] For the purpose of calculating the phase diagram, therefore, the CsI-based (α) phase is treated as a Henrian solution, with a Henrian activity coefficient for KI in CsI at the eutectic temperature given by

$$RT \ln \gamma_B = 15\,000 \text{ J mol}^{-1}. \quad (117)$$

For the β-phase, the expression

$$G^E(s,\beta) = x_A x_B (5000 + 15\,000 x_A) \text{ J mol}^{-1} \quad (118)$$

was used. Both quantities were assumed to be independent of temperature. The phase diagram, calculated with Eqs. (116)–(118) shows a calculated eutectic at 536 °C, $x_B = 0.39$. The calculated limits of solid solubility at the eutectic temperature are $x_B = 0.07, 0.65$. The solid phase boundaries, as calculated, are tentative only, since the question of the nature of the solid state of this system is unresolved. The calculated liquidus carries a significant uncertainty, since the spread in the reported minimum temperature is so great (65 °C).

Probable maximum inaccuracy in calculated liquidus (Fig. 39): ± 40 °C.

CsI(A)+RbI(B)

Data defining the liquidus and solidus of this system have been tabulated in one study,[226] obtained from thermal analysis. A minimum liquidus temperature is reported, with complete solid solubility. The experimental data[226] show, however, the liquidus to be cusp-shaped at the minimum, which is thermodynamically inconsistent. Available data on the minimum are summarized as follows:

T/°C	x_B	Ref.
566	0.35	226
578	0.35	232

Although this system has been assumed to be characterized by the presence of continuous solid solution at the liquidus temperature,[226,232] this cannot be correct since, at these temperatures, CsI and RbI have different crystal structures (CsI, Pm3m and RbI, Fm3m). Thus there should be a region of solid–solid immiscibility and the system would then show a eutectic rather than a minimum. Markarov and Pankov[233] prepared solid solutions at 25 °C from saturated aqueous solution. The solubility isotherm was obtained by radioactive isotopic analysis of Rb and Cs in the solid phases. In addition, the water activity of these solutions was determined by the isopiestic method. From a knowledge of the activities of the mixed salts in aqueous solution in equilibrium with the solid phase, activity coefficients in the solid could be inferred. The miscibility gap in solid solutions was found to be defined by $x_B = 0.163, 0.922$. The excess Gibbs energy of homogeneous solid solutions outside this gap can be represented approximately by the following equation:

$$G^E(s) = 5118 x_A x_B \text{ J mol}^{-1}. \quad (119)$$

The excess enthalpy of the liquid has been measured by direct calorimetry by Kleppa and co-workers[84,214] at 700 and 740 °C, respectively, at the 1:1 composition only. In the later work[214] precautions were taken to exclude oxygen from the molten salts, and these results[214] are used here:

$$H^E(l) = 89 x_A x_B \text{ J mol}^{-1}. \quad (120)$$

The calculation of the phase diagram for this system is unusually difficult, not only because the nature of the solid state is unresolved at present, but also by the small temperature range (~70 °C) covered by the diagram,[226] which magnifies the effects of scatter in the data. It was decided to represent the solid state by the use of two Henrian activity coefficients, relative to the solid standard state at the eutectic temperature:

for CsI in RbI

$$RT \ln \gamma_A = 4000 \text{ J mol}^{-1}, \quad (121)$$

for RbI in CsI

$$RT \ln \gamma_B = 4000 \text{ J mol}^{-1}, \quad (122)$$

and these were assumed to be temperature independent. With the use of Eqs. (120) to (122) a phase diagram was calculated, which has a calculated eutectic at 580 °C, $x_B = 0.493$. The calculated limits of solid solubility at this temperature are $x_B = 0.36, 0.64$. The calculated solubility limits at 25 °C are $x_B = 0.17, 0.84$, in good agreement with experiment.[233] The calculated eutectic temperature is close to the most recently determined "minimum" (Ref. 232), and the calculated liquidus and solidus lie within the experimental phase boundaries.[226] The calculated solid phase boundaries, for reasons cited earlier, are to be regarded as suggestive only.

Probable maximum inaccuracy in calculated liquidus (Fig. 40): ± 25 °C.

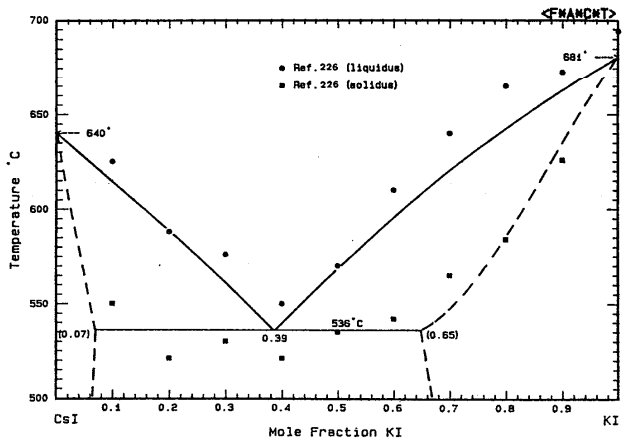

FIG. 39. The system CsI(A) + KI(B).

3.2. Common-Cation Systems

a. Lithium

LiCl(A)+LiF(B)

Liquidus data points were obtained in four studies[234–237] by thermal analysis[234,236,237] and the visual-polythermal method.[235] Data were tabulated in Refs. 234–236 and appear in Ref. 237 only as points on a phase diagram. The liquidus curve defined by Johnson and Hathaway's[237] points read off the published diagram coincided (within 3 °C) with that of Haendler *et al.*[236] Reported eutectic data are summarized as follows:

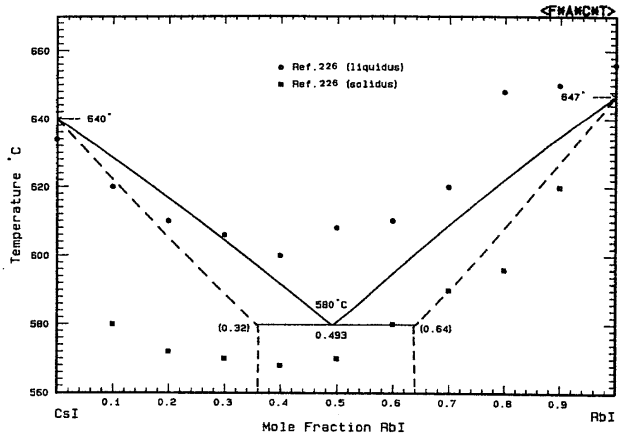

FIG. 40. The system CsI(A) + RbI(B).

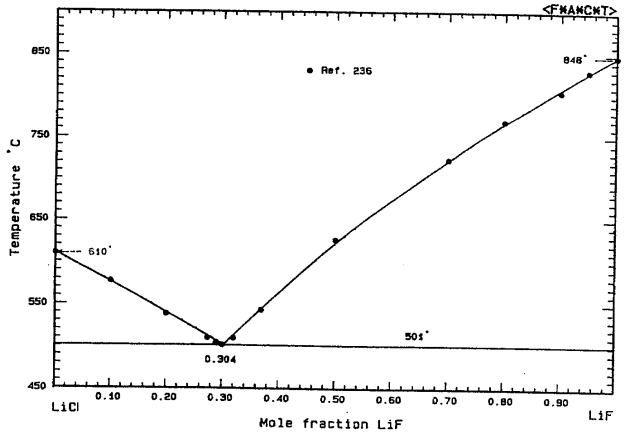

FIG. 41. The system LiCl(A) + LiF(B).

T/°C	x_B	Ref.
485	0.264	234
484	0.305	235
501	0.305	236
501	0.3	237
498	0.28	238
498	0.29	37
498	0.295	239
497	0.3	98
488	0.25	240
498	0.3	241

The reported eutectic temperatures cluster either near 485 or 500 °C. The two most recent independent liquidus data sets[236,237] are virtually coincidental, and so the data of Ref. 236 were used for the present calculations.

Eutectic arrests were observed in three studies[234,236,237] and can be bracketed by the interval $0.08 \leqslant x_B \leqslant 0.95$. The limiting liquidus slopes indicate zero solubility, within experimental uncertainty. Zero solubility was assumed in the present work.

There are no reported measurements of the excess enthalpy of the liquid.

A phase diagram was calculated with an excess enthalpy of the liquid given by

$$H^E(1) = -1000 x_A x_B \text{ J mol}^{-1} \quad (123)$$

which was assumed to be independent of temperature, and with an excess entropy of zero. The calculated eutectic is 501 °C, $x_B = 0.304$. The calculated liquidus lies within 5 °C of the experimental points.[236]

Probable maximum inaccuracy in calculated diagram (Fig. 41): ± 5 °C.

LiBr(A)+LiF(B)

Data defining the liquidus were obtained in two studies,[178,234] both by means of thermal analysis. The data were tabulated in the earlier,[234] but not in the later[178] work; these latter were read off the published phase diagram.[178] The following is a summary of reported eutectics.

T/°C	x_B	Ref.
453	0.29	234
448	0.24	178
458	0.23	242
448	0.25	243

The liquidi of Refs. 234 and 178 lie within 5 °C of one another on the LiBr side, but on the other side Bochvar's[234] is consistently below that of Ref. 178. The limiting slope of the liquidus[178] corresponds to that expected for zero solid solubility at the LiF extreme. The fact that Bochvar's liquidus is everywhere below that of Ref. 178 suggests that the later results[178] are closer to true behavior. The phase diagram of Ref. 178 was therefore adopted as a guide to the construction of the phase diagram.

Eutectic arrests were observed[234] in the interval $0.12 \leqslant x_B \leqslant 0.97$. This observation, together with the experimental limiting liquidus slopes, indicates limited, if any, solid solubility. None was assumed in the present calculations.

There is no report of the excess enthalpy of the liquid. Two excess enthalpy and two excess entropy coefficients were obtained from an optimization performed on the liquidus data[178]:

$$H^E(1) = x_A x_B (1677 + 8567 x_B) \text{ J mol}^{-1}, \quad (124)$$

$$S^E(1) = x_A x_B (9.431 + 0.812 x_B) \text{ J mol}^{-1} \text{ K}^{-1}. \quad (125)$$

It must, however, be emphasized that the data are insufficient to permit both H^E and S^E to be determined independently. Hence, Eqs. (124) and (125) must be considered as only tentative, pending verification. The sum $G^E - H^E - TS^E$ is probably quite accurate over the temperature range of the liquidus.

The phase diagram calculated with Eqs. (124) and (125) reproduced the experimental eutectic[178] exactly, and the calculated liquidus is everywhere within 5 °C of the experimental.[178]

Probable maximum inaccuracy of calculated diagram (Fig. 42): ± 5 °C.

LiF(A)+LiI(B)

There is only one report on this system,[237] in which tabulated liquidus data points were obtained from the thermal analysis. The experimental eutectic is 411 °C, $x_B = 0.835$. The eutectic arrest was observed in the interval $0.1 \leqslant x_B \leqslant 0.95$. The limiting liquidus slope at the LiI side indicates zero solid solubility there. At the LiF extreme, LiI solubility in LiF of 10 mol % or greater is possible, accord-

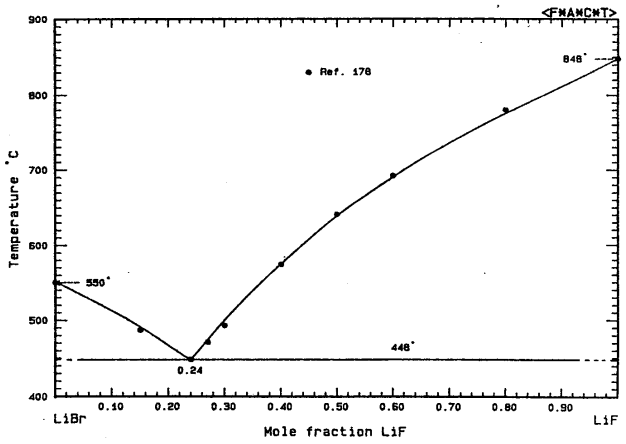

FIG. 42. The system LiBr(A) + LiF(B).

ing to the limiting slope. There are no other experimental data to support this possibility. For the calculation of the phase diagram, therefore, zero solubility was assumed at both extremes and all data points[237] were used in the optimization. The experimental procedure and purification of the salts[237] were done with particular care.

There are no reported measurements of the excess enthalpy of the liquid.

A phase diagram was calculated with the use of Eqs. (126) and (127):

$$H^{E}(l) = -1391 x_A x_B \text{ J mol}^{-1}, \quad (126)$$

$$S^{E}(l) = x_A x_B(-10.286 + 16.836 x_B - 8.065 x_B^2) \text{ J mol}^{-1}\text{ K}^{-1}. \quad (127)$$

It must, however, be emphasized that the data are insufficient to permit both H^E and S^E to be determined independently. Hence, Eqs. (126) and (127) must be considered as only tentative, pending verification. The sum $G^E = H^E - TS^E$ is probably quite accurate over the temperature range of the liquidus. The calculated eutectic is 414 °C, $x_B = 0.834$, and the calculated liquidus lies everywhere within 4° of the experimental points.[237]

Probable maximum inaccuracy in calculated diagram (Fig. 43): ± 5 °C.

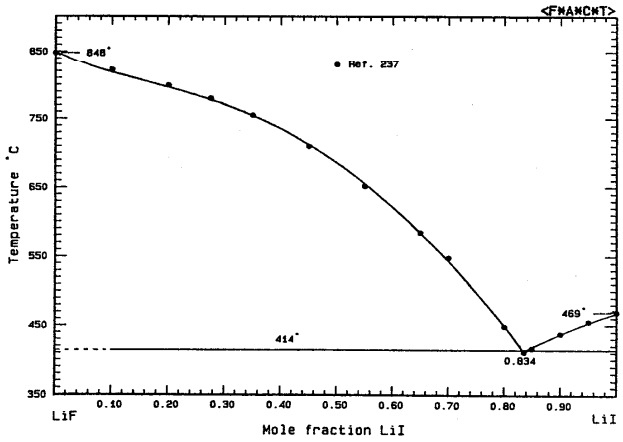

FIG. 43. The system LiF(A) + LiI(B).

LiBr(A) + LiCl(B)

Liquidus data points, obtained from cooling curves, have been tabulated in one report.[234] The system is one with complete solid solubility at the liquidus temperature. Data on the minimum are summarized as follows:

T/°C	x_B	Ref.
522	≈0.36	234
522	0.40	182

The experimental liquidus[234] is shown to be quite flat over a 0.2-unit mole fraction range, so that the composition at the minimum is somewhat uncertain. There are no reported measurements of the solidus.

The excess enthalpy of the liquid has been measured by direct calorimetry at 630 °C by Kleppa and coworkers.[244,245] The later data[245] are both more numerous and cover a wider composition range than the earlier.[244] The result[245] is used here:

$$H^{E}(l) = x_A x_B(80 + 113 x_B) \text{ J mol}^{-1}. \quad (128)$$

A phase diagram was calculated with the use of Eqs. (128) and (129)

$$G^{E}(s) = 5000 x_A x_B \text{ J mol}^{-1}, \quad (129)$$

and both quantities were assumed to be independent of temperature. The calculated minimum is 522 °C, $x_B = 0.36$. The calculated liquidus agrees with the experimental[234] on the LiBr side, but is consistently above experiment on the LiCl side. In a preliminary calculation, it was found that if the liquidus were to follow faithfully the experimental data on the LiCl side, an improbably asymmetric expression for $G^E(s)$—four terms in Eqs. (129)—would be required. Since the simple expression shown here by Eq. (129) allows the minimum to be reproduced accurately, we have constructed the phase diagram (Fig. 44) on this basis. Since there are no other existing liquidus or solidus data, this discrepancy cannot be resolved and the calculated phase boundaries are suggestive only. The calculated consolute temperature for solid demixing is 24 °C.

Probable maximum inaccuracy in calculated diagram (Fig. 44): + 20 °C.

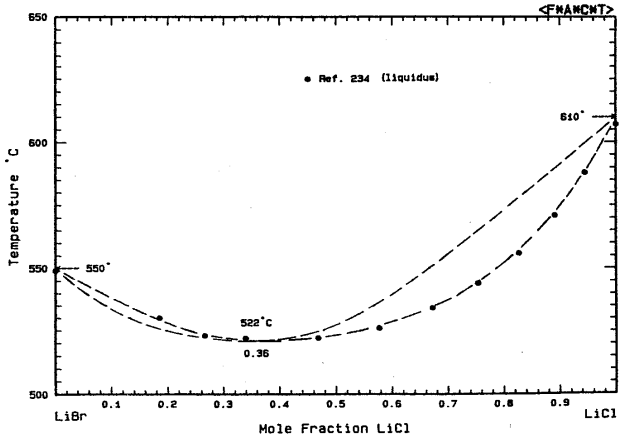

FIG. 44. The system LiBr(A) + LiCl(B).

LiCl(A)+LiI(B)

Liquidus data points were determined by thermal analysis and tabulated in one study only.[246] The eutectic was found to be 368 °C, $x_B = 0.654$, and the eutectic arrest was observed in the composition interval $0.05 \leqslant x_B \leqslant 0.95$. The limiting liquidus slopes at either extreme do not indicate the presence of solid solubility, and none was assumed in the present calculations.

The excess enthalpy of the liquid was measured by direct calorimetry at 633 °C by Melnichak and Kleppa,[245] and their result is used here:

$$H^E(l) = x_A x_B (1393 + 628x_A) \text{ J mol}^{-1}. \quad (130)$$

Although Johnson and Hathaway's[246] is the only measurement of the liquidus, it was performed with particular care, especially in the preparation of LiI, which is notoriously difficult to obtain in a sufficiently pure state. A phase diagram was calculated, based on Eq. (130) and two excess entropy coefficients from an optimization of the data[246]:

$$S^E(l) = x_A x_B (2.204 - 3.122x_A) \text{ J mol}^{-1}. \quad (131)$$

The experimental eutectic is reproduced exactly, though the calculated liquidus falls slightly below the observed (within 10 °C).

Probable maximum inaccuracy in calculated diagram (Fig. 45): ± 10 °C.

LiBr(A)+LiI(B)

The only reported phase diagram data for this system are for the minimum only,[247,248] obtained from thermal analysis.

T/°C	x_B	Ref.
418	≈0.6	247
417	0.6	248

The excess enthalpy of the liquid has been measured at 633 °C by direct calorimetry by Melnichak and Kleppa,[245] whose result is used here:

$$H^E(l) = x_A x_B (818 + 17x_A) \text{ J mol}^{-1}. \quad (132)$$

That this system is one with a minimum and continuous solid solution is consistent with the fact that the other related systems M||Br, I(M = Na, K, Rb, or Cs) are all of this same type. A phase diagram was calculated with the use of Eqs. (132) and (133)

$$G^E(s) = 8000x_A x_B \text{ J mol}^{-1} \quad (133)$$

both quantities being assumed temperature independent. The calculated minimum is 418 °C, $x_B = 0.63$. The calculated consolute temperature for solid demixing is 202 °C.

Probable maximum inaccuracy in calculated diagram (Fig. 46): ± 15 °C.

b. Sodium

NaCl(A)+NaF(B)

Data defining the liquidus have been tabulated in five studies,[237,249–252] from thermal analysis[237,249,250,252] and visual-polythermal[251] methods. A eutectic summary is given as follows:

T/°C	x_B	Ref.
680	0.35	249
675	0.345	250
675	0.34	251
680	0.335	252
680	0.33	237
678	0.34	253
676	0.345	254
682	0.263	255
675	0.346	256
669	0.328	257
680	0.33	258

Eutectic arrests were observed by Grjotheim *et al.*[252] in the range $0.01 \leqslant x_B \leqslant 0.99$. Wolters[250] made optical studies of thin sections of solidified melts and concluded that solid phases were pure salts. Thus there is no appreciable solid solubility in this system, and this conclusion is corroborated by the limiting liquidus slopes of all investigators.[237,249–252] There are no reported measurements of the excess enthalpy of the liquid.

The most thorough and careful work on this system is found in the most recent studies.[237,252] The combined liquidus points of these reports were used in the thermodynamic optimization. Two excess enthalpy terms for the liquid were calculated:

$$H^E(l) = x_A x_B (1416 + 1283x_B) \text{ J mol}^{-1} \quad (134)$$

which were assumed to be independent of temperature.

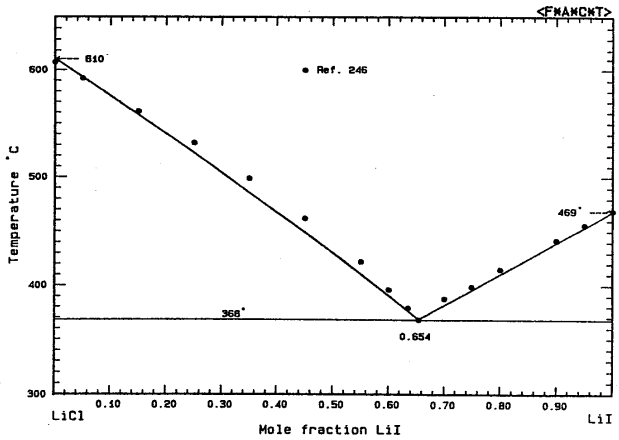

FIG. 45. The system LiCl(A) + LiI(B).

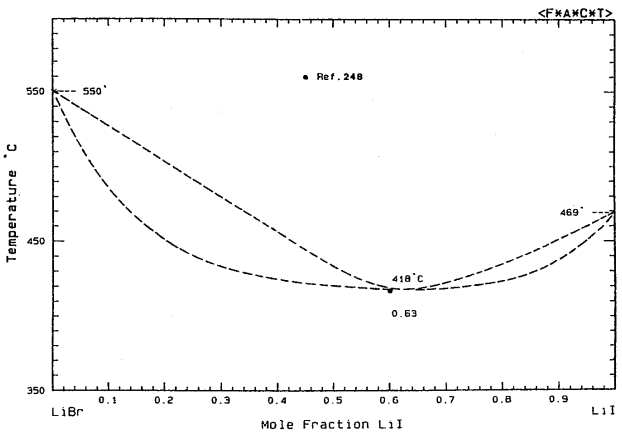

FIG. 46. The system LiBr(A) + LiI(B).

Here, $S^E(1)$ was assumed to be zero. Equation (134) was used to calculate the phase diagram, and the calculated liquidus is everywhere within 5 °C of the experimental points.[237,252] The calculated eutectic is 681 °C, $x_B = 0.333$.

Probable maximum inaccuracy in calculated diagram (Fig. 47): ± 5 °C.

NaBr(A)+NaF(B)

Data defining the liquidus have been obtained by thermal analysis[259] and by the visual-polythermal method.[51] Results for the eutectic may be summarized as follows:

T/°C	x_B	Ref.
662	0.27	259
642	0.27	51
640	0.27	260
656	0.28	261

The data of Ref. 51 are tabulated, and those of Ref. 259 are available only as points on a phase diagram. The melting point of NaBr reported in Ref. 259 is 18 °C higher than the accepted value, and liquidus data points in this early work all lie above those of the later.[51] The data of Dombrovskaya and Koloskova[51] were therefore taken as the basis of the present calculations.

In neither of these studies[51,259] were eutectic arrests recorded. The limiting liquidus slope at the NaBr extreme does not suggest solid solubility; on the NaF side the data do not extend far enough in order to allow an estimate of solubility. In the present calculations, zero solid solubility was assumed at both extremes.

There are no reports of the excess enthalpy of the liquid. A thermodynamic optimization using the chosen liquidus data[51] yielded the expression:

$$H^E(1) = x_A x_B(-700 + 4895x_B) \text{ J mol}^{-1} \quad (135)$$

which quantity was assumed to be independent of temperature. $S^E(1)$ was assumed to be zero. The phase diagram calculated with the use of Eq. (135) showed a calculated eutectic of 640 °C, $x_B = 0.28$, and the calculated liquidus lies within 10 °C of the experimental points,[51] allowing for the low reported melting point of NaBr.

Probable maximum inaccuracy in calculated diagram (Fig. 48): ± 10 °C.

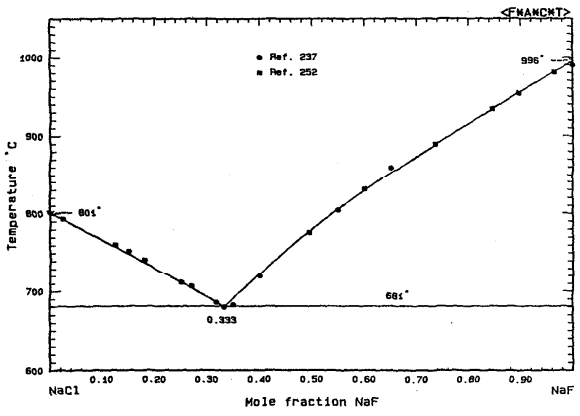

FIG. 47. The system NaCl(A) + NaF(B).

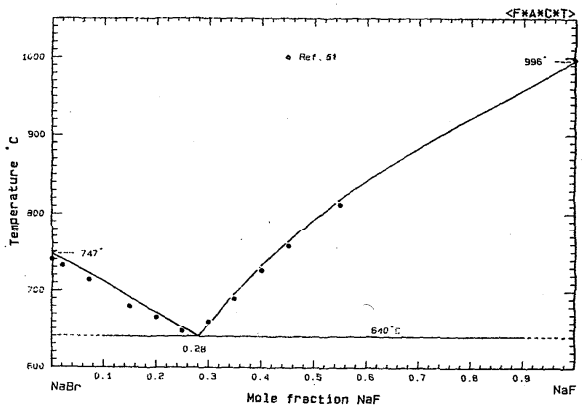

FIG. 48. The system NaBr(A) + NaF(B).

NaF(A)+NaI(B)

Data defining the liquidus have been reported in three studies,[219,237,259] from thermal analysis[237,259] and visual-polythermal methods.[219] The following table summarizes the reported eutectic data.

T/°C	x_B	Ref.
617	0.79	259
603	0.82	219
597	0.82	237
603	0.82	262

Liquidus data were tabulated only in Refs. 219 and 237. The data of Johnson and Hathaway[237] appear to be the most carefully obtained of these reports, and were chosen as the basis of the present calculations. There are no reports of the excess enthalpy of the liquid.

Eutectic arrests were recorded only in Ref. 237 in the range $0.45 \leqslant x_B \leqslant 0.95$. The limiting liquidus slope at the NaI extreme suggests little or no solid solubility, and none was assumed in the present work. At the NaF extreme, the liquidus data of Ref. 219 extend only to $x_B = 0.2$, and thus a definite statement on solid solubility at this end cannot be made. Solid solubility cannot be ruled out, but if present it is probably not extensive, since similar systems M||F,I (M = Li,K,Cs) do not display solid solubility at this end. None was assumed in this work.

A thermodynamic optimization was performed on the liquidus data of Ref. 237, which yielded two excess enthalpy terms

$$H^E(1) = x_A x_B(8739 - 7663x_B) \text{ J mol}^{-1} \quad (136)$$

which were assumed to be independent of temperature. $S^E(1)$ was assumed to be zero. A phase diagram calculated with Eq. (136) yielded a calculated eutectic of 596 °C, $x_B = 0.814$. The calculated liquidus lies within 10 °C of the combined experimental points.[219,237]

Probable maximum inaccuracy in calculated diagram (Fig. 49): ± 10 °C.

NaBr(A)+NaCl(B)

Data defining the liquidus have been reported in four studies,[189,259,263,264] all from thermal analysis. All show a

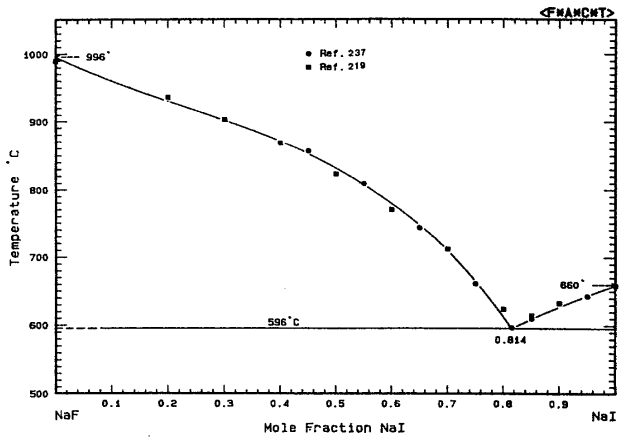

FIG. 49. The system NaF(A) + NaI(B).

shallow minimum and complete solid solubility at the liquidus temperature. Data for the minimum are summarized as follows:

T/°C	x_B	Ref.
765	~0.25	259
744	≈0.3	263
743	0.4	189
738	0.16	264
731	0.28	265
740	0.50	198

Data in Refs. 189, 263, and 264 have been tabulated and in Ref. 259 appear on a phase diagram only. Liquidus data of Refs. 189, 263, and 264 show up to 10 °C scatter, especially near the minimum. One reported melting point is lower than accepted (Ref. 264, by 5 °C) and two NaCl melting points higher (Refs. 263 and 189, by 7 and 4 °C, respectively). Thus, as a guide for the present calculations the data points of Gromakov and Gromakova[264] on the NaCl side, and of Amadori[263] and Bellanca[189] on the NaBr side were retained.

Solidus data points were obtained from cooling curves in Refs. 189 and 264. These solidi differ by as much as 10 °C. The data of Bellanca[189] indicate that liquidus and solidus are 2–3 °C apart at the minimum, which is not thermodynamically permitted.

The excess enthalpy of the liquid has been measured by direct calorimetry by Kleppa and co-workers[244,245] and others,[193,266] in the range 800–860 °C. The most extensive data are the more recent of Kleppa[245] at 811 °C and are used here:

$$H^E(l) = x_A x_B (293 + 105 x_B) \text{ J mol}^{-1}. \quad (137)$$

The activity of NaBr in the liquid has been deduced from emf measurements at 800 °C.[268–271]

The enthalpy of formation of metastable solid solutions at 25 °C has been measured calorimetrically in two independent studies.[126,267] Data of both studies may be represented by the equation:

$$H^E(s) = 5490 x_A x_B \text{ J mol}^{-1} \quad (138)$$

with a rms deviation of 40 J mol^{-1}.

A phase diagram was calculated with the use of Eqs. (137) and (139):

$$G^E(s) = x_A x_B (5490 - 2.373T) \text{ J mol}^{-1} \quad (139)$$

with the assumption that $S^E(l) = 0$. Equation (139) was based on Eq. (138) and the liquidus defined by data of Refs. 189, 263, and 264. The calculated minimum is 741 °C, $x_B = 0.24$. The calculated liquidus is within 5 °C of the selected reference data points.[189,263,264] The calculated solidus falls closer to Bellanca's[189] than to Gromakov's[264] on the NaCl side, where differences are not masked by experimental scatter. Equation (139) reproduces the excess enthalpies of Eq. (138) exactly. The calculated consolute temperature for solid demixing is 15 °C (there are no experimental data for comparison).

Probable maximum inaccuracy in calculated liquidus (Fig. 50): ± 5 °C.

Probable maximum inaccuracy in calculated solidus (Fig. 50): ± 10 °C.

NaCl(A)+NaI(B)

Data defining the liquidus were obtained from thermal analysis[237,272] and the visual-polythermal method.[273] Data were tabulated in each case. Reported eutectic data are summarized in the following table:

T/°C	x_B	Ref.
578	0.63	272
573	0.615	237
585	0.625	273
570	0.625	265

The liquidus of the most recent work[237] was taken as a guide for the present calculations.

The limits of the eutectic isothermal were determined from thermal analysis by Ref. 272 as $x_B = 0.04, 0.75$ and by Ref. 265 as $x_B = 0.023, 0.76$. In addition, Amadori[272] obtained two points on the NaI solidus. The activity of NaBr in the liquid at 800 °C has been deduced from emf measurements.[269]

The excess enthalpy of the liquid has been measured by direct calorimetry at 812[245] and 860 °C.[274] The data of Melnichak and Kleppa[245] are both more numerous and cover a wider concentration range than the earlier work,[274] and these[245] therefore are used here:

$$H^E(l) = x_A x_B (1619 + 640 x_A) \text{ J mol}^{-1}. \quad (140)$$

Two excess entropy terms for the liquid were included

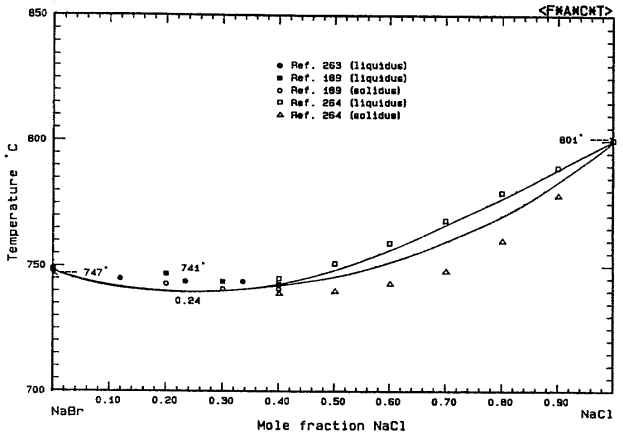

FIG. 50. The system NaBr(A) + NaCl(B).

$$S^E(l) = x_A x_B (0.2 + 4.6x_B) \text{ J mol}^{-1} \text{ K}^{-1} \quad (141)$$

in order to reproduce the experimental liquidus.[237]

Two solid solution Henrian activity coefficients, relative to the solid standard state, were calculated to reproduce the experimental limits of solid solubility[265,272] at the eutectic temperature. They were assumed to be temperature independent. For NaI in NaCl:

$$RT \ln \gamma_B = 21\,066 \text{ J mol}^{-1}; \quad (142)$$

and for NaCl in NaI:

$$RT \ln \gamma_A = 9649 \text{ J mol}^{-1}. \quad (143)$$

A phase diagram calculated with Eqs. (140)–(143) showed a calculated eutectic of 574 °C, $x_B = 0.60$. The calculated limits of solid solubility at the eutectic temperature are $x_B = 0.04$, 0.76. The calculated liquidus falls with 5 °C of the experimental,[237] and the calculated NaI solidus is within 10 °C of the two experimental points.[272]

Probable maximum inaccuracy in calculated diagram (Fig. 51): + 10 °C.

NaBr(A)+NaI(B)

Data defining the liquidus have been obtained from thermal analysis and tabulated in two studies.[263,275] Reported data for the minimum are summarized as follows:

T/°C	x_B	Ref.
645	0.7084	263
650	0.65	275
636	0.67	265
635	0.76	276

The minimum is shallow and neither its temperature nor composition is known very precisely. Of the two tabulated sets of data,[263,275] Obukhov[275] reports a NaI melting point 10 °C higher than the accepted value; Amadori's[263] is 2 °C higher. Thus although Amadori's is the older work, it was chosen for the present calculations since the minimum is on the NaI side of the diagram. On the NaBr side, the two liquidi[263,275] agree within 5 °C. The activity of NaBr in the liquid at 800 °C has been deduced from emf measurements.[269]

The excess enthalpy of the liquid has been measured by direct calorimetry at 812 °C by Melnichak and Kleppa,[245] whose result is used here:

$$H^E(l) = x_A x_B (632 + 21x_A) \text{ J mol}^{-1}. \quad (144)$$

The enthalpy of formation of metastable solid solutions has been measured calorimetrically at 25 °C [126] and the results can be represented by the following equation:

$$H^E(s) = 10\,041 x_A x_B \text{ J mol}^{-1} \quad (145)$$

within 120 J mol^{-1}. An x-ray study of a 1:1 solid at room temperature revealed limited solubility.[149] There are no reported measurements of the solidus.

A phase diagram was calculated, based on Eq. (144), with $S^E(l) = 0$, and the following temperature-independent excess Gibbs energy of the solid:

$$G^E(s) = x_A x_B (6730 - 1600x_B) \text{ J mol}^{-1}. \quad (146)$$

The calculated minimum is 645 °C, $x_B = 0.69$. The calculated consolute temperature for solid demixing is 92 °C, and the calculated limits of solubility at 25 °C are $x_B = 0.11$ and 0.78. These results are consistent with experiment.[149] The calculated liquidus lies within 5 °C of the experimental data.[263]

Probable maximum inaccuracy of calculated liquidus (Fig. 52): ± 5 °C.

Probable maximum inaccuracy of calculated solidus (Fig. 52): ± 10 °C.

c. Potassium

KCl(A)+KF(B)

Data defining the liquidus were obtained from thermal analysis and tabulated in Ref. 249. In that report the experimental melting point of KF is 11 °C higher than the accepted value. A summary of reported eutectic data is as follows:

T/°C	x_B	Ref.
605	0.45	249
603	0.45	256
606	0.45	277
605	0.461	258

Plato[249] observed eutectic arrests in the interval $0.1 < x_B < 0.92$. The limiting liquidus slope at the KF extreme does not suggest the presence of solid solubility there. At the KCl extreme, the slope is consistent with a solid solution of as much as 8 mol % KF in KCl at the eutectic temperature. In the absence of other data, however, this figure

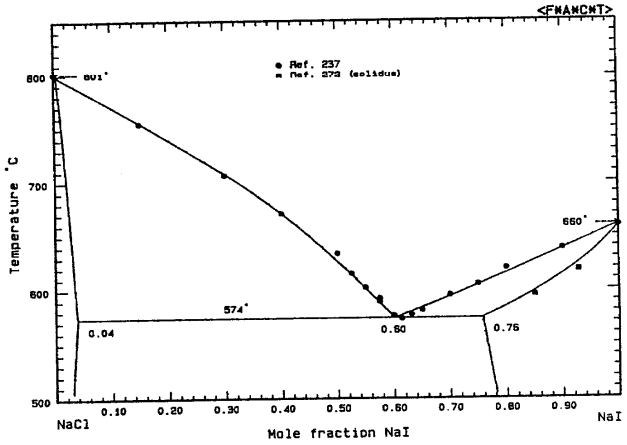

FIG. 51. The system NaCl(A) + NaI(B).

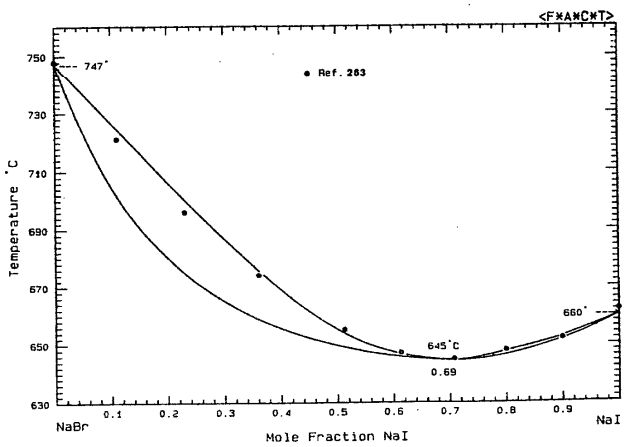

FIG. 52. The system NaBr(A) + NaI(B).

cannot be sustained. Zero solid solubility was therefore assumed at both extremes in the present calculations.

There are no reports of the excess enthalpy of the liquid, and so three coefficients were calculated from a thermodynamic optimization performed on the data[249]:

$$H^{E}(1) = x_A x_B (3066 - 10\,621 x_B + 9125 x_B^2)\ \text{J mol}^{-1}. \quad (147)$$

This quantity was assumed to be independent of temperature. Here, $S^{E}(1)$ was assumed to be zero. A phase diagram calculated with the use of Eq. (147) shows a calculated eutectic of 605 °C, $x_B = 0.45$. The calculated liquidus lies within 5 °C of the experimental data.[249]

Probable maximum inaccuracy in calculated diagram (Fig. 53): ± 15 °C.

KBr(A)+KF(B)

Data defining the liquidus were obtained from thermal analysis[178,278] and by the visual-polythermal method.[51] The data are tabulated in Refs. 51 and 278 and appear only as points on a phase diagram in Ref. 178. In this latter case,[178] the data points were read off the published diagram. A summary of reported eutectic data is as follows:

T/°C	x_B	Ref.
582	0.40	278
585	0.39	178
576	0.40	51
580	0.40	180
576	0.40	260

Liquidi of Refs. 178 and 51 are consistent with each other, while that of Ref. 278 differs by as much as 20 °C from Refs. 51 and 178. The later data[51,178] were therefore chosen for the present calculations. There are no reported measurements of the excess enthalpy of the liquid.

Eutectic arrests were observed[278] in the interval $0.03 \leqslant x_B \leqslant 0.97$, and the limiting liquidus slopes[51,178] indicate little or no solid solubility at either extreme. None was assumed in the present work.

Two excess enthalpy coefficients were calculated from the combined liquidus data points of Refs. 51 and 178:

$$H^{E}(1) = x_A x_B (-1034 + 401 x_B)\ \text{J mol}^{-1} \quad (148)$$

and this quantity was assumed to be temperature independent. $S^{E}(1)$ was assumed to be zero. The phase diagram calculated with Eq. (148) has a calculated eutectic of 580 °C, $x_B = 0.403$. The calculated liquidus lies within 10 °C of the experimental points.[51,178]

Probable maximum inaccuracy in calculated diagram (Fig. 54): ± 10 °C.

KF(A)+KI(B)

Data defining the liquidus have been obtained in two studies,[219,259] both by thermal analysis. Only in Ref. 219 are the data tabulated, and these were taken as a guide for the present calculations. In neither case[219,259] were eutectic arrests reported. The data for the eutectic may be summarized as follows:

T/°C	x_B	Ref.
580	0.7	259
544	0.66	219, 220

The limiting liquidus slopes at either extreme[219] do not indicate solid solubility, and none was assumed in the present work.

There are no reported measurements of the excess enthalpy of the liquid. Two coefficients were calculated from an optimization of the liquidus data[219]:

$$H^{E}(1) = x_A x_B (2230 - 6473 x_B)\ \text{J mol}^{-1}. \quad (149)$$

This quantity was assumed to be independent of temperature. Here, $S^{E}(1)$ was assumed to be zero. A phase diagram calculated with Eq. (149) shows a calculated eutectic of 543 °C, $x_B = 0.67$. The calculated liquidus lies within 10 °C of the experimental data.[219]

Probable maximum inaccuracy in calculated diagram (Fig. 55): ± 10 °C.

KBr(A)+KCl(B)

Data defining the liquidus have been obtained in several studies,[145,189,259,279,280] all by thermal analysis. The data are tabulated in Refs. 189, 279, and 280 and appear only as points on a phase diagram in Refs. 145 and 259. A summary of data for the minimum is given as follows:

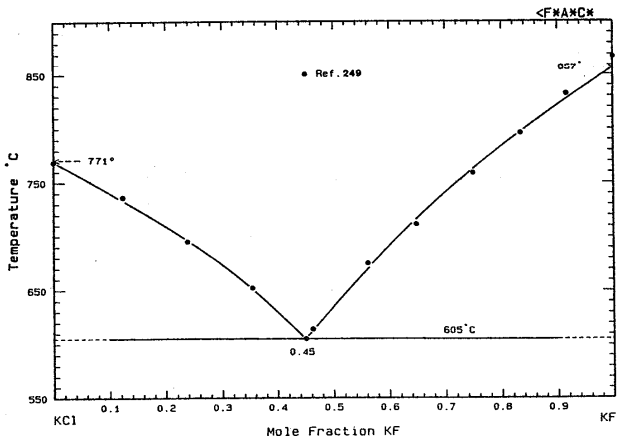

FIG. 53. The system KCl(A) + KF(B).

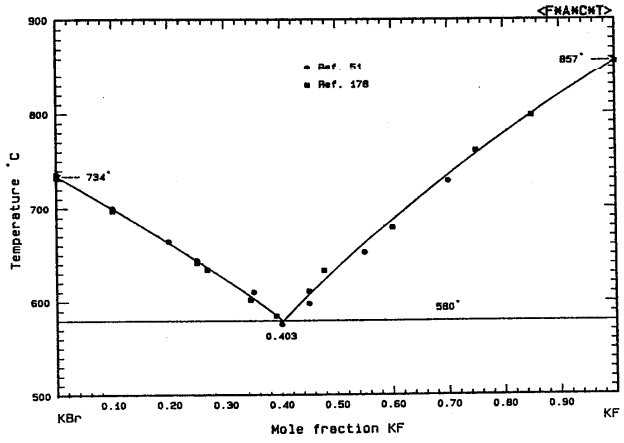

FIG. 54. The system KBr(A) + KF(B).

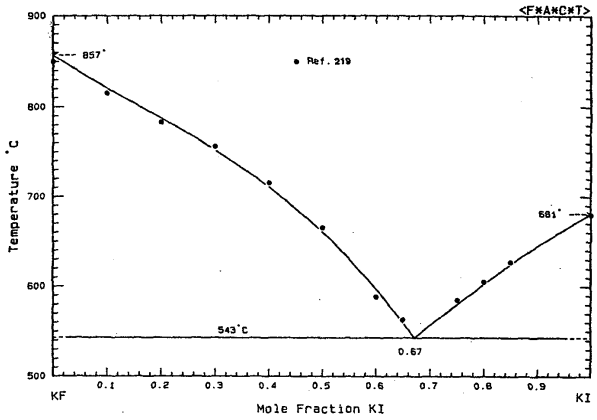

FIG. 55. The system KF(A) + KI(B).

T/°C	x_B	Ref.
740	0.32	259
716	0.4	279
734	0.32	280
728	0.30	189
740	0.32	145
720	0.3	198

The differences between observed and accepted melting points of the pure salts are appreciable: KBr (-2 to $+16$ °C) and KCl (-2 to $+19$ °C). In this respect the latest report[198] is closest to accepted values, and so the true minimum temperature is here taken to be more probably nearer to 720 °C than to the higher observed values.

The activity of KBr in the liquid at 800 °C has been deduced from emf measurements.[270,271]

Points on the solidus were obtained by thermal analysis in two of the studies.[189,279] The two experimental solidi are in poor agreement. Solid solutions, prepared from quenched melts, were examined by x-ray diffraction at room temperature.[148,281] The results indicate complete miscibility.

The excess enthalpy of the solid has been measured calorimetrically at 25 °C by a number of authors.[282,285–289] The solutions were prepared from quenched melts[282,285–288] or by crystallization from aqueous solution.[289] The results of all these studies can be represented by the expression:

$$H^E(s) = (3780 \pm 400)x_A x_B \text{ J mol}^{-1}. \quad (150)$$

The excess Gibbs energy of solid solutions at 25 °C was derived from the solubilities of the single and mixed salts in aqueous solution and the measured activity coefficients in saturated aqueous solution.[290] The results may be represented by the following equation:

$$G^E(s) = (3300 \pm 170)x_A x_B \text{ J mol}^{-1}. \quad (151)$$

The excess Gibbs energy of solid solutions at 700 °C was derived from equilibration of solutions with HCl–HBr mixtures,[291] and the result is

$$G^E(s) = (5020 \pm 840)x_A x_B \text{ J mol}^{-1}. \quad (152)$$

A third determination of $G^E(s)$ is reported by Miller and Skudlarski[283] from mass spectrometry:

$$G^E(s) = (1944 \pm 123)x_A x_B \text{ J mol}^{-1}. \quad (153)$$

Equations (150)–(153) suggest that the excess entropy of the solid is close to zero.

Mustajoki[284] measured the heat capacity of mixed crystals and the pure salts by an adiabatic method in the temperature interval 50–450 °C. His results were not precise enough to be used in an optimization.

The excess enthalpy of the liquid has been measured by direct calorimetry at temperatures between 800 and 890 °C.[193,244,245] The earlier data[193,244] are very sparse, and so Kleppa's later results[245] are used here:

$$H^E(l) = x_A x_B (146 + 109x_B) \text{ J mol}^{-1}. \quad (154)$$

A phase diagram was calculated with the use of Eqs. (154) and (155):

$$G^E(s) = 3500x_A x_B \quad (155)$$

both quantities being assumed independent of temperature. The calculated minimum is 717 °C, $x_B = 0.36$. The calculated consolute temperature for solid demixing is -66 °C. The phase diagram, as calculated, is deemed to be a reasonable representation of the experimental data, which are not in good accord among themselves. In addition, the value chosen for $G^E(s)$, Eq. (155), is consistent with experimentally derived values, Eqs. (151) and (152).

Probable maximum inaccuracy in calculated diagram (Fig. 56): ± 15 °C.

KCl(A)+KI(B)

Data defining the liquidus have been tabulated in six reports[106,273,279,280,292,293] and appear only as points on a phase diagram in Ref. 259. Le Chatelier[106] recorded the temperature at which crystals first appeared; the other investigators used thermal analysis. The system has been regarded by some as one within a minimum and complete solid solubility[106,273,279] or as a eutectic with limited solid solubility.[259,280,292,293] The data for the minimum and eutectic may be summarized as follows:

	T/°C	x_B	Ref.
Eutectic	600	0.51	280
	598	0.51	292
	637	0.53	259
	598	0.5	293
Minimum	580	≈0.5	106
	584	0.55	279
	≈590	0.55	273

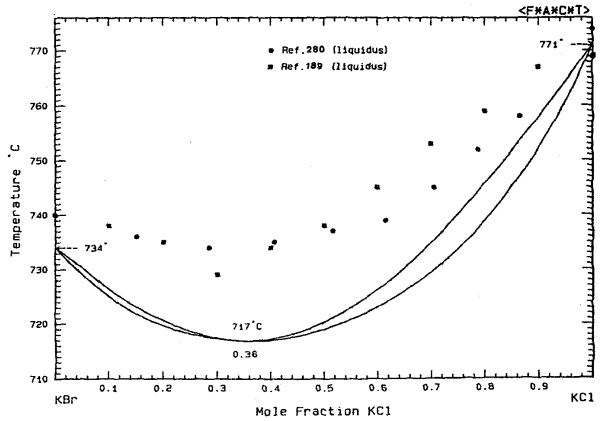

FIG. 56. The system KBr(A) + KCl(B).

The scatter among the liquidus data points of the later investigators[273,279,280,292,293] is as much as 24 °C, and the minimum (or eutectic) temperature is not well defined.

Points on the solidus were obtained by thermal analysis in Refs. 279, 280, and 292. All reports indicate extensive solid solubility on the KI side; this is confirmed by the limiting liquidus slope.[273,279,280,292,293] On the KCl side, the limiting slope indicates quite clear only limited solubility. Thus Wrzesnewsky's[279] solidus is in error, and support is given instead to Amadori's data.[280,292] His earlier[280] data indicate a KI solubility in KCl of 10 mol %, and his later re-investigation[292] indicates 5 mol %.

Wrzesnewsky[279] reported third temperature arrests, which are about 100 °C below his reported solidus. He ascribes this envelope to demixing of solid solutions. This is unlikely, as the envelope as reported is concave upward, whereas a solubility gap is indicated by a curve which is concave downward. Tamman and Ruppelt[175] recorded the onset and completion of turbidity in slowly heated and cooled solidified melts, as shown by transmitted light. At a given composition the transformation from complete translucence to complete turbidity occupied a temperature interval of between 50 and 100 °C. The data do not allow any unambiguous conclusion to be drawn, although the suggested general shape of the envelope is concave downward. Thus the nature of the solid state of this system has not been resolved by experiment.

The excess enthalpy of the liquid has been measured by direct calorimetry at 812 °C by Melnichak and Kleppa,[245] whose result is used here:

$$H^{E}(l) = x_A x_B (1238 + 268x_A) \text{ J mol}^{-1}. \quad (156)$$

A phase diagram was calculated with the use of Eq. (156) following Amadori,[280,292] with the assumption of limited solid solubility at the KCl side. Here, $S^{E}(l)$ was assumed to be zero. A Henrian activity coefficient for KI in KCl at the eutectic temperature was used:

$$RT \ln \gamma_B = 20\,000 \text{ J mol}^{-1}, \quad (157)$$

and the solid solution at the KI side was taken to be regular with an excess Gibbs energy given by

$$G^{E}(s) = 13\,500 x_A x_B \text{ J mol}^{-1}. \quad (158)$$

The quantities in Eqs. (156)–(158) were all assumed to be temperature independent. The calculate eutectic is 598 °C, $x_B = 0.497$ and the calculated liquidus is within 10 °C of experiment.[280,292] The calculated limits of solid solubility are $x_B = 0.04$, 0.55 at the eutectic temperature. The calculated solidus on the KI side falls below the experimental,[280] and for reasons stated above the solid phase boundaries of this system remain poorly defined.

Probable maximum inaccuracy in calculated liquidus (Fig. 57): ± 10 °C.

Probable maximum inaccuracy in calculated solidus (Fig. 57): ± 25 °C.

KBr(A)+KI(B)

Data defining the liquidus have been obtained in four studies,[259,279,280,294] all through thermal analysis. The data in Refs. 279 and 280 are tabulated and appear only as points on a phase diagram.[259,294] Points were read off the diagram in the latest work.[294] Data for the minimum may be summarized as follows:

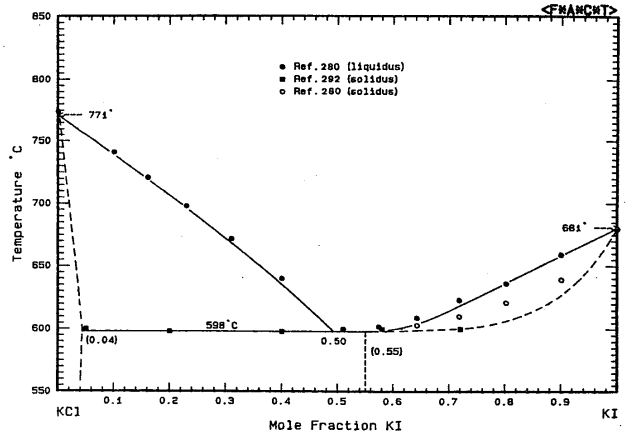

FIG. 57. The system KCl(A) + KI(B).

T/°C	x_B	Ref.
705	...	259
664	≈0.68	280
589	0.5	279
663	0.65	294

The liquidi of Refs. 280 and 294 are remarkably concordant (within 2 °C). The high minimum temperature of Ref. 259 is rejected because the melting points of the pure salts are 16 and 24 °C higher than accepted values. The low value[279] is rejected also because it entails a consolute temperature for solid–solid demixing of ≈450 °C, which is not supported by experimental data.[175,296] The liquidi of Refs. 280 and 294 were therefore chosen as a basis for the present calculations.

Data defining the solidus have been obtained by thermal analysis.[279,294] For the reason given above, Wrznewsky's[279] data are rejected and the data of the later work[294] are retained. The data were read off the published phase diagram.[294]

The excess enthalpy of the liquid has been measured by direct calorimetry at 812 °C by Melnichak and Kleppa,[245] whose result is used here:

$$H^{E}(l) = x_A x_B (452 - 13x_A) \text{ J mol}^{-1}. \quad (159)$$

The solid state of this system has been the object of a number of studies.[126,148,150,175,295–301] Lattice constants of quenched solid solutions, obtained by x-ray diffraction, are reported.[148,150,295,296] The optical transmission during heating and cooling was recorded.[175] The excess enthalpy of metastable quenched single-phase solid solutions has been measured calorimetrically at 25 °C[126] and the results may be represented by the following equation:

$$H^{E}(s, 25\,°C) = 7354 x_A x_B \text{ J mol}^{-1} \quad (160)$$

with a rms deviation of 74 J mol^{-1}. The excess Gibbs energy has been determined from the aqueous solubility isotherm, together with data from isopiestic measurements on saturated solutions of the single and mixed salts at 25 °C.[297] The results may be represented by the following equation:

$$G^{E}(s, 25\,°C) = 5151 x_A x_B \text{ J mol}^{-1} \quad (161)$$

with a rms deviation of 47 J mol^{-1}. Although the determination of this quantity is indirect, its magnitude is of the same order as H^E(s) in Eq. (160). This is its significance for the present considerations. The limits of solid solubility at 25 °C have been determined from x-ray studies and from the aqueous solubility isotherm. The results are summarized here:

x_B	Ref.	Method
0.07, 0.76	298	aq
0.06, 0.75	301	aq
···, 0.80–0.85	148	x ray
0.16, 0.89	297	aq
0.14, 0.80	299	aq
0.14, 0.79	300	aq
0.12, 0.80	296	x ray

From their x-ray study, Luova and Tannila[296] deduce a consolute point for solid–solid demixing of 205 °C, $x_B = 0.34$. From the optical transmission work,[175] it can be concluded only that the consolute temperature is above 200 °C and that the phase envelope is skewed toward the KBr side.

In the present analysis the solid solubility limits at room temperature[148,296,297,299,300] were taken as the basis, together with Eqs. (160) and (161), for the thermodynamic properties of the solid state at low temperature. The phase diagram calculated with the use of Eqs. (159) and (162), with $S^E(1) = 0$,

$$G^E(s) = x_A x_B (7067 - 2.743T) \text{ J mol}^{-1} \qquad (162)$$

shows a calculated minimum at 663 °C, $x_B = 0.67$, and the calculated liquidus and solidus lie within 2 °C of experimental data.[280,294] The calculated limits of solid solubility at 25 °C are $x_B = 0.14, 0.86$, in good agreement with the experiment. The calculated excess Gibbs energy at 25 °C, from Eq. (162), is $6250 x_A x_B$ J mol^{-1}, which compares favorably with the experiment, Eqs. (160) and (161). However, the calculated consolute point for solid–solid demixing is 88 °C, $x_B = 0.5$, which is significantly different from the experiment.[175,296] It is thus not possible to reconcile all the reported data on the solid state, and the calculated solid–solid phase boundary is only suggestive.

Probable maximum inaccuracy in calculated liquidus (Fig. 58): ± 2 °C.

Probable maximum inaccuracy in calculated solidus (Fig. 58): ± 4 °C.

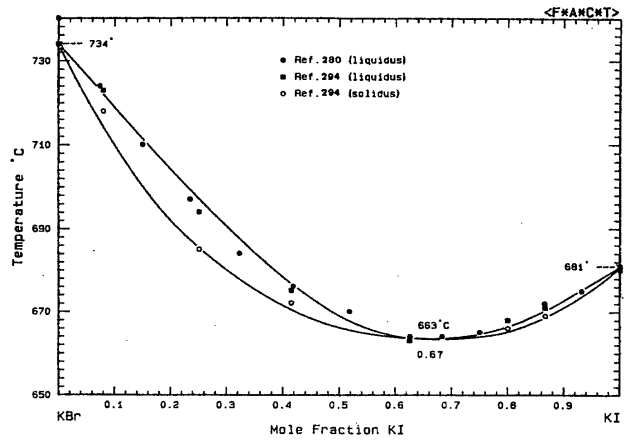

FIG. 58. The system KBr(A) + KI(B).

d. Rubidium

RbCl(A)+RbF(B)

Data defining the liquidus have been obtained by the visual-polythermal method and tabulated in Ref. 302. The reported eutectic is 545 °C, $x_B = 0.47$. Another determination of the eutectic alone was reported[37] as 532°, $x_B = 0.53$. Eutectic arrests were observed[302] only in the interval $0.3 < x_B < 0.6$. The limiting liquidus slope at the RbF extreme suggests little or no solid solubility; the data on the RbCl side do not extend far enough in order to allow an estimate of solubility. Zero solid solubility was assumed at both extremes.

No experimental excess enthalpy of the liquid is available, and so two coefficients for this quantity were calculated from the experimental data[302]:

$$H^E(1) = x_A x_B (5207 - 6894 x_B) \text{ J mol}^{-1}, \qquad (163)$$

which were assumed to be temperature independent. $S^E(1)$ was assumed to be zero. A phase diagram was calculated with the use of Eq. (163) and the calculated eutectic is 543 °C, $x_B = 0.48$. The observed[302] melting point of RbF is 13 °C lower than the accepted value. The calculated liquidus lies within 10 °C of the experimental[302] points.

Probable maximum inaccuracy in calculated diagram (Fig. 59): ± 15 °C.

RbBr(A)+RbF(B)

Data defining the liquidus are available in one study[184] obtained by thermal analysis. The data appear only as points in a phase diagram, from which they were read. The reported eutectic is 509 °C, $x_B = 0.46$. The authors observed the eutectic arrest only near the eutectic composition; the limiting liquidus slopes at either extreme indicate, however, little or no solid solubility. None was assumed in the present calculations. There are no reported data for the excess enthalpy of the liquid.

Three excess enthalpy coefficients for the liquid were calculated from the experimental liquidus data:

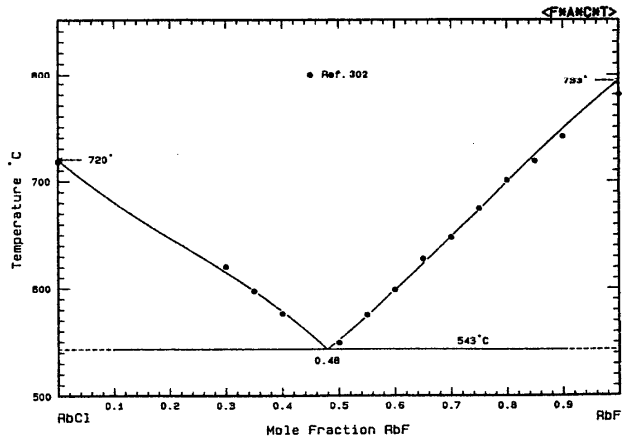

FIG. 59. The system RbCl(A) + RbF(B).

$$H^E(1) = x_A x_B(-1628 - 407x_B - 2254x_B^2)\ \text{J mol}^{-1}. \quad (164)$$

This quantity was assumed to be temperature independent and $S^E(1)$ was taken to be zero. A phase diagram was calculated with the use of Eq. (164). The calculated eutectic is identical to the experimental[184] and the calculated liquidus lies within 2 °C of the experimental points.

Probable maximum inaccuracy in calculated diagram (Fig. 60): ± 5 °C.

RbF(A)+RbI(B)

No phase diagram or excess thermodynamic property data are available for this system. A tentative phase diagram can however be calculated, based on a few assumptions drawn from analogous alkali halide binary systems, all of which have been evaluated. Thus the present system is a member of the series M‖F,I (M = Li,Na,K,Rb,Cs). All the other members of this series are simple eutectics with little or no solid solubility (the same is true for the system Rb‖F,Br). Therefore, it is reasonable to suppose that the present system is a simple eutectic with zero solid solubility.

An estimate of the excess Gibbs energy of the liquid is needed. Systems closely analogous to the one under discussion are M‖F,I (M = K,Cs), and Rb‖F,Br. The excess enthalpy of the liquid at $x = 0.5$ for these three systems, deduced from the phase diagram data, are − 252, − 1620, and − 599 J mol^{-1}, respectively (the excess entropy of the liquid was assumed to be zero in all cases). On the assumption that, for the present system, $S^E(1) = 0$ and that the liquid is a regular solution with an excess enthalpy given by

$$H^E(1) = -3700 x_A x_B\ \text{J mol}^{-1}, \quad (165)$$

i.e., approximately a mean of the neighboring analogous systems M‖F,I (M = K,Cs), a phase diagram was calculated. The calculated eutectic is 485 °C, $x_B = 0.57$. This eutectic temperature is a reasonable interpolation from the two neighboring analogous systems, as may be seen in the table:

Melting points (°C)

A	B
KF (857)	KI (681)
RbF (793)	RbI (647)
CsF (703)	CsI (640)

Eutectic

°C	x_B
543	0.671
485	0.57
431	0.533

Probable maximum inaccuracy in calculated diagram (Fig. 61): ± 30 °C.

RbBr(A)+RbCl(B)

Data defining the liquidus have been obtained by the visual-polythermal method and tabulated in two reports.[303,304] A summary of the available data for the minimum is given by the following:

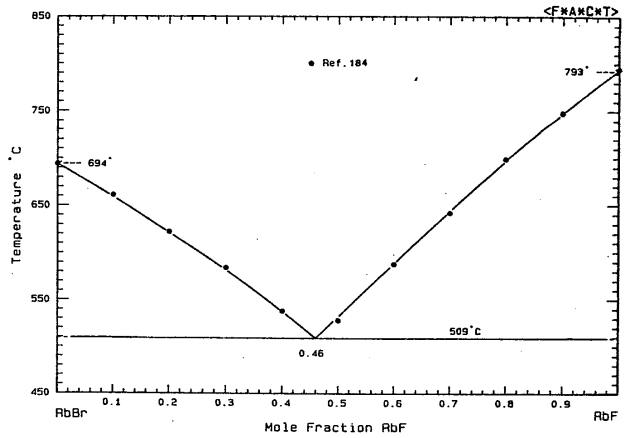

FIG. 60. The system RbBr(A) + RbF(B).

T/°C	x_B	Ref.
690	...	303
669	0.23	304
686	≈0.5	305

The minimum temperature cannot be defined easily in this work, since the melting points of the pure components (RbBr, 694 °C; RbCl, 720 °C) are quite close. In addition, the observed melting points[303–305] deviate from the accepted values appreciably: RbBr (− 4, − 13, and − 4 °C) and RbCl (+ 6 °C for all three reports). In Ref. 303 the liquidus is flat in the interval $0 \leqslant x_B \leqslant 0.65$.

Solid solutions over the entire composition range were examined by x-ray diffraction at 25 °C.[149,150,206,306] All reports indicated homogeneous solution. Hovi[307] estimated a consolute temperature for solid demixing of − 100 °C, from theoretical considerations.

The excess enthalpy of the liquid has been measured by direct calorimetry in three reports[244,245,308] at 800, 860, and 731 °C, respectively. The earlier data[244,308] are very sparse, but the later work[245] was performed over the entire composition range at a temperature closest to the liquidus temperatures. These results[245] are used here:

$$H^E(1) = x_A x_B(121 + 46x_B)\ \text{J mol}^{-1}. \quad (166)$$

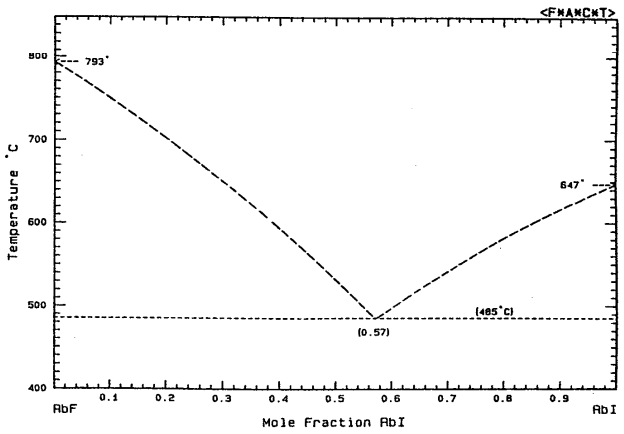

FIG. 61. The system RbF(A) + RbI(B).

A phase diagram was calculated with the use of Eqs. (166) and (167)

$$G^{E}(s) = 2000 x_A x_B \text{ J mol}^{-1}, \quad (167)$$

where both quantities were assumed to be temperature independent. $S^{E}(1)$ was assumed to be zero. The calculated minimum is 682 °C, $x_B = 0.38$, which is approximately the mean of the observed values.[303–305] The calculated consolute temperature for solid demixing is − 154 °C.

Probable maximum inaccuracy in calculated diagram (Fig. 62): ± 15 °C.

RbCl(A)+RbI(B)

Data defining the liquidus have been tabulated in two reports[309,310] from thermal analysis[310] and the visual-polythermal method.[309,310] Different investigators have described this system as one having a eutectic or a minimum; data for the eutectic or minimum may be summarized:

	T/°C	x_B	Ref.
Eutectic	563	0.55	309
	570	0.56	311
Minimum	560	0.55	310

There is no consensus on the extent of solid solubility in this system. Data defining the solidus were obtained[309] by thermal analysis. These investigators[309] state that solid solutions exist in the interval $0.125 \leqslant x_B \leqslant 1$. On the RbI side the liquidus of both studies[309,310] agree with 10 °C, but not elsewhere. The solidus points of Ref. 309 on the RbI side clearly suggest solid solubility as far as the eutectic. The limiting slopes of both liquidi,[309,310] however, are consistent only with zero solid solubility on this side of the diagram. Thus although both reported liquidi are remarkably concordant in this composition region, both are thermodynamically inconsistent with their authors' assumption of extensive solid solubility. There are no reported investigations of the solid state of this system at lower temperatures, which might help to resolve this question.

The excess enthalpy of the liquid has been measured by direct calorimetry at 740 °C[245] and the result is used here:

$$H^{E}(1) = x_A x_B (1138 - 63 x_A) \text{ J mol}^{-1}. \quad (168)$$

For the calculation of the phase diagram of this system, the choice between eutectic and minimum temperature types cannot be unambiguously made from reported data.[309,310] Preliminary attempts to reproduce the observed liquids by treating the system as a eutectic, with no or extensive solid solubility on both sides, were unsatisfactory. The calculated diagram shown in the figure was obtained with the assumption of complete solid solubility and the use of Eqs. (168) and (169) (both quantities were assumed to be temperature independent) and with $S^{E}(1) = 0$:

$$G^{E}(s) = x_A x_B (8943 + 4450 x_B) \text{ J mol}^{-1}. \quad (169)$$

The calculated minimum is 560 °C, $x_B = 0.58$. The calculated liquidus falls between the experimental points[309,310] on the RbCl side, but above the experimental points on the RbI side. This poor fit follows from the thermodynamic inconsistency mentioned earlier between the observed limiting liquidus slopes and the assumption of complete solid solubility. The analogous systems M||Cl,I (M = Na, K, or Cs) have all been treated successfully as involving extensive (but not complete) solid solubility. The entire phase diagram, as calculated, is tentative since it has not been possible to reconcile all the pertinent reported data. The calculated consolute point for solid–solid demixing is 440 °C, $x_B = 0.58$.

Probable maximum inaccuracy in calculated liquidus (Fig. 63): ± 20 °C.

RbBr(A)+RbI(B)

Data defining the liquidus have been obtained by the visual-polythermal method and tabulated in Ref. 304. The reported minimum is 618 °C, $x_B = 0.50$. A re-determination of the minimum alone[312] showed 617 °C, $x_B = 0.5$. Ahtee[150,313] examined solid solutions over the whole composition range by x-ray diffraction, and reported a consolute point for solid demixing at 76 °C, $x_B = 0.35$. The excess enthalpy of solid solution has been measured at 25 °C by solution calorimetry at the 1:1 composition[314] and in the intervals $x_B < 0.31$, $x_B > 0.74$.[315] Koski's[314] result is $H^{E}(s) = 1380$ J mol^{-1} at $x = 0.5$. From later x-ray measurements on the solid, it was reported that the consolute point is 149 °C, $x_B = 0.35$, and that the miscibility limits at room temperature are $x_B = 0.04, 0.82$.[332]

The excess enthalpy of the liquid has been measured by

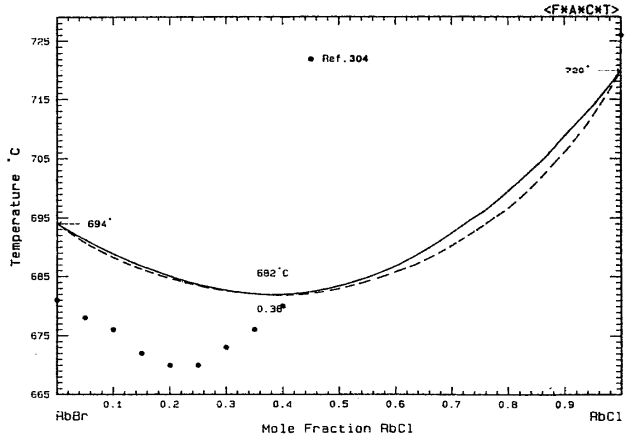

FIG. 62. The system RbBr(A) + RbCl(B).

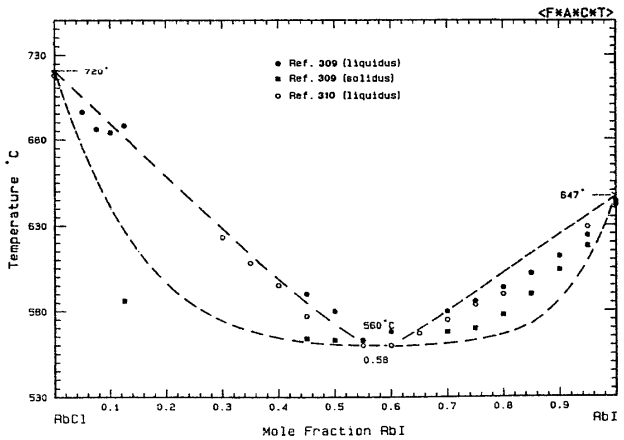

FIG. 63. The system RbCl(A) + RbI(B).

direct calorimetry at 740 °C by Melnichak and Kleppa,[245] whose result is used here:

$$H^E(1) = x_A x_B (418 - 59x_A) \text{ J mol}^{-1}. \quad (170)$$

A phase diagram was calculated with the use of Eqs. (170) and (171),

$$G^E(s) = x_A x_B (3700 + 3700x_A) \text{ J mol}^{-1}, \quad (171)$$

in which both quantities were assumed to be temperature independent. $S^E(1)$ was assumed to be zero. The calculated minimum is 618 °C, $x_B = 0.52$. The calculated liquidus follows the experimental[304] points within the error in the observed melting points of the pure salts (RbBr, 13 °C; RbI, 5 °C). The calculated consolute point for solid demixing is 115 °C, $x_B = 0.34$, which reproduces the observed asymmetry.[313,332] In addition, the temperature-independent $G^E(s)$ at $x = 0.5$, according to Eq. (171), is 1388 J mol^{-1}, which is the same as Koski's result[314] at 25 °C:

Probable maximum inaccuracy of calculated diagram (Fig. 64): ± 10 °C.

e. Cesium

CsCl(A)+CsF(B)

The only reported datum for this system is a determination of the eutectic by Bukhalova and Sementsova,[98] who supply neither tabulated nor plotted phase diagram data. Their result is 440 °C, $x_B = 0.49$. There are no data concerning solid solubility, but consideration of other eutectic systems of this type (Cs‖F,Br and Rb‖F,Cl) suggests little or no solubility; none was assumed in the present calculations. There are no experimental reported data for the excess enthalpy of the liquid or solid.

A phase diagram was calculated, based on an excess enthalpy of the liquid given by

$$H^E(1) = x_A x_B (2700 - 7713x_B) \text{ J mol}^{-1} \quad (172)$$

which was assumed to be temperature independent. The calculated eutectic is 440 °C, $x_B = 0.496$, which agrees with the experimental datum.[98] The calculated Pm3m→Fm3m transition for CsCl on the liquidus is 470 °C.

Probable maximum inaccuracy in calculated diagram (Fig. 65): ± 20 °C.

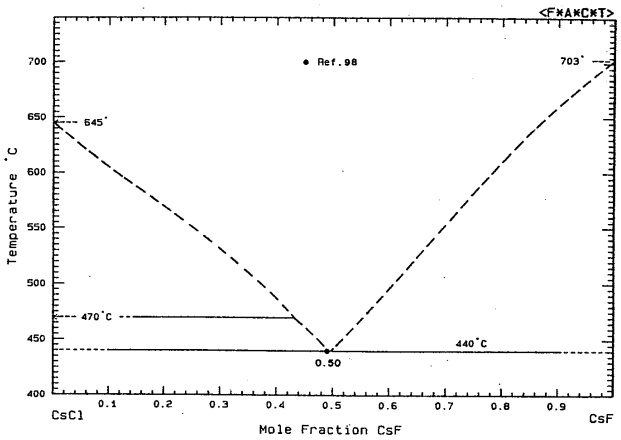

FIG. 65. The system CsCl(A) + CsF(B).

CsBr(A)+CsF(B)

Data defining the liquidus have been obtained by both thermal analysis and the visual-polythermal method and tabulated in Ref. 316. The observed eutectic is 438 °C, $x_B = 0.485$. The eutectic arrest was observed in the interval $0.025 \leqslant x_B \leqslant 0.975$ indicating little if any solid solubility. The limiting slopes at both extremes confirm this finding, and so zero solid solubility was assumed in the present calculations.

There are no reported data for the excess enthalpy of the liquid. Two excess enthalpy coefficients were calculated by an optimization performed on the observed[316] data:

$$H^E(1) = x_A x_B (-3414 - 1213x_B) \text{ J mol}^{-1}. \quad (173)$$

A phase diagram was calculated with the use of Eq. (173), with $S^E(1) = 0$, and the calculated eutectic is 436 °C, $x_B = 0.485$. The average deviation of the calculated liquidus from the experimental data[316] is 10 °C.

Probable maximum inaccuracy in calculated diagram (Fig. 66): ± 10 °C.

CsF(A)+CsI(B)

Data defining the liquidus have been obtained by both thermal analysis and visual-polythermal methods and tabulated in Ref. 316. The observed eutectic is 430 °C, x_B

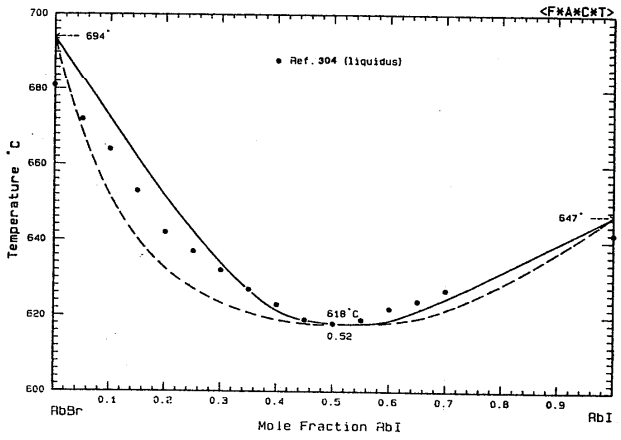

FIG. 64. The system RbBr(A) + RbI(B).

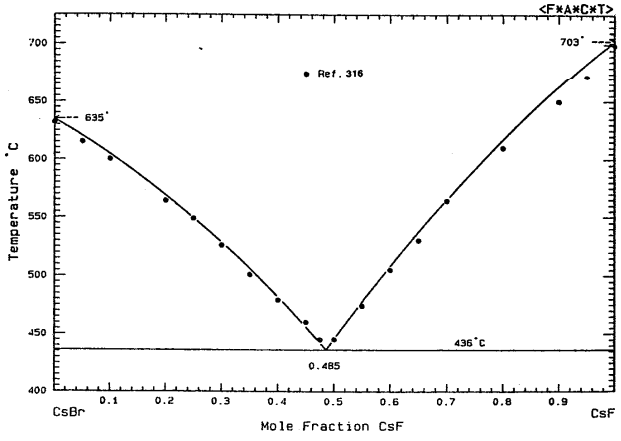

FIG. 66. The system CsBr(A) + CsF(B).

$= 0.535$. The eutectic arrest was observed in the interval $0.025 \leqslant x_B \leqslant 0.975$, indicating little or no solid solubility. This was confirmed by the limiting liquidus slopes at either extreme, and hence zero solid solubility was assumed in the present calculations. There are no reported data for the excess enthalpy of the liquid, and three coefficients were calculated from an optimization performed on the phase diagram data[316]:

$$H^E(1) = x_A x_B(-6523 + 5342x_B - 10\,517x_B^2)\ \text{J mol}^{-1}. \quad (174)$$

A phase diagram was calculated with the use of Eq. (174), with $S^E(1) = 0$, which shows a calculated eutectic of 431 °C, $x_B = 0.53$. The calculated liquidus lies within 10 °C of the experimental points,[316] except near the CsI extreme; the observed[316] melting point of CsI is however 19 °C lower than the accepted value.

Probable maximum inaccuracy in calculated diagram (Fig. 67): ± 15 °C.

CsBr(A)+CsCl(B)

Data defining the liquidus have been obtained by the visual-polythermal method and tabulated in Ref. 317. The system is described[317] as one having a minimum at 613 °C, $x_B = 0.425$. These authors assumed complete solid solubility at the liquidus temperature. Natarajan *et al.*[318] reported in another context the datum that the melting point of a solid solution at $x_B = 0.4$ was 614 °C. For the purpose of calculating a phase diagram, Il'yasov's[317] data were adopted as guide for the location of the liquidus. The temperature range covered by the solid–liquid phase diagram is remarkably small (≈30 °C), which might magnify the effect of errors in the observed[317] melting points of the pure salts (CsBr, + 6 °C; CsCl, − 5 °C).

The excess enthalpy of the liquid has been measured by direct calorimetry at 731,[245] 800,[244] and 860 °C.[274] The most recent results[245] are also the most complete, and are used here in the form:

$$H^E(1) = 63x_A x_B\ \text{J mol}^{-1}. \quad (175)$$

The solid state of this system has been the object of numerous studies Refs. 143, 149, 150, 156, 159, 160, 161, 281, 318, 319, 320, and 330. X-ray diffraction was used at room temperature[149,150,281,318,319,330] and at high temperature.[143,161,318,330] Also used were thermal analysis[143,156,161,318,330] and conductivity.[161,330] At room temperature the system is completely homogeneous. The Pm3m→Fm3m transition temperature of CsCl is raised by the addition of CsBr; the composition dependence[161,318,330] is obscured somewhat by apparent thermal hysteresis. Weijma and Arends[161] used both conductivity and thermal analysis, and the results of these methods are quite concordant. Their results are accordingly used here as a guide for the solid solution behavior of this system. Since the data[161] appear only in a diagram, points were read off the envelope at 0.1-mole fraction intervals, in the range $0.5 \leqslant x_B \leqslant 1$. The temperature spread of all reported CsCl transition temperatures, at a given composition, is between 30 and 50 °C.[161,318,330]

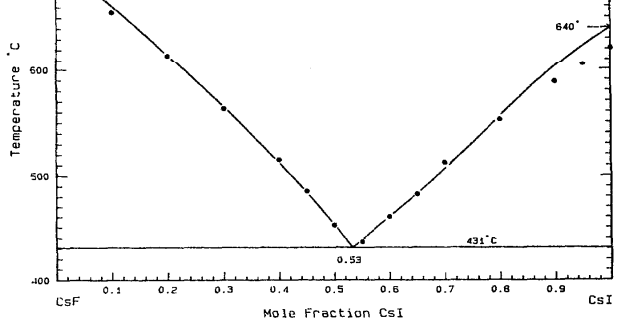

FIG. 67. The system CsF(A) + CsI(B).

Since, at the observed liquidus temperature, CsBr and CsCl exhibit different crystal structures, the phase diagram is expected to be one with a eutectic rather than a minimum and with a region of coexistence of the two solid phases. The phase diagram has been calculated on the assumption of the existence of two solid phases (α, CsCl-structure; β, NaCl-structure). The $\alpha \rightarrow \beta$ transition for CsBr is hypothetical, since the α-solid melts before transforming. Nevertheless, an extrapolated transition temperature of 880 °C[161] is assumed, with the following Gibbs energy of transformation:

$$\Delta_{trs}G\ (\text{CsBr}) = 4483 - 3.89T\ \text{J mol}^{-1}. \quad (176)$$

Weijma and Arends[161] obtained the hypothetical transition temperature by combining the known transition properties of CsCl with their measurements of the variation of the CsCl enthalpy of transition with CsBr content in solution. A simple thermodynamic equilibrium equation was used. The enthalpy and entropy of CsBr transition shown in Eq. (176) are not those deduced by Ref. 161, but are adjustable parameters obtained by fitting the calculated phase diagram to experimental data. The transition properties of CsCl and CsBr used in the present calculations may be compared in the table:

	T_{trs} (°C)	$\Delta_{trs}H$ (J mol^{-1})	$\Delta_{trs}S$ (J mol^{-1} K^{-1})
CsCl	470	3766	5.07
CsBr	880*	4483*	3.89*

where the asterisk indicates a hypothetical quantity. The data for CsCl in this table were taken from the standard reference used in the present work.[9] The two solid phases were assumed to be regular, with temperature-independent excess Gibbs energies given by

$$G^E(s,\alpha) = 1123x_A x_B\ \text{J mol}^{-1}, \quad (177)$$

$$G^E(s,\beta) = 0. \quad (178)$$

A phase diagram was calculated with the use of Eqs. (175) to (178). The calculated eutectic is 613 °C, $x_B = 0.43$, identical with the reported[317] minimum. The calculated liquidus agrees with the experimental[317] within the error limits of the melting points of the pure salts. The solid solubility limits at the eutectic temperature are $x_B = 0.39, 0.47$; such a narrow two-phase region is not easily detected by thermal

analysis or x-ray diffraction at high temperature. The calculated two-phase region, terminating at pure CsCl, falls within the envelope reported by Weijma and Arends.[161] The calculated solid–liquid two-phase regions are very narrow ($\approx$2 °C), which is corroborated by the results of zone-melting experiments.[305] The complete phase diagram [Figs. 68(a) and 68(b)], as calculated, represents experimental solid–liquid and solid–solid data in a thermodynamically consistent and faithful manner, given the uncertainties in experimental quantities. The solid phase boundaries must remain tentative, however, until more refined experimental work is done.

Probable maximum inaccuracy in calculated liquidus [Fig. 68(a)]: ± 5 °C.

CsCl(A)+CsI(B)

Data defining the liquidus have been tabulated in one investigation,[207] obtained by the visual-polythermal method. The reported eutectic is 502 °C, $x_B = 0.47$. Other authors,[321] using thermal analysis, reported solid solubility defined by $x_B = 0.15, 0.80$, and a eutectic at 493 °C, $x_B = 0.48$. Weyand,[143] who investigated this system briefly using thermal analysis, confirmed that the system is eutectic and reported solid solubility limits of $x_B < 0.1$ and > 0.88. He also reported that the CsCl Pm3m→Fm3m transformation temperature was decreased in the presence of CsI.

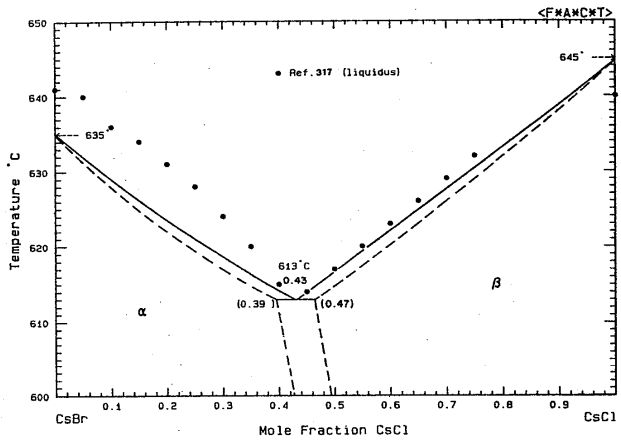

FIG. 68a. The system CsBr(A) + CsCl(B), high temperature.

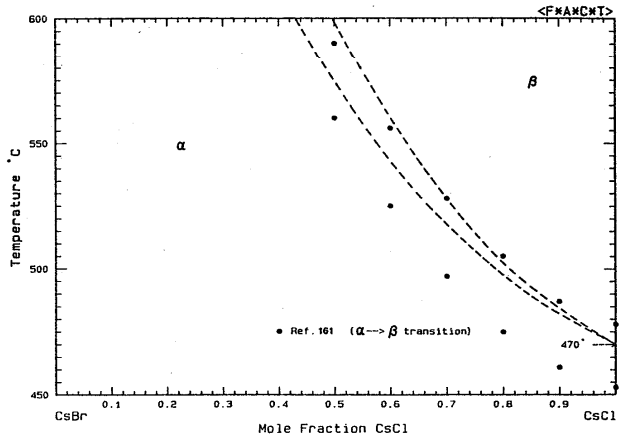

FIG. 68b. The system CsBr(A) + CsCl(B), low temperature.

The excess enthalpy of the liquid has been measured at 698 °C by direct calorimetry by Melnichak and Kleppa,[245] whose result is used here:

$$H^E(l) = x_A x_B (745 - 167 x_A) \text{ J mol}^{-1}. \quad (179)$$

Since, at the liquidus temperature, CsCl and CsI exhibit different crystal structures, two solid phases were assumed in order to calculate the phase diagram. A Henrian activity coefficient, relative to the solid standard state, was assigned to each phase:

For CsI in CsCl (NaCl-type structure)

$$RT \ln \gamma_B = 8418 \text{ J mol}^{-1}. \quad (180)$$

For CsCl in CsI (CsCl-type structure)

$$RT \ln \gamma_B = 12\,118 \text{ J mol}^{-1}. \quad (181)$$

The quantities in Eqs. (179) to (181) were all assumed to be temperature independent. A phase diagram was calculated with the use of these three quantities, which shows a calculate eutectic of 502 °C, $x_B = 0.48$, and solid solubility limits of $x_B = 0.24, 0.88$ at the eutectic temperature. The transformation temperature of pure CsCl is 470 °C, but this is not shown on the calculated diagram since there are no quantitative data on its composition dependence. The solid phase boundaries remain suggestive only, since there are few experimental data. The calculated liquidus is everywhere within 5 °C of the experimental[207] points.

Probable maximum inaccuracy in calculated liquidus (Fig. 69): ± 10 °C.

CsBr(A)+CsI(B)

Data defining the liquidus are tabulated in one study,[207] obtained by the visual-polythermal method. The observed minimum is 578 °C, $x_B = 0.48$. There are no data for the solidus. The excess enthalpy of the liquid has been measured at 698° by direct calorimetry by Melnichak and Kleppa,[245] whose result is used here:

$$H^E(l) = x_A x_B (364 - 15 x_A) \text{ J mol}^{-1}. \quad (182)$$

The limits of solid solubility at 25 °C have been determined by x-ray diffraction on the quenched melt[150] and by a radio isotopic analysis of the solid solution prepared from saturated aqueous solutions.[322] The results are indicated as follows:

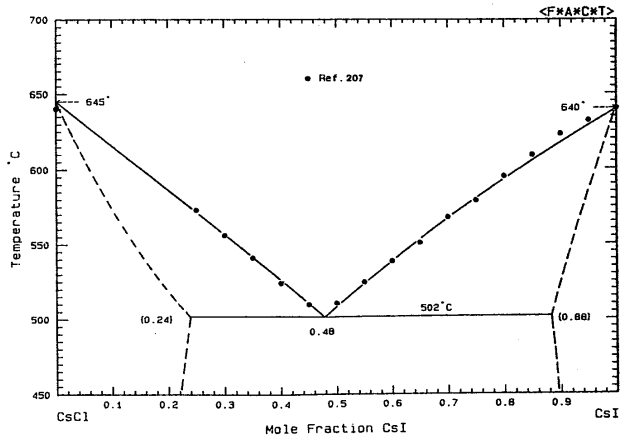

FIG. 69. The system CsCl(A) + CsI(B).

x_B	Ref.
0.06, 0.86	150
0.11, 0.82	322

The excess enthalpy of the solid at $x = 0.5$ has been measured by solution calorimetry[314] at 25 °C, and was found to be 2200 J mol^{-1}.

A phase diagram was calculated, with the use of Eqs. (182) and (183)

$$G^E(s) = 6500 x_A x_B \text{ J mol}^{-1} \quad (183)$$

both quantities being assumed independent of temperature. Equation (183) is a reasonable estimate, since the excess enthalpy (or excess Gibbs energy) of the solid at 25 °C may be represented by the function $8800 x_A x_B$.[314] The calculated minimum is 578 °C, $x_B = 0.49$. The calculated liquidus lies within 1 °C of the experimental[207] on the CsBr side, and within 8 °C on the CsI side, where there is much greater scatter in the measured data. The calculated solid miscibility limits at 25 °C are $x_B = 0.12, 0.88$, which are in good agreement with experiment.[150,322] The calculated consolute temperature for solid demixing is 113 °C.

Probable maximum inaccuracy in calculated liquidus (Fig. 70): ± 10 °C.

Probable maximun inaccuracy in calculated solidus (Fig. 70): ± 15 °C.

4. Acknowledgments

The authors would like to thank Dr. A. Carl Maso for his assistance with several of the evaluations. This work was supported in part by funds provided by the U.S. Department of Energy through the Joint Program on Critical Compilation of Physical and Chemical Data coordinated through the Office of Standard Reference Data, National Bureau of Standards (NBS), in support of the NBS–American Ceramic Society Phase Diagrams for Ceramists Data Center. Funds were also provided by the Natural Sciences and Engineering Research Council of Canada. Thanks are due to Daniel Cook for drawing and labeling the phase diagrams.

5. Appendix

In this section we present summaries of basic data input to (Table A1) and output from (Tables A2–A6 inclusive)

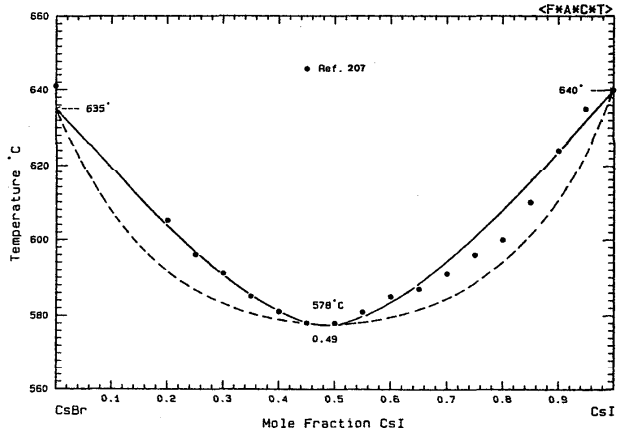

FIG. 70. The system CsBr(A) + CsI(B).

the evaluations of Sec. 3. Tables A7 and A8 are classificatory. Table A1 is self-explanatory.

Tables A2 and A3 summarize the excess thermodynamic properties of the liquid state for all systems, in the form of Legendre polynomial coefficients. A Legendre series is a series expansion in terms of orthogonal Legendre polynomials.[323] To three terms, the Legendre expansions for H^E and S^E are

$$H^E/x_A x_B = a_0 + a_1(2x_B - 1) + a_2(6x_B^2 - 6x_B + 1), \quad (A1)$$

$$S^E/x_A x_B = b_0 + b_1(2x_B - 1) + b_2(6x_B^2 - 6x_B + 1). \quad (A2)$$

The coefficients a_0, a_1, a_2, b_0, b_1, and b_2 may be obtained from the coefficients h_0, h_1, h_2, s_0, s_1, and s_2 of Eqs. (8) and (9) of Sec. 2 by simple linear combination. That is, Eq. (8) of Sec. 2, when truncated after three terms may be rearranged as

$$\frac{H^E}{x_A x_B} = \left(h_0 + \frac{h_1}{2} + \frac{h_2}{3}\right) + \left(\frac{h_1}{2} + \frac{h_2}{2}\right) x_B + \left(\frac{h_2}{6}\right) x_B^2 \quad (A3)$$

so that $a_2 = h_2/6$, $a_1 = (h_1 + h_2)/2$, and $a_0 = (h_0 + h_1/2 + h_2/3)$. Similar relationships permit b_0, b_1, and b_2 to be calculated from the coefficients s_0, s_1, and s_2.

The Legendre coefficients in Tables A2 and A3 were thus calculated from the power series coefficients given in Sec. 3 for each system. The advantage of the Legendre representation is that the coefficients a_1 and b_1 are uncorrelated due to the orthogonality condition. That is, the numerical value of any coefficient is independent of the total number of coefficients used in the series.[323] Hence, Legendre coefficients of several different binary solutions can be directly compared in searching for empirical correlations, whereas simple power series coefficients cannot. As an example of such an empirical correlation, in Fig. 71 the three Legendre coefficients a_0, a_1, and a_2 for the excess enthalpy of all Li-containing common-anion systems are plotted versus the ionic size parameter function $[(d_A + d_B)/(d_A - d_B)]^2$, where d is the collision diameter of the two ions of a salt [e.g., for NaCl, $d = (r_+ + r_-)$, where r_+ and r_- are the ionic radii]. This function is given by Conformal Ionic Solution Theory.[324] An approximate monotonic dependence is observed.

One of the results of the computer optimization of phase diagram data, described in Sec. 2, is the deduction of Gibbs energies of fusion and of formation of intermediate compounds, whether melting congruently or incongruently. Table A4 is a summary of such data for all compounds found in this evaluation.

Tables A5 and A6 summarize the excess thermodynamic properties of the solid state of those systems in which there is appreciable solid solubility. They are expressed either as regular (sometimes subregular) or Henrian solutions, according to case. Tables A7 and A8 are self-explanatory.

TABLE A1. Melting points (T°_{fus}) and Gibbs energies of fusion ($\Delta_{fus}G^\circ$) of pure halides[a] ($\Delta_{fus}G^\circ = a + bT + cT^2 + dT^3 + eT\ln T + f/T$ J mol^{-1})

	T°_{fus} (K)	$a\times10^{-3}$	b	$c\times10^{3}$	$d\times10^{6}$	e	$f\times10^{-5}$
LiF	1121.3	14.518	128.435	8.709	0	−21.494	−2.65
NaF	1269.0	10.847	156.584	4.950	0	−23.978	−1.07
KF	1130.0	13.763	127.035	7.211	0	−20.962	0
RbF	1066.0[b]	2.388	251.453	19.268	0	−39.367	2.51
CsF	976.0	3.451	176.219	8.872	0	−27.372	0
LiCl	883.0	4.420	197.318	16.435	0	−31.966	0
NaCl	1073.8	7.735	202.091	11.925	0	−31.824	0
KCl	1044.0	4.755	215.399	12.734	0	−33.581	1.82
RbCl	993.0[c]	7.759	96.729	5.209	0	−15.899	0
CsCl[d]	918.0	1.755	116.390	2.469	0	−17.673	0
LiBr	823.0	2.079	215.437	20.682	0	−35.070	2.97
NaBr	1020.0	18.327	75.124	6.657	0	−14.418	0
KBr	1007.0	17.680	2.955	−22.782	7.504	−0.703	−3.24
RbBr[e]	967.0[f]	10.054	110.999	5.335	0	−18.410	0
CsBr	908.0	1.890	189.667	5.419	0	−28.874	0
LiI	742.0	6.591	121.310	14.046	0	−21.275	0
NaI	933.0	13.940	88.680	6.027	0	−15.975	0
KI	954.0	4.656	211.209	14.460	0	−33.547	2.46
RbI[g]	920.0[h]	12.280	107.227	5.502	0	−18.410	0
CsI	913.0[i]	48.639	−358.103	−21.213	0	47.488	4.04

[a]Data have been taken from the standard Ref. 9 unless otherwise indicated.
[b]The melting point of RbF is that of Holm[24] who took particular care in its purification. The heat of fusion at this temperature is 22 930 J mol^{-1}, obtained from the heat content measurements of Kaylor, Walden, and Smith (Ref. 325).
[c]The melting point of RbCl has been updated (Ref. 136).
[d]The values given are for the β-form (high temperature) of CsCl. For the $\alpha\rightarrow\beta$ transition of this salt, the following thermodynamic quantities were used: $T^\circ_{trs} = 743$ K; $\Delta_{trs}G^\circ = -1806 + 87.773T + 8.580\times10^{-3}T^2 - 13.874T\ln T$ J mol^{-1}.
[e]The $\Delta_{fus}G^\circ$ of RbBr has been calculated on the assumption that the heat of fusion at the melting point is 22 868 J mol^{-1}. This corrected value was obtained from the entropy of fusion 23.648 J mol^{-1} K^{-1}, estimated by the interpolation method of Richter and co-workers (Ref. 326 and 327).
[f]The melting point of RbBr has been updated (Ref. 184).
[g]The $\Delta_{fus}G^\circ$ of RbI has been calculated on the assumption that the heat of fusion is 24 560 J mol^{-1}, as measured calorimetrically (Ref. 328).
[h]The melting point of RbI has been revised upward. A more recent representative value was taken from a standard reference (Ref. 329).
[i]The melting point of CsI has been revised upward (Ref. 207).

TABLE A2. Excess enthalpy and entropy of the liquid state for the 40 common-anion systems expressed as Legendre polynomials

$$H^E(l)/x_Ax_B = a_0 + a_1(2x_B - 1) + a_2(6x_B^2 - 6x_B + 1)\ \text{J mol}^{-1}$$
$$S^E(l)/x_Ax_B = b_0 + b_1(2x_B - 1) + b_2(6x_B^2 - 6x_B + 1)\ \text{J mol}^{-1}\ \text{K}^{-1}$$

System A-B	a_0	a_1	a_2	b_0	b_1	b_2
LiF-NaF	−7 381	184	0	−2.169	−0.562	0
LiF-KF	−18 275	1765	789	−2.948	1.573	0
LiF-RbF	−20 292	3138	0	−8.991	7.512	−5.663
LiF-CsF	−15 695	3726	921	0	0	0
NaF-KF	−335	0	0	2.541	0	0
NaF-RbF	375	0	0	−2.156	−0.282	−0.784
NaF-CsF	2 314	−1359	0	0	0	0
KF-RbF	360	0	0	0	0	0
KF-CsF	2 028	0	0	0	0	0
RbF-CsF	0	0	0	0	0	0
LiCl-NaCl	−4 686	0	0	0	0	0
LiCl-KCl	−17 758	189	0	−5.148	−2.479	0
LiCl-RbCl	−20 933	2408	663	−10.715	−3.363	0
LiCl-CsCl	−24 694	3723	1513	−18.899	−1.643	0
NaCl-KCl	−2 186	136	0	0	0	0
NaCl-RbCl	−3 389	168	0	−3.300	−2.623	0
NaCl-CsCl	−4 101	−209	0	−5.695	−5.832	0
KCl-RbCl	84	0	0	0	0	0
KCl-CsCl	795	0	0	0	0	0
RbCl-CsCl	335	0	0	0	0	0
LiBr-NaBr	−3 264	293	0	0	0	0

TABLE A2. (Continued)

System A-B	a_0	a_1	a_2	b_0	b_1	b_2
LiBr-KBr	− 14 428	878	327	− 1.441	− 1.819	0
LiBr-RbBr	− 18 857	2009	781	0	0	0
LiBr-CsBr	− 22 552	3242	648	− 6.648	− 11.029	2.509
NaBr-KBr	− 2 259	125	0	0	0	0
NaBr-RbBr	− 3 682	230	0	0	0	0
NaBr-CsBr	− 4 832	105	0	0	0	0
KBr-RbBr	0	0	0	0	0	0
KBr-CsBr	377	0	0	0	0	0
RbBr-CsBr	230	0	0	0	0	0
LiI-NaI	− 4 165	270	0	0	0	0
LiI-KI	− 12 805	1412	0	− 3.277	2.730	0
LiI-RbI	− 17 560	2176	0	− 0.934	6.254	0
LiI-CsI	− 21 175	3812	0	0	0	0
NaI-KI	− 2 217	105	0	0	0	0
NaI-RbI	− 3 767	199	0	− 4386	0	0
NaI-CsI	− 5 717	278	0	1.801	2.567	0
KI-RbI	− 80	0	0	0	0	0
KI-CsI	− 59	0	0	0	0	0
RbI-CsI	89	0	0	0	0	0

TABLE A3. Excess enthalpy and entropy of the liquid state for the 30 common-cation systems, expressed as Legendre polynomials

$$H^E(1)/x_A x_B = a_0 + a_1(2x_B - 1) + a_2(6x_B^2 - 6x_B + 1)\ \text{J mol}^{-1}$$

$$S^E(1)/x_A x_B = b_0 + b_1(2x_B - 1) + b_2(6x_B^2 - 6x_B + 1)\ \text{J mol}^{-1}$$

System A-B	a_0	a_1	a_2	b_0	b_1	b_2
LiF-LiCl	− 1000	0	0	0	0	0
LiF-LiBr	5960	− 4284	0	9.837	− 0.406	0
LiF-LiI	− 1391	0	0	− 4.556	4.386	− 1.344
LiCl-LiBr	136	− 57	0	0	0	0
LiCl-LiI	1707	− 314	0	0.643	− 1.561	0
LiBr-LiI	826	− 9	0	0	0	0
NaF-NaCl	2057	− 642	0	0	0	0
NaF-NaBr	1747	− 2448	0	0	0	0
NaF-NaI	4907	− 3832	0	0	0	0
NaCl-NaBr	345	− 53	0	0	0	0
NaCl-NaI	1939	− 320	0	2.5	2.3	0
NaBr-NaI	642	− 11	0	0	0	0
KF-KCl	798	749	1521	0	0	0
KF-KBr	− 833	− 200	0	0	0	0
KF-KI	− 1007	− 3237	0	0	0	0
KCl-KBr	170	− 55	0	0	0	0
KCl-KI	1372	− 134	0	0	0	0
KBr-KI	446	7	0	0	0	0
RbF-RbCl	1760	3447	0	0	0	0
RbF-RbBr	− 2583	1330	− 376	0	0	0
RbF-RbI	− 3700	0	0	0	0	0
RbCl-RbBr	144	− 23	0	0	0	0
RbCl-RbI	1107	32	0	0	0	0
RbBr-RbI	389	30	0	0	0	0
CsF-CsCl	− 1156	3857	0	0	0	0
CsF-CsBr	− 4020	607	0	0	0	0
CsF-CsI	− 7358	− 2588	− 1753	0	0	0
CsCl-CsBr	63	0	0	0	0	0
CsCl-CsI	662	84	0	0	0	0
CsBr-CsI	332	31	0	0	0	0

TABLE A4. Gibbs energies of fusion and of formation (from pure liquid components) of intermediate solid compounds calculated in this work

$\Delta_{fus}G^\circ = a + bT(\mathrm{K})$ J mol^{-1}

$\Delta_f G^\circ = a' + b'T(\mathrm{K})$ J mol^{-1}

Compound	a	b	a'	b'
(LiF)0.5(CsF)0.5	17 950	− 23.400	− 22 300	18.011
(LiF)0.5(RbF)0.5	13 700	− 18.316	− 18 811	14.093
(LiCl)0.5(RbCl)0.5	8 128.9	− 13.575	− 13 445	10.492
(LiCl)0.67(CsCl)0.33	16 340	− 24.519	− 22 172	24.336
(LiBr)0.5(RbBr)0.5	10 176	− 18.550	− 12 382	8.000
(LiBr)0.5(CsBr)0.5	11 559	− 19.802	− 11 438	6.000
(LiI)0.5(RbI)0.5	20 168	− 37.643	− 22 505	28.274

TABLE A5. Summary of the thermodynamic properties of the solid state in common-cation systems. Units: J mol^{-1}

System (A)-(B)	$G^E(s)/x_A x_B$	Henrian solutions
LiCl-LiBr	5000	
LiBr-LiI	8000	
NaCl-NaBr	5490 − 2.373 T(K)	
NaCl-NaI		$RT\ln\gamma_A = 9\,649$ $RT\ln\gamma_B = 21\,066$
NaBr-NaI	$6730 - 1600x_B$	
KCl-KBr	3500	
KCl-KI	(β-solid) 13 500	$RT\ln\gamma_B = 20\,000$
KBr-KI	7067 − 2.743 T(K)	
RbCl-RbBr	2000	
RbCl-RbI	$8943 + 4450x_B$	
RbBr-RbI	$3700 + 3700x_A$	
CsCl-CsBr	(α-solid) 1123 (β-solid) 0	
CsCl-CsI		$RT\ln\gamma_A = 12\,118$ $RT\ln\gamma_B = 8\,418$
CsBr-CsI	6500	

TABLE A6. Summary of the thermodynamic properties of the solid state in common-anion systems. Units: J mol^{-1}

System (A)-(B)	$G^E(s)/x_A x_B$	Henrian solutions
LiF-NaF		$RT\ln\gamma_A = 18\,895$
NaF-KF		$RT\ln\gamma_A = 24\,770$
KF-RbF	2500	
KF-CsF		$RT\ln\gamma_A = 10\,448$
RbF-CsF	2000	
LiCl-NaCl	$9800 - 5200x_B$	
NaCl-KCl	$14\,333 + 3278x_A + 32.796T(\mathrm{K}) - 5.598\,T\ln T$	
NaCl-RbCl		$RT\ln\gamma_A = 18\,325$ $RT\ln\gamma_B = 31\,027$
KCl-CsCl	$5957 + 6044x_A$	
RbCl-CsCl	2500	
LiBr-NaBr	$8500 - 1500x_B$	
NaBr-KBr	$11\,004 + 78.782T(\mathrm{K}) - 12.088\,T\ln T$	
KBr-RbBr	2000	
KBr-CsBr	(β-solid) 9000	$RT\ln\gamma_A = 8\,000$
RbBr-CsBr	(β-solid) $1000 + 2000x_B$	$RT\ln\gamma_A = 3\,000$
LiI-NaI	4000	
NaI-KI	$10\,014 + 3073x_A - 18.203\,T(\mathrm{K}) + 1.831\,T\ln T$	
NaI-RbI	15 190	
KI-RbI	1700	
KI-CsI	(β-solid) $5000 + 15\,000x_B$	$RT\ln\gamma_A = 15\,000$
RbI-CsI		$RT\ln\gamma_A = 4\,000$ $RT\ln\gamma_B = 4\,000$

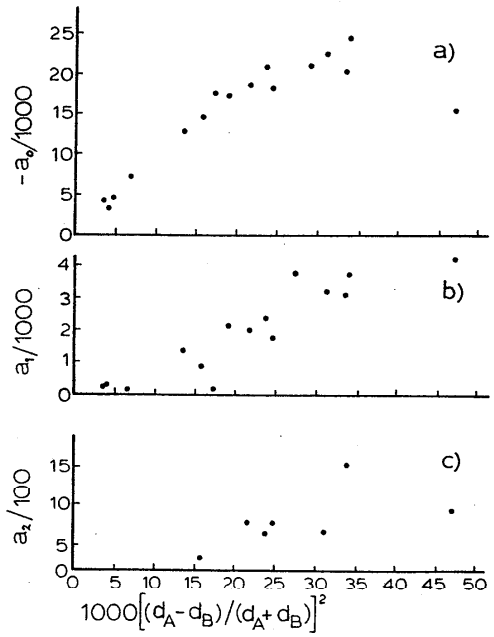

FIG. 71. The three Legendre polynomial coefficients (a_0,a_1,a_2) for the excess enthalpy function $H^E(l)/x_A x_B$ of the Li-containing common-anion systems. Source: Table A2. Unit: J mol^{-1}. The abscissa is the function of ionic radii, used by Reiss, Katz, and Kleppa (Ref. 324) and described in the text.

TABLE A7. Classification of the 70 binary alkali halide phase diagrams according to type

Common anion	Common cation
Simple eutectic[a]	
LiF-KF	LiF-LiCl
NaF-RbF	LiF-LiBr
NaF-CsF	LiF-LiI
LiCl-KCl	LiCl-LiI
NaCl-CsCl	NaF-NaCl
LiBr-KBr	NaF-NaBr
NaBr-RbBr	NaF-NaI
NaBr-CsBr	KF-KCl
LiI-KI	KF-KBr
LiI-CsI	KF-KI
NaI-CsI	RbF-RbCl
	RbF-RbBr
	RbF-RbI
	CsF-CsCl
	CsF-CsBr
	CsF-CsI
Eutectic (limited SS)[b]	
LiF-NaF	
NaF-KF	
NaCl-RbCl	
Eutectic (extensive SS)[c]	
KF-CsF	NaCl-NaI
KBr-CSBr	KCl-KI
RbBr-CsBr	CsCl-CsBr
NaI-RbI	CsCl-CsI
KI-CsI	
RbI-CsI	

TABLE A7. (Continued)

Common anion	Common cation
Eutectic (with compound)[d]	
LiF-RbF	
LiF-CsF	
LiCl-RbCl	
LiCl-CsCl	
LiBr-RbBr	
LiBr-CsBr	
LiI-RbI	
Complete SS[e]	
KF-RbF	LiCl-LiBr
RbF-CsF	LiBr-LiI
LiCl-NaCl	NaCl-NaBr
NaCl-KCl	NaBr-NaI
KCl-RbCl	KCl-KBr
KCl-CsCl	KBr-KI
RbCl-CsCl	RbCl-RbBr
LiBr-NaBr	RbCl-RbI
NaBr-KBr	RbBr-RbI
KBr-RbBr	CsBr-CsI
LiI-NaI	
NaI-KI	
KI-RbI	

[a] Very limited or no solid solubility, no compounds.
[b] Solid solubility less than 10 mol %.
[c] Solid solubility greater than 10 mol %.
[d] Congruently or incongruently melting compound.
[e] At liquidus temperature.

TABLE A8. Phase diagram types among series of binary alkali halide systems

Eutectics	Complete solid solubility
Common anion	
Li, K‖X(X = F, Cl, Br, I)	Li, Na‖X(X = Cl, Br, I)
Li, Rb‖X(X = F, Cl, Br, I)	Na, K‖X(X = Cl, Br, I)
Li, Cs‖X(X = F, Cl, Br, I)	K, Rb‖X(X = F, Cl, Br, I)
Na, Rb‖X(X = F, Cl, Br, I)	
Na, Cs‖X(X = F, Cl, Br, I)	
Common cation	
M‖F, X(M = Li, Na, K, Rb, Cs) (X = Cl, Br, I)	M‖Cl, Br(M = Li, Na, K, Rb) M‖Br, I(M = Li, Na, K, Rb, Cs)

6. References

[1] *Handbook of Solid–Liquid Equilibria in Systems of Anhydrous Inorganic Salts,* TT 69-55079/1, AEC-tr-6983/1, UC-4, edited by N. K. Voskresenskaya (U. S. Atomic Energy Commission and National Science Foundation, Washington, DC, 1970), Vol. 1.
[2] R. E. Thoma, Adv. Molten Salt Chem. **3**, 275 (1975).
[3] "Phase Diagrams of Nuclear Reactor Materials," ORNL-2548, edited by R. E. Thoma, Oak Ridge National Laboratory, Oak Ridge, TN, 1959.
[4] *Binary Phase Diagrams of Halide Salts,* U.S. Atomic Energy Commission Contract AT(30-1) 2723, edited by W. D. Robertson (Clearinghouse for Federal Scientific and Technical Information, Washington, DC, 1966), Vol. 2.
[5] *Physical Properties Data Compilations Relevant to Energy Storage. I. Molten Salts: Eutectic Data,* NSRDS-NBS 61, Part 1, edited by G. J. Janz, C. B. Allen, J. R. Downey, and R. P. T. Tomkins (National Bureau of Standards, Washington, DC, 1978).
[6] J. Wisniak, *Phase Diagrams: A Literature Source Book* (Elsevier, New York, 1981), Vols. 1 and 2.
[7] *Phase Diagrams for Ceramists,* edited by E. M. Levin, C. R. Robbins, H. F. McMurdie, R. S. Roth, T. Negas, and L. P. Cook (American Ceramic Society, Columbus, OH, 1964–1983), Vols. 1–5.
[8] J. Wisniak and A. Tamir, *Mixing and Excess Thermodynamic Properties: A Literature Source Book* (Elsevier, New York, 1978).
[9] I. Barin, O. Knacke, and O. Kubaschewski, *Thermochemical Properties of Inorganic Substances* (Springer, Berlin, 1977).
[10] C. W. Bale and A. D. Pelton, Metall. Trans. **14B**, 77 (1983).
[11] W. T. Thompson, C. W. Bale, and A. D. Pelton, "F*A*C*T (Facility for the Analysis of Chemical Thermodynamics) Users' Manual" (Programs FITBIN and POTCOMP) (Ecole Polytechnique/McGill University, Montreal, 1985).
[12] A. D. Pelton, "Phase Diagrams," in *Physical Metallurgy,* 3rd ed., edited by R. W. Cahn and P. Haasen (North–Holland, New York, 1983), p. 328.
[13] I. Ansara, Int. Metall. Rev. **24**, 20 (1979).
[14] P. J. Spencer and I. Barin, Mater. Eng. Appl. **1**, 167 (1979).
[15] A. D. Pelton and C. W. Bale, "Thermodynamic Analysis of Ionic Systems at High Temperature," NACE Symposium on High Temperature Corrosion, National Association of Corrosion Engineers, San Diego, CA, 1981.
[16] C. W. Bale and A. D. Pelton, CALPHAD J. **6**, 255 (1982).
[17] P. L. Lin, A. D. Pelton, and C. W. Bale, J. Am. Ceram. Soc. **62**, 414 (1979).
[18] L. S. Hersh and O. J. Kleppa, J. Chem. Phys. **42**, 1309 (1965).
[19] D. Topor and L. Topor, J. Chim. Phys. **68**, 1464 (1971).
[20] T. Forland and L. U. Thulin, Acta Chem. Scand. **21**, 1121 (1967).
[21] M. Itoh, T. Sasamoto, and T. Sata, Bull. Chem. Soc. Jpn. **54**, 3391 (1981).
[22] A. G. Bergman and E. P. Dergunov, C. R. Acad. Sci. URSS **31**, 755 (1941).
[23] N. N. Volkov and T. F. Shvab, Izv. Fiz.-Khim. Nauchno.-Issled. Inst. Irkutsk. Gos. Univ. **2**, 60 (1953).
[24] J. L. Holm, Acta Chem. Scand. **19**, 638 (1965).
[25] J. L. Holm and B. J. Holm, Thermochim. Acta **6**, 375 (1973).
[26] J. L. Holm and O. J. Kleppa, J. Chem. Phys. **49**, 2425 (1968).
[27] A. C. Macleod and J. Cleland, J. Chem. Thermodyn. **7**, 103 (1975).
[28] K. C. Hong and O. J. Kleppa. J. Chem. Thermodyn. **8**, 31 (1976).
[29] A. G. Bergman and S. P. Pavlenko, C. R. Acad. Sci. URSS **30**, 812 (1941).
[30] N. N. Volkov and L. A. Dubinskaya, Izv. Fiz.-Khim. Nauchno.-Issled. Inst. Irkutsk. Gos. Univ. **2**, 45 (1953).
[31] A. G. Bergman and N. A. Bychkova-Schul'ga, Russ. J. Inorg. Chem. **2**, 276 (1957).
[32] A. G. Bergman and V. P. Goryacheva, Russ. J. Inorg. Chem. **7**, 1359 (1962).
[33] E. Aukrust, B. Bjorge, H. Flood, and T. Forland, Ann. N.Y. Acad. Sci. **79**, 830 (1960).
[34] G. A. Bukhalova, Z. N. Topshinoeva, and V. G. Akhtyrskii, Zh. Neorg. Khim. **19**, 235 (1974).
[35] R. A. Gilbert, J. Phys. Chem. **67**, 1143 (1963).
[36] E. P. Dergunov, Dokl. Akad. Nauk SSSR **58**, 1369 (1947).
[37] N. N. Volkov and G. P. Tumash, Izv. Fiz.-Khim. Nauchno.-Issled. Inst. Irkutsk. Gos. Univ. **2**, 41 (1953).
[38] C. J. Barton, L. M. Bratcher, T. N. McVay, and W. R. Grimes, in "Phase Diagrams of Nuclear Reactor Materials," edited by R. E. Thoma, ORNL Report 2548, Oak Ridge National Laboratory, TN, 1959, p. 16.
[39] R. E. Thoma, Adv. Molten Salt Chem. **3**, 275 (1975).
[40] J. H. Burns and W. R. Busing, Inorg. Chem. **4**, 1510 (1965).
[41] G. Flor, C. Margheritis, and C. Sinistri, J. Chem. Eng. Data **24**, 361 (1979).
[42] G. A. Bukhalova and D. V. Sementsova, Russ. J. Inorg. Chem. **10**, 1024 (1965).
[43] E. M. Levin, C. R. Robbins, and H. F. McMurdie, *Phase Diagrams for Ceramists,* 1969 Supplement (The American Ceramic Society, Columbus, OH, 1969), Fig. 3332.
[44] See Ref. 38, p. 17.

[45]G. A. Bukhalova and Z. P. Babaeva, Russ. J. Inorg. Chem. **11**, 220 (1966).
[46]E. P. Babaeva and G. A. Bukhalova, Russ. J. Inorg. Chem. **11**, 351, (1966).
[47]G. A. Bukhalova and E. P. Babaeva, Russ. J. Inorg. Chem. **10**, 1027 (1965).
[48]G. A. Bukhalova and D. V. Sementsova, Russ. J. Inorg. Chem. **10**, 1029 (1965).
[49]D. L. Deadmore and J. S. Machin, J. Phys. Chem. **64**, 824 (1960).
[50]N. S. Kurnakov and S. F. Zhemchuzhnyi, Z. Anorg. Chem. **52**, 186 (1907).
[51]N. S. Dombrovskaya and Z. A. Koloskova, Izv. Sek. Fiz.-Khim. Anal. Inst. Obshch. Neorg. Khim. Akad. Nauk. SSSR **10**, 211 (1938).
[52]A. G. Bergman and I. N. Nikonova, Zh. Obshch. Khim. **12**, 449 (1942).
[53]A. G. Bergman and G. I. Nagornyi, Bull. Acad. Sci. URSS Classe Sci. Chim. **5**, 328 (1943).
[54]F. P. Platonov, Tr. Mosk. S'kh. Akad. **36**, 42 (1946).
[55]See Ref. 38, p. 19.
[56]R. G. Samuseva and V. E. Plyushchev, Russ. J. Inorg. Chem. **6**, 1092 (1961).
[57]Z. A. Mateiko, G. A. Bukhalova, and D. V. Sementsova, Izv. Vyssh. Uchebn. Zaved. Khim. Khim. Tekhnol. **10**, 856 (1967).
[58]E. P. Dergunov and A. G. Bergman, Zh. Fiz. Khim. **22**, 625 (1948).
[59]See Ref. 38, p. 20.
[60]R. G. Samuseva and V. E. Plyushchev, Russ. J. Inorg. Chem. **10**, 688 (1965).
[61]D. V. Sementsova and G. A. Bukhalova, Izv. Vyssh. Uchebn. Zaved. Khim. Khim. Tekhnol. **11**, 240 (1968).
[62]I. N. Belyaev and O. Ya. Revina, Russ. J. Inorg. Chem. **11**, 1041 (1966).
[63]S. Zhemchuzhnyi and F. Rambach, Z. Anorg. Chem. **65**, 403 (1910).
[64]W. Schaefer, Neues Jahrb. Mineral. Geol. Palaeontol. Abh. Abt. A **43**, 132 (1920).
[65]F. E. E. Lamplough, Proc. Cambridge Philos. Soc. **16**, 193 (1912).
[66]M. A. Klochko, Zh. Obshch. Khim. **3**, 1026 (1933).
[67]A. G. Bergman and E. K. Akopov, Izv. Sek. Fiz.-Khim. Anal. Inst. Obshch. Neorg. Khim. Akad. Nauk SSSR **23**, 222 (1953).
[68]A. S. Arabadzhan and A. G. Bergman, Russ. J. Inorg. Chem. **7**, 1152 (1962).
[69]G. A. Bukhalova and A. S. Arabadzhan, Russ. J. Inorg. Chem. **7**, 1154 (1962).
[70]S. D. Gromakov and L. M. Gromakova, Zh. Fiz. Khim. **27**, 1545 (1953).
[71]E. K. Akopov, Russ. J. Inorg. Chem. **1**, 148 (1956).
[72]A. K. Akopov and A. G. Bergman, Russ. J. Inorg. Chem. **11**, 937 (1966).
[73]A. G. Bergman, E. L. Kozachenko, and S. I. Berezina, Russ. J. Inorg. Chem. **9**, 663 (1964).
[74]T. P. Bortnikova, E. K. Akopov, and V. A. Ocheretnyi, Zh. Neorg. Khim. **19**, 1066 (1974).
[75]V. N. Derkacheva and K. V. Gontar, Zh. Prikl. Khim. (Leningrad) **50**, 668 (1977).
[76]A. N. Kruglov and M. E. Prostakov, Zh. Neorg. Khim. **26**, 1975 (1981).
[77]A. V. Storonkin, O. D. Grebennikova, I. V. Krivousova, I. V. Kozhina, and I. V. Vasil'kova, Vestn. Leningr. Univ. Fiz. Khim. **2**, 70 (1973).
[78]A. S. Chesnokov, Kh. L. Strelets, E. F. Klyuchnikova, and V. N. Veretinskii, Tr. Vses. Nauchno.-Issled. Proekten. Inst. Alyum. Magnievoi. Elektrodnoi. Promsti. **72**, 90 (1970).
[79]V. N. Derkacheva and E. Ya. Khardikova, Zh. Prikl. Khim. **48**, 1159 (1975).
[80]See Ref. 43, Fig. 3083.
[81]C. N. R. Rao and M. Natarajan, *Crystal Structure Transformations in Binary Halides*, NSRDS-NBS 41 (U.S. Dept. of Commerce, Washington, DC, 1972).
[82]T. M. Tsushba, B. S. Sherchenko, and I. K. Tovmas'yan, Zh. Neorg. Khim. **21**, 1894 (1976).
[83]A. Smits, J. Elgersma, and M. E. Hardenberg, Rec. Trav. Chim. Pays-Bas **43**, 671 (1924).
[84]L. S. Hersh and O. J. Kleppa, J. Chem. Phys. **42**, 1309 (1965).
[85]T. W. Richards and W. B. Meldrum, J. Am. Chem. Soc. **39**, 1816 (1917).
[86]H. Keitel, Neues Jahrb. Mineral. Geol. Palaeontol. Abh. Abt. **52A**, 378 (1925).
[87]E. Elchardus and P. Laffitte, Bull. Soc. Chim. France **51**, 1572 (1932).
[88]I. G. Murgulescu and S. Sternberg, Z. Phys. Chem. (Leipzig) **219**, 114 (1962).
[89]W. K. Behl, AD Report No. 752087, National Technical Information Service, Springfield, 1972.
[90]L. U. Thulin, O. Waernes, and T. Ostvold, Acta Chem. Scand. Ser. A **30**, 731 (1976).
[91]B. F. Markov, T. A. Fishura, and A. N. Budarina, Rev. Roum. Chim. **20**, 597 (1975).
[92]I. I. Il'yasov, K. I. Iskandarov, and Yu. G. Litvinov, Russ. J. Inorg. Chem. **21**, 473 (1976).
[93]H.-C. Gaebell, G. Meyer, and R. Hoppe, Mater. Res. Bull. **18**, 429 (1983).
[94]T. P. Bortnikova and E. K. Akopov, Zh. Neorg. Khim. **21**, 3158 (1976).
[95]E. Korreng, Z. Anorg. Chem. **91**, 194 (1915).
[96]E. P. Dergunov, Zh. Fiz. Khim. **25**, 584 (1951).
[97]I. I. Il'yasov, K. I. Iskandarov, M. Davranov, and R. N. Berdieva, Zh. Neorg. Khim. **20**, 250 (1975).
[98]G. A. Bukhalova and D. V. Sementsova, Zh. Neorg. Khim. **10**, 1886 (1965).
[99]D. S. Lesnykh and S. A. Chernyakhovskaya, Zh. Neorg. Khim. **12**, 3178 (1967).
[100]G. A. Bukhalova and V. M. Burlakova, Zh. Neorg. Khim. **11**, 2812 (1966).
[101]Zh. G. Moiseenko, E. K. Akopov, and L. A. Panieva, Zh. Neorg. Khim. **17**, 3098 (1972).
[102]I. I. Il'yasov, Yu. G. Litvinov, and M. K. Kydynov, Zh. Neorg. Khim. **21**, 1578 (1976).
[103]H.-C. Gaebell, G. Meyer, and R. Hoppe, Z. Anorg. Allg. Chem. **498**, 94 (1983).
[104]B. P. Burylev and V. L. Mironov, Izv. Ser.-Kavk. Nauchn. Tsentra Vyssh. Shk., Ser. Estestv Nauk **4**, 61 (1976).
[105]B. P. Burylev, Izv. Sev.-Kavk. Nauchn. Tsentra Vyssh. Shk., Ser. Estestv Nauk **3**, 67 (1982).
[106]H. Le Chatelier, Compt. Rend. Hebd. Acad. Sci. **118**, 350 (1894).
[107]H. Gensky, Neues Jahrb. Mineral. Geol. Palaeontol. Abh. Abt. A **36**, 513 (1913).
[108]K. Treis, Neues Jahrb. Mineral. Geol. Palaeontol. Beil. Abh. Abt. A **37**, 766 (1914).
[109]F. Landsberry and R. A. Page, J. Soc. Chem. Ind. **39**, 37 (1920).
[110]G. A. Abramov, Metallurgia. **10**, 82 (1935).
[111]A. G. Bergman and I. N. Nikonova, Zh. Obshch. Khim. **12**, 460 (1942).
[112]N. I. Myaz', Nauchn. Rab. Stud. L'vov Gosud. Univ. **2**, 25 (1949).
[113]E. Scheil and H. Stadelmaier, Z. Metallkd. **43**, 227 (1952).
[114]E. K. Akopov and A. G. Bergman, Zh. Obshch. Khim. **24**, 1524 (1954).
[115]G. A. Bukhalova and A. G. Bergman, Zh. Prikl. Khim. **28**, 1266 (1955).
[116]A. G. Bergman and V. V. Rubleva, J. Gen. Chem. USSR **26**, 747 (1956).
[117]D. S. Coleman and P. D. A. Lacy, Mater. Res. Bull. **2**, 935 (1967).
[118]A. D. Pelton, A. Gabriel, and J. Sangster, J. Chem. Soc. Faraday Trans. 1, **81**, 1167 (1985).
[119]M. V. Kamenetskii, Tsvetn. Metall. **31**, 39 (1958).
[120]R. Nacken, Sitzungsber. Preuss. Akad. Wiss., Phys. Math. Kl. **1**, 192 (1918).
[121]A. J. H. Bunk and G. W. Tichelaar, Konikl. Ned. Akad. Wet. Proc., Ser. B **56**, 378 (1953).
[122]W. T. Barrett and W. E. Wallace, J. Am. Chem. Soc. **76**, 366 (1954).
[123]Nguyen-Ba-Chanh, J. Chim. Phys. **61**, 1428 (1964).
[124]Yu. I. Vesnin and S. P. Zakovryashin, Solid State Commun. **31**, 635 (1979).
[125]G. Graeffe and M. Nurmia, Z. Naturforsch. A **21**, 165 (1966).
[126]M. W. Lister and N. F. Meyers, J. Phys. Chem. **62**, 145 (1958).
[127]R. G. Wolfson and W. Kobes, Mater. Res. Bull. **2**, 263 (1967).
[128]A. Benrath and J. Wainoff, Z. Phys. Chem. **77**, 257 (1911).
[129]J. J. Egan and J. Bracker, U.S. Atomic Energy Commission Report BNL 6589 (1962).
[130]C. Krohn and Z. Moser, KGL Norske Videsnk. Selsk. Skr. No. 9 (1967).
[131]J. Guion, M. Blander, D. Hengstenberg, and K. Hagemark, J. Phys. Chem. **72**, 2086 (1968).
[132]V. I. Glazov, Khim. Tekhnol. Oksid. Magrit. Materialov., No. 3, 130 (1977).
[133]N. L. Yarym-Agaev and G. V. Mel'nik, Zh. Fiz. Khim. **39**, 2650 (1965).
[134]N. L. Yarum-Agaev and L. D. Afanasenko, Russ. J. Phys. Chem. **48**, 666 (1974).
[135]E. Kordes and F. Raaz, Z. Anorg. Chem. **181**, 225 (1929).
[136]A. D. Pelton and S. N. Flengas, Can. J. Chem. **48**, 3483 (1970).
[137]P. S. Shapkin, P. V. Vasil'kova, and M. P. Susarev, Russ. J. Inorg. Chem. **12**, 1493 (1967).
[138]J. M. Short and R. Roy, J. Am. Ceram. Soc. **47**, 149 (1964).
[139]A. Tsubuki, S. Maezawa, K. Niki, and T. Tomonari, High Temp. Sci. **5**, 68 (1973).
[140]I. I. Il'yasov and A. G. Bergman, Zh. Neorg. Khim. **7**, 695 (1962).

[141]N. M. Ryutkina, N. V. Maksina, and N. A. Finkel'shtein, Zh. Neorg. Khim. **18**, 1101 (1973).
[142]E. K. Akopov and T. P. Bortnikova, Zh. Neorg. Khim. **18**, 498 (1973).
[143]J. D. Weyand, Diss. Abstr. Int. B **32**, 7014 (1972).
[144]H. T. Fullam, Mater. Res. Bull. **7**, 289 (1972).
[145]G. Tamman and W. Krings, Z. Anorg. Chem. **130**, 229 (1923).
[146]O. S. Dombrovskaya, Zh. Obshch. Khim. **3**, 1022 (1933).
[147]See Ref. 43, Fig. 3051.
[148]R. J. Havighurst, E. Mack, and F. C. Blake, J. Am. Chem. Soc. **47**, 29 (1925).
[149]E. B. Thomas and L. J. Wood, J. Am. Chem. Soc. **57**, 822 (1935).
[150]M. Ahtee, Ann. Acad. Sci. Fenn. Ser. A6, No. 312 (1969).
[151]O. S. Dombrovskaya, Zh. Obshch. Khim. **3**, 1017 (1933).
[152]I. V. Vasil'kova, A. I. Efimov, L. V. Ryazantseva, and A. V. Storonkin, Russ. J. Phys. Chem. **51**, 480 (1977).
[153]I. I. Il'yasov and A. G. Bergman, Russ. J. Inorg. Chem. **7**, 355 (1962).
[154]E. K. Akopov, L. A. Vashchenko, and L. A. Panieva, Zh. Neorg. Khim. **24**, 2774 (1979).
[155]See Ref. 43, Fig. 3024.
[156]K. J. Rao, G. V. S. Rao, and C. N. R. Rao, Trans. Faraday Soc. **63**, 1013 (1967).
[157]A. Tsubuki, S. Maezawa, K. Niki, and T. Tomonari, High Temp. Sci. **5**, 68 (1973).
[158]S. S. Batsanov, V. P. Bokarev, and I. Kh. Moroz, Russ. J. Inorg. Chem. **26**, 1557 (1981).
[159]J. Arends and H. Nijboer, Phys. Status Solidi **26**, 537 (1968).
[160]A. K. Shukla, J. C. Ahluwalia, and C. N. R. Rao, J. Chem. Soc. Faraday Trans. 1, **72**, 1288 (1976).
[161]H. Weijma and J. Arends, Phys. Status Solidi **35**, 205 (1969).
[162]L. J. Wood, C. Sweeney, and M. T. Derbes, J. Am. Chem. Soc. **81**, 6148 (1959).
[163]L. J. Wood, G. J. Riconalla, and J. D. Laposa, J. Phys.Chem. **65**, 377 (1961).
[164]*JANAF Thermochemical Tables,* 2nd ed. (U.S. GPO, Washington, DC 1971), NSRDS-NBS 37.
[165]B. L. Seleznev and Yu. G. Vlasov, Russ. J. Phys. Chem. **50**, 971 (1976).
[166]H. Koski, Suom. Kemistil. B **43**, 482 (1970).
[167]H. Koski, Ann. Acad. Sci. Fenn. Ser. A6, No. 314 (1969).
[168]L. L. Makarov and Yu. G. Vlasov, Dokl. Akad. Nauk SSSR **120**, 111 (1958).
[169]S. M. Arkhipov, N. I. Kashina, and V. A. Kuzina, Zh. Neorg. Khim. **15**, 1640 (1970).
[170]G. Kellner, Z. Anorg. Allg. Chem. **99**, 137 (1917).
[171]A. I. Agaev, Uch. Zap. Azerb. Gos. Univ. Ser. Fiz. Mat. Khim. Nauk, No. 2, 61 (1961).
[172]N. N. Volkov and M. N. Zakhvalinskii, Izv. Fiz.-Khim. Nauchno.-Issled. Inst. Irkutsk. Go. Univ. **2**, 69 (1953).
[173]V. V. Bugaenko, R. V. Chernov, and Yu. P. Krasan, Ukr. Khim. Zh. Russ. Ed. **43**, 1215 (1977).
[174]T. M. Tsushba, B. S. Shevchenko, and I. K. Tovmas'yan, Zh. Neorg. Khim. **21**, 1894 (1976).
[175]G. Tamman and A. Ruppelt, Z. Anorg. Allg. Chem. **197**, 65 (1931).
[176]D. Doornhof, H. J. Van Wijk, and H. A. J. Oonk, Thermochim. Acta **76**, 171 (1984).
[177]P. D. Garn, Bell Lab. Rec. **33**, 452 (1955).
[178]C. Margheritis, G. Flor, and C. Sinistri, Z. Naturforsch A **34**, 836 (1979).
[179]N. A. Reshetnikov and G. M. Unshakov, Izv. Fiz.-Khim. Nauchno.-Issled. Inst. Irkutsk. Gos. Univ. **2**, 23 (1953).
[180]N. N. Volkov and L. A. Dubinskaya, Izv. Fiz. Khim. Nauchno.-Issled. Inst. Irkutsk. Gos. Univ. **2**, 45 (1953).
[181]G. G. Diogenov, N. N. Nurminskii, and E. A. Anisimova, Trudy Irkutsk. Politekh. Inst. **69**, 119 (1971).
[182]A. S. Arabadzhan and A. G. Bergman, Zh. Neorg. Khim. **8**, 365 (1963).
[183]I. I. Il'yasov, K. I. Iskandarov, and A. G. Palobekov, Izv. Vyssh. Uchebn. Zaved. Khim. Khim. Tekhnol. **17**, 611 (1974).
[184]G. Flor, C. Margheritis, and C. Sinistri, J. Chem. Eng. Data **24**, 361 (1979).
[185]G. G. Diogenov and V. I. Ermachkov, Zh. Neorg. Khim. **12**, 827 (1967).
[186]I. I. Il'yasov, M. Davranov, and I. I. Grudyanov, Zh. Neorg. Khim. **20**, 232 (1975).
[187]V. E. Plyushchev and R. G. Samuseva, Russ. J. Inorg. Chem. **9**, 1177 (1964).
[188]D. S. Lesnykh and E. P. Garmatina, Zh. Neorg. Khim. **12**, 1307 (1967).
[189]A. Bellanca, Period. Mineral. **10**, 9 (1939).
[190]G. M. Unzhakov, Izv. Fiz.-Khim. Nauchno.-Issled. Inst. Irkutsk. Gos. Univ. **2**, 10 (1953).
[191]I. I. Il'yasov, V. N. Mirsoyapov, and Yu. V. Korotkov, Zh. Neorg. Khim. **4**, 909 (1959).
[192]I. I. Il'yasov, Russ. J. Inorg. Chem. **7**, 86 (1962).
[193]I. G. Murgulescu and D. I. Marchidan, Rev. Roum. Chim. **9**, 793 (1964).
[194]Nguyen-Ba-Chanh, J. Chim. Phys. **61**, 1428 (1964).
[195]V. Sabet and T. Ostvold, Acta Chem. Scand. **27**, 396 (1973).
[196]R. G. Samuseva and V. E. Plyushchev, Russ. J. Inorg. Chem. **9**, 1315 (1964).
[197]I. I. Il'yasov and V. V. Volchankaya, Zh. Neorg. Khim. **27**, 3211 (1982).
[198]I. K. Tovmas'yan, T. M. Tsushba, and V. P. Radina, Russ. J. Inorg. Chem. **15**, 1311 (1970).
[199]R. G. Samuseva and V. E. Plyushchev, Russ. J. Inorg. Chem. **6**, 1096 (1961).
[200]I. I. Il'yasov, Ukr. Khim. Zh. Russ. Ed. **31**, 930 (1965).
[201]I. I. Il'yasov, Zh. Neorg. Khim. **10**, 2324 (1965).
[202]V. A. Isaenko, Zh. Neorg. Khim. **22**, 1674 (1977).
[203]V. P. Bokarev and A. V. Parshukov, Russ. J. Inorg. Chem. **27**, 1650 (1982).
[204]G. G. Diogenov and V. I. Ermachkov, Zh. Neorg. Khim. **12**, 573 (1967).
[205]M. Davranov, I. I. Il'yasov, and M. Ashurova, Zh. Neorg. Khim. **19**, 1628 (1974).
[206]G. S. Durham, L. Alexander, D. Pitman, H. Golub, and H. Klug, J. Phys. Chem. **59**, 561 (1955).
[207]I. I. Il'yasov and A. G. Bergman, Russ. J. Inorg. Chem. **9**, 768 (1964).
[208]I. K. Tovmas'yan, T. M. Tsushba, and A. G. Bergman, Russ. J. Inorg. Chem. **15**, 1172 (1970).
[209]K. I. Iskandarov, Yu. G. Litvinov, and I. I. Il'yasov, Zh. Neorg. Khim. **21**, 1990 (1976).
[210]A. G. Dudareva, A. K. Molodkin, Yu. E. Bogatov, V. V. Kurilkin, P. I. Fedorov, and A. I. Ezhov, Zh. Neorg. Khim. **21**, 1905 (1976).
[211]S. D. Dionisev and L. A. Ryazantseva, Russ. J. Inorg. Chem. **27**, 1066 (1982).
[212]Yu. G. Vlasov, B. L. Seleznov, and V. V. Kolodnikov, Zh. Fiz. Khim. **47**, 2170 (1973).
[213]H. Ohno and K. Furukawa, J. Nucl. Mater. **64**, 37 (1977).
[214]M. E. Melnichak and O. J. Kleppa, J. Chem. Phys. **52**, 1790 (1970).
[215]D. B. Leiser and O. J. Whittemore, J. Am. Ceram. Soc. **50**, 60 (1967).
[216]C. H. Liu and L. R. Lieto, J. Chem. Eng. Data **14**, 83 (1969).
[217]R. Sridhar, C. E. Johnson, and E. J. Cairns, J. Chem. Eng. Data **15**, 244 (1970).
[218]H. C. Gaebell and G. Meyer, Mater. Res. Bull. **18**, 1353 (1983).
[219]A. G. Bergman and F. P. Platonov, Izv. Sekt. Fiz.-Khim. Anal. Inst. Obshch. Neorg. Khim. Akad. Nauk SSSR **11**, 253 (1937).
[220]F. P. Platonov, Tr. Mosk. Skh. Akad. **36**, 42 (1946).
[221]I. I. Il'yasov, G. G. Shchemeleva, and A. G. Bergman, Russ. J. Inorg. Chem. **6**, 355 (1961).
[222]A. Gobaoz and S. Zuca, Rev. Roum. Chim. **11**, 183 (1966).
[223]L. S. Hersh and O. J. Kleppa, Trans. Faraday Soc. **59**, 1850 (1963).
[224]I. I. Il'yasov, Russ. J. Inorg. Chem. **11**, 115 (1966).
[225]I. I. Il'yasov and A. G. Bergman, Zh. Neorg. Khim. **11**, 681 (1966).
[226]R. G. Samuseva and V. E. Plyushchev, Russ. J. Inorg. Chem. **9**, 1313 (1964).
[227]I. I. Il'yasov, M. Davranov, and K. I. Iskandarov, Russ. J. Inorg. Chem. **21**, 759 (1976).
[228]L. L. Makarov and D. Yu. Stupin, Russ. J. Phys. Chem. **35**, 363 (1961).
[229]H. A. C. McKay and J. K. Perring, Trans. Faraday Soc. **49**, 163 (1953).
[230]I. I. Il'yasov and A. G. Bergman, Zh. Neorg. Khim. **10**, 681 (1965).
[231]I. I. Il'yasov, N. I. Chaurski, and D. G. Barsegov, Zh. Neorg. Khim. **11**, 1984 (1966).
[232]I. I. Il'yasov, M. Davranov, and K. I. Iskandarov, Zh. Neorg. Khim. **19**, 1919 (1974).
[233]L. L. Makarov and A. G. Pankov, Russ. J. Phys. Chem. **36**, 1209 (1962).
[234]A. A. Bochvar, Z. Anorg. Allg. Chem. **210**, 163 (1933).
[235]A. G. Bergman and E. I. Banashek, Izv. Sekt. Fiz.-Khim. Anal. Inst. Obshch. Neorg. Khim. Akad. Nauk SSSR **23**, 201 (1953).
[236]H. M. Haendler, P. S. Sennett, and C. M. Wheeler, J. Electrochem. Soc. **106**, 264 (1959).
[237]C. E. Johnson and E. J. Hathaway, J. Electrochem. Soc. **118**, 631 (1971).
[238]G. A. Bukhalova and A. G. Bergman, Dokl. Akad. Nauk SSSR **66**, 67 (1949).
[239]A. G. Bergman, E. L. Kozachenko, and S. I. Berezina, Zh. Neorg. Khim. **9**, 663 (1964).

[240]A. G. Bergman and A. S. Arabadzhan, Zh. Neorg. Khim. **8**, 1228 (1963).
[241]S. I. Berezina, A. G. Bergman, and E. L. Bakumskaya, Russ. J. Inorg. Chem. **8**, 1118 (1963).
[242]N. N. Volkov and M. N. Zakhvalinskii, Izv. Fiz.-Khim. Nauchno.-Issled. Inst. Irkutsk. Gos. Univ. **2**, 45 (1953).
[243]A. G. Bergman and A. S. Arabadzhan, Zh. Neorg. Khim. **8**, 1228 (1963).
[244]O. J. Kleppa, L. S. Hersh, and J. M. Toguri, Acta Chem. Scand. **17**, 2681 (1963).
[245]M. E. Melnichak and O. J. Kleppa, J. Chem. Phys. **57**, 5231 (1972).
[246]C. E. Johnson and E. J. Hathaway, J. Chem. Eng. Data **14**, 174 (1969).
[247]E. J. Cairns, C. E. Crouthamel, A. K. Fisher, M. S. Foster, J. C. Hesson, C. E. Johnson, H. Shimotoke, and A. D. Tevelbauch, Argonne Natl. Lab. Report No. ANL-7316, 219 (1967).
[248]G. Flor, C. Margheritis, and C. Sinistri, J. Chem. Eng. Data **26**, 152 (1981).
[249]W. Plato, Z. Phys. Chem. **58**, 350 (1907).
[250]A. Wolters, Neues Jahrb. Mineral. Geol. Palaeontol. Abh. Abt. A **30**, 55 (1910).
[251]G. A. Bukhalova, Izv. Sek. Fiz.-Khim. Anal. Inst. Obshch. Neorg. Khim. Akad. Nauk SSSR **26**, 138 (1955).
[252]K. Grjotheim, T. Halvorsen, and J. L. Holm, Acta Chem. Scand. **21**, 2300 (1967).
[253]G. A. Bukhalova, Zh. Neorg. Khim. **4**, 117 (1959).
[254]N. N. Volkov and A. G. Bergman, C. R. Acad. Sci. URSS **27**, 967 (1940).
[255]M. A. Kuvakin and P. S. Kusakin, Zh. Neorg. Khim. **4**, 2577 (1959).
[256]R. F. Rea, J. Am. Ceram. Soc. **21**, 98 (1938).
[257]V. N. Storozhenko, S. F. Vazhenin, and L. N. Antipin, Zh. Fiz. Khim. **39**, 524 (1965).
[258]M. Ishaque, Bull. Soc. Chim. France 127 (1952).
[259]O. Ruff and W. Plato, Berichte **36**, 2357 (1903).
[260]V. D. Polyakov, Izv. Sekt. Fiz.-Khim. Anal. Inst. Obshch. Neorg. Khim. Acad. Nauk SSSR **13**, 299 (1940).
[261]N. N. Volkov and M. N. Zakhvalinskii, Izv. Fiz.-Khim. Nauchno.-Issled. Inst. Irkutsk. Gos. Univ. **2**, 69 (1953).
[262]N. S. Dombrovskaya, Izv. Sekt. Fiz.-Khim. Anal. Inst. Obshch. Neorg. Khim. Acad. Nauk SSSR **20**, 124 (1950).
[263]M. Amadori, Atti R. Accad. Naz. Lincei Mem. Cl. Sci. Fis. Mat. Nat. II **21**, 467 (1912).
[264]S. P. Gromakov and L. M. Gromakova, Zh. Fiz. Khim. **29**, 746 (1955).
[265]E. Schobert, Neues Jahrb. Mineral. Geol. Palaeont. Abh. Abt. **2**, 186 (1913).
[266]T. Ostvold, Acta Chem. Scand. **25**, 2302 (1971).
[267]M. A. Fineman and W. E. Wallace, J. Am. Chem. Soc. **70**, 4165 (1948).
[268]S. Sternberg and C. Herdlicka, Rev. Roum. Chim. **11**, 29 (1966).
[269]S. Sternberg and C. Herdlicka, Rev. Roum. Chim. **12**, 771 (1967).
[270]T. Ostvold, Acta Chem. Scand. **22**, 435 (1968).
[271]T. Ostvold, in *Molten Salts*, NSRDS-NBS 28 (National Bureau of Standards, Washington, DC, 1969), Vol. 2, Sec. 1.
[272]See Ref. 263, p. 471.
[273]I. I. Il'yasov and A. G. Bergman, J. Gen. Chem. USSR **26**, 1457 (1956).
[274]D. I. Marchidan and C. Telea, Rev. Roum. Chim. **13**, 291 (1968).
[275]A. P. Obukhov, Zh. Obshch. Khim. **3**, 787 (1933).
[276]S. Okada, S. Voshizawa, and N. Watanabe, J. Chem. Soc. Jpn. **56**, 79 (1953).
[277]I. E. Krauze and A. G. Bergman, C. R. Acad. URSS **35**, 20 (1942).
[278]N. S. Kurnakov and J. B. Wrzesnewsky, Z. Anorg. Chem. **74**, 89 (1912).
[279]J. B. Wrzesnewsky, Z. Anorg. Chem. **74**, 95 (1912).
[280]M. Amadori and G. Pampanini, Atti R. Accad. Naz. Lincei Mem. Cl. Sci. Fis. Mat. Nat. II, **20**, 572 (1911).
[281]H. L. Link and L. J. Wood, J. Am. Chem. Soc. **62**, 766 (1940).
[282]N. Fontell, Soc. Sci. Fenn. Comment. Physico-Math. X(6), 1 (1939).
[283]M. Miller and K. Skudlarski, Ber. Bunsenges. Phys. Chem. **89**, 916 (1985).
[284]A. Mustajoki, Ann. Acad. Sci. Fenn. Ser. A1 **98**, 7 (1951).
[285]V. Hovi, Ann. Acad. Sci. Fenn. A1 **55**, 1 (1948).
[286]M. M. Popoff and S. F. Jaworoskaja, Z. Phys. Chem. **167A**, 180 (1933).
[287]M. M. Popoff, Z. Phys. Chem. **147A**, 302 (1930).
[288]M. S. Ivankina, Izv. Tomsk. Politekh. Inst. **95**, 192 (1958).
[289]N. Fontell, V. Hovi, and H. Mikkola, Ann. Acad. Sci. Fenn. A1 **54**, 1 (1949).
[290]W. H. McCoy and W. E. Wallace, J. Am. Chem. Soc. **78**, 5995 (1956).
[291]H. Brodowsky and W. Kock, Ber. Bunsenges. Phys. Chem. **79**, 985 (1975).
[292]See Ref. 263, p. 606.
[293]E. M. Chernotordik, Zh. Obshch. Khim. **4**, 459 (1934).
[294]P. Luova and M. Muurinen, Ann. Univ. Turku. Ser. A 1, 110 (1967).
[295]E. T. Teatum and N. O. Smith, J. Phys. Chem. **61**, 697 (1957).
[296]P. Luova and O. Tannila, Suom. Kemistil. B **39**, 220 (1966).
[297]L. L. Makarov and K. K. Evstrop'ev, Russ. J. Phys. Chem. **34**, 934 (1960).
[298]G. Bruni and M. Amadori, Atti R. Inst. Veneto Sci. Lett. Arti Cl. Sci. Mat. Nat. II **71** (1911/12).
[299]M. Kantola, P. Luova, and L. Vinko, Ann. Acad. Sci. Fenn. Ser. A 6, (1964).
[300]P. Luova, Suom. Kemistil. B **38**, 32 (1965).
[301]M. Amadori and G. Pampanini, Atti R. Accad. Naz. Lincei, Mem. Cl. Sci. Fis., Mat. Nat. II **20**, 478 (1911).
[302]E. I. Banashek, Izv. Sek. Fiz.-Khim. Anal. Inst. Obshch. Neorg. Khim. Akad. Nauk SSSR **20**, 109 (1950).
[303]I. K. Tovmas'yan, T. M. Tsushba, and A. G. Bergman, Soviet Prog. Chem. **36**, 27 (1970).
[304]I. I. Il'yasov and V. V. Volchanskaya, Soviet Prog. Chem. **40**, 56 (1974).
[305]V. A. Isaenko, N. A. Volchenkova, and A. N. Kirgintsev, Russ. J. Inorg. Chem. **21**, 1577 (1976).
[306]V. Hovi, Suom. Kemistil. B **28**, 127 (1955).
[307]V. Hovi, Suom. Kemistil. B **27**, 33 (1954).
[308]I. G. Murgulescu and D. I. Marchidan, Rev. Roum. Chim. **11**, 1031 (1966).
[309]I. K. Tovmas'yan and V. I. Sholokhova, Soviet Prog. Chem. **39**, 55 (1973).
[310]I. I. Il'yasov and Yu. G. Litvinov, Soviet. Prog. Chem. **40**, 28 (1974).
[311]V. I. Sholokhova, Dokl. Mezhvus. Nauch.-Teor. Konf. Aspir. Rostov-na-Donu Pedagog. Inst. 430 (1971).
[312]I.I. Il'yasov, K. I. Iskandarov, M. Kidynov, R. N. Berdieva, and M. Davranov, Ukr. Khim. Zh. Russ. Ed. **41**, 490 (1975).
[313]M. Ahtee and H. Koski, Ann. Acad. Sci. Fenn. Ser. A6, No. 297 (1968).
[314]H. Koski, Thermochim. Acta **5**, 360 (1973).
[315]V. P. Belousov, Y. G. Vlasov, and B. L. Seleznev, Izv. Vyssh. Uchebn. Zaved. Khim. Khim. Tekhnol. **20**, 76 (1977).
[316]G. A. Bukhalova, G. A. Shegurova, T. M. Khliyan, and E. S. Yagub'yan, Russ. J. Inorg. Chem. **18**, 583 (1973).
[317]I. I. Il'yasov, Russ. J. Inorg. Chem. **9**, 766 (1964).
[318]M. Natarajan, K. J. Rao, and C.N.R. Rao, Trans. Faraday Soc. **66**, 2497 (1970).
[319]V. Hovi, Ann. Univ. Turku, Ser. A I **26** (1957).
[320]A. V. Storonkin, M. M. Shul'ts, and W. Korchagin, Fiz.-Khim. Svoistva Rastvorov, Leningr. Gos. Univ. 227 (1964).
[321]G. A. Bukhalova, G. A. Shegurova, and E. S. Yagub'yan, Russ. J. Inorg. Chem. **18**, 1370 (1973).
[322]Y. G. Vlasov, B. L. Seleznev, and E. A. Elchin, Zh. Neorg. Khim. **17**, 3069 (1972).
[323]C. W. Bale and A. D. Pelton, Metall. Trans. **5**, 2323 (1974).
[324]H. Reiss, J. L. Katz, and O. J. Kleppa, J. Chem. Phys. **36**, 144 (1962).
[325]C. E. Kaylor, G. E. Walden, and D. F. Smith, J. Am. Chem. Soc. **81**, 4172 (1957).
[326]J. Richter and W. Vreuls, Ber. Bunsenges. Phys. Chem. **83**, 1023 (1979).
[327]J. Richter, W. Vreuls, and W. Winthagen, Ber. Bunsenges. Phys. Chem. **84**, 231 (1980).
[328]J. Bousquet, G. Perachon, and J.-C. Remy, Bull. Soc. Chim. Fr. **1**, 238 (1967).
[329]*Handbook of Chemistry and Physics*, 65th ed., edited by R. C. Weast (CRC Press, Boca Raton, FL, 1984).
[330]L. J. Wood, W. Secunda, and C. H. McBride, J. Am. Chem. Soc. **80**, 307 (1958).
[331]O. Kaposi, L. Bencze, and L. V. Zhuravleva, J. Chem. Thermodyn. **18**, 635 (1986).
[332]M. M. Reventos, N. B. Chanh, and J. M. Amigo, Acta Geol. Hisp. **19**, 223 (1984).